

12-2018

# Investigating the Role of Carotenoids in Membrane Organization of *Pantoea* sp. YR343

Sushmitha Vijaya Kumar

*University of Tennessee*, [svijaya3@vols.utk.edu](mailto:svijaya3@vols.utk.edu)

---

## Recommended Citation

Vijaya Kumar, Sushmitha, "Investigating the Role of Carotenoids in Membrane Organization of *Pantoea* sp. YR343. " PhD diss., University of Tennessee, 2018.  
[https://trace.tennessee.edu/utk\\_graddiss/5304](https://trace.tennessee.edu/utk_graddiss/5304)

This Dissertation is brought to you for free and open access by the Graduate School at Trace: Tennessee Research and Creative Exchange. It has been accepted for inclusion in Doctoral Dissertations by an authorized administrator of Trace: Tennessee Research and Creative Exchange. For more information, please contact [trace@utk.edu](mailto:trace@utk.edu).

To the Graduate Council:

I am submitting herewith a dissertation written by Sushmitha Vijaya Kumar entitled "Investigating the Role of Carotenoids in Membrane Organization of *Pantoea* sp. YR343." I have examined the final electronic copy of this dissertation for form and content and recommend that it be accepted in partial fulfillment of the requirements for the degree of Doctor of Philosophy, with a major in Life Sciences.

Jennifer Morrell-Falvey, Major Professor

We have read this dissertation and recommend its acceptance:

Gladys Alexandre, Francisco Barrera, Dale Pelletier, Robert Standaert

Accepted for the Council:

Carolyn R. Hodges

Vice Provost and Dean of the Graduate School

(Original signatures are on file with official student records.)

---

**Investigating the Role of Carotenoids in Membrane Organization of *Pantoea* sp.  
YR343**

**A Dissertation Presented for the  
Doctor of Philosophy  
Degree  
The University of Tennessee, Knoxville**

**Sushmitha Vijaya Kumar  
December 2018**

## **DEDICATION**

*To my family for their unconditional love and support*

*And*

*To Siva Karthik, you are my rock*

## ACKNOWLEDGEMENTS

There have been many people who have walked alongside me for the past few years for whom I am grateful for. First and foremost, I would like to thank my advisor Dr. Jennifer Morrell-Falvey for her continued support, guidance and patience. I am grateful for the freedom she provided me, that helped me become a better researcher. All in all, I am lucky to have you as my mentor. I also would like to thank my committee members, Dr. Dale Pelletier, Dr. Gladys Alexandre, Dr. Robert Standaert and Dr. Francisco Barrera for your valuable suggestions and support.

I am much obliged to Dr. Mitchel Doktycz, Dr. Graham Taylor and Dr. Dave Alison for their continued support in the lab. Dr. Amber Bible, thank you for being an awesome mentor and for all the scientific discussions. It has been so much fun working alongside you and I truly admire your work ethics. Many thanks to Cathy for being an awesome secretary. To all my lab members at ORNL, I have thoroughly enjoyed working alongside you. This work would not be completed without friends like you.

I would like to thank Dr. Albrecht von Arnim for recruiting me and also for the valuable advice along the way. To Terrie Yeatts, for all the help. Many thanks to everyone in the GST program. To my doctors, for being very accommodating and helping me finish this journey strong.

To my loving and supportive family, my parents, Latha and A. R. Vijaya Kumar, thanks for letting me chase my dreams and being so patient. Many thanks to my sister Samyuktha and brother-in law Srikant, for supporting me at every step of the way. To my handsome nephew Reyansh, who thinks greatly of his aunt. Finally, to my best friend Karthik, words cannot describe how instrumental you have been in this journey of mine. Your kindness, patience and continued love has helped enjoy this journey. I am so grateful for you.

## ABSTRACT

Bacterial cell membranes are complex mixtures of lipids and proteins, the combination of which confers biophysical properties to the membrane and allows it to respond to environmental conditions. *Pantoea* sp. YR343 is a plant-associated gram-negative gamma-proteobacteria characterized by the presence of carotenoids in the membrane. *Pantoea* sp. YR343 mutants lacking phytoene synthase (encoded by *crtB*), which catalyzes the first step in carotenoid biosynthesis, failed to produce carotenoids and displayed enhanced sensitivity to reactive oxygen species. The *crtB* mutant also displayed unexpected defects in biofilm formation, secretion of indole-3-acetic acid, and root colonization compared to wildtype cells. We hypothesized that the phenotypic defects observed in the *crtB* mutant were due to the changes in both lipid and protein composition which modulate the biophysical properties of the membrane and influence signaling and transport.

Mass spectrometry analysis of the lipid head and tails revealed a significant abundance of phosphatidylethanolamine and unsaturated fatty acids in the *crtB* mutant cells. Using both fluorescence anisotropy (FA) and atomic force microscopy on whole cells, we showed that the *crtB* mutant membranes were less fluid when compared to wildtype membranes. We further characterized the membranes using spheroplasts and natural extract vesicles, which showed that presence of the outer wall does not impact membrane fluidity, but the presence of membrane proteins and carotenoids do have a strong impact. Proteomic profiling of wildtype and *crtB* mutant membranes revealed a significant loss of several membrane protein classes in the *crtB* mutant. Among the different classes of proteins, signaling and transport, outer membrane biogenesis and cell motility protein classes were the most affected in the mutant. The loss of specific protein classes may explain, at least in part, the phenotypic defects associated with the *crtB* mutant.

Our study highlights the importance of carotenoids beyond its anti-oxidant potential. Loss of bacterial carotenoids changes membrane organization and dynamics by affecting the composition and distribution of both lipids and membrane proteins. Importantly, carotenoids regulate membrane fluidity, which is an important parameter for bacterial adaptation and survival.

## TABLE OF CONTENTS

<b>CHAPTER 1 Background and Overview</b>	1
The Lipid Bilayer	3
Distribution and role of sterols in cell membranes	4
Membrane phase transition	5
Membrane organization and lipid rafts	5
Membrane fluidity	7
Carotenoids- properties and functions	8
Role of carotenoids in membrane fluidity	9
Plant-microbe interaction	10
<i>Pantoea</i> sp. YR343	11
$\Delta crtB$ , a carotenoid deficient strain of <i>Pantoea</i> sp. YR343	11
References	14
Appendix	22
<b>CHAPTER 2 Deletion of carotenoids from membranes of <i>Pantoea</i> sp. YR343 results in altered lipid composition and changes in membrane biophysical properties</b>	27
Abstract	28
Introduction	28
Results	30
Discussion	33
Materials and methods	35
References	40
Appendix	45
<b>CHAPTER 3 Loss of carotenoids leads to changes in membrane protein classes in <i>Pantoea</i> sp. YR343</b>	56
Abstract	57
Introduction	57
Results and Discussion	59
Materials and methods	68
References	73
Appendix	79
<b>CHAPTER 4 Conclusions and Future Directions</b>	101
References	105
<b>APPENDIX</b>	106
Appendix-A	107
References	112
Appendix-B	113
<b>VITA</b>	138

## LIST OF FIGURES

Figure 1.1	Schematic representation of biological membranes with a heterogenous distribution of phospholipids and proteins	23
Figure 1.2.	A simplified model of lipid rafts in eukaryotic membranes	24
Figure 1.3.	Biosynthesis and functions of carotenoids	25
Figure 1.4	Phenotypic defects associated with $\Delta crtB$ mutant	26
Figure 2.1	<i>crtB</i> deletion causes changes in membrane lipid head group composition	46
Figure 2.2	Significant decrease in % abundance of unsaturated fatty acids (C16:1 and C18:1) in the $\Delta crtB$ mutant cells	48
Figure 2.3	Representative AFM deflection images of <i>Pantoea</i> sp. YR343 and $\Delta crtB$ cells at 28°C and 45°C	50
Figure 2.4	Atomic force microscopy (AFM) reveals less elastic $\Delta crtB$ mutant cell	51
Figure 2.5	Fluorescence anisotropy with DPH indicates a rigid $\Delta crtB$ mutant membrane	52
Figure 2.6	Removal of outer membrane reveals no difference in fluorescence polarization between <i>Pantoea</i> sp. YR343 and $\Delta crtB$ mutant spheroplast	53
Figure 2.7	Properties of extruded vesicles of <i>Pantoea</i> sp. YR343 and $\Delta crtB$ mutant	54
Figure 2.8	Fluorescence anisotropy with DPH on natural extract vesicles indicates a fluid $\Delta crtB$ mutant membrane	55
Figure 3.1	Identification and analysis of the proteins identified in whole cell, membrane pellet, DRM and DSM fractions of <i>Pantoea</i> sp. YR343 and $\Delta crtB$ mutant cells	80
Figure 3.2	Histogram representing the % of proteins with predicted transmembrane helix domains (THMM) for each sample	81
Figure 3.3	Hierarchical clustering of all proteins identified in all four fractions of <i>Pantoea</i> sp. YR343 and $\Delta crtB$ mutant	82
Figure 3.4	Volcano plot illustrating significantly differentially abundant proteins	83
Figure 3.5	Top orthologous groups for all significant proteins in whole cell, membrane pellet, DRM and DSM samples	88
Figure 3.6	Clustered heatmap of gene expression in <i>Pantoea</i> sp. YR343 and $\Delta crtB$ mutant	89
Figure 3.7	Loss of carotenoids affects bacterial cell motility	93



## LIST OF TABLES

Table 2.1	Normalized $\mu\text{m}$ concentration of all lipid head groups identified by lipidomics	47
Table 2.2	<i>crtB</i> deletion causes changes in membrane fatty acid composition	49
Table 3.1	Whole-genome gene ontology (GO) term annotation using Blast2GO software	84
Table 3.2	List of significantly upregulated or downregulated proteins involved in cell wall/ membrane/ envelope biogenesis	90
Table 3.3	List of significantly upregulated or downregulated proteins involved in cell motility	94
Table 3.4	List of significantly upregulated or downregulated proteins involved in lipid transport and metabolism	96
Table 3.5	List of significantly upregulated or downregulated proteins involved in signal transduction mechanism	98
Table A.1	List of primers used in this study	111
Table B.1	List of transcripts upregulated in $\Delta\text{crtB}$ mutant cells	113
Table B.1	List of transcripts downregulated in $\Delta\text{crtB}$ mutant cells	114

## ABBREVIATIONS

GPI- Glycosylphosphatidylinositol-anchored  
GPCR- G-protein coupled receptors  
DRM- detergent-resistant membrane  
PE- phosphatidylethanolamine  
IAA- indole-3 acetic acid  
LB- Luria-Bertani medium  
PS- Phosphatidylserine  
PG- Phosphatidylglycerol  
PA- Phosphatidic acid  
GC-FAME-Gas-chromatography-fatty acid methyl ester  
AFM- Atomic force microscopy  
DPH-1,6-diphenyl-1,3,5- hexatriene  
DSM- Detergent-sensitive membrane  
MP- Membrane pellet  
FC- Fold change  
GO- Gene Ontology  
MCP- Methyl-accepting chemotaxis proteins  
COG- Cluster of orthologous groups  
UDP- Undecaprenyl-phosphate  
TM- Transmembrane  
SP- Signal peptide  
 $\mu$ l- Microliter

**CHAPTER-1**  
**Background and Overview**

Chapter 1 is reproduced in part with permission.

Bible, A. N., Fletcher, S. J., Pelletier, D. A., Schadt, C. W., Jawdy, S. S., Weston, D. J., ... Morrell-Falvey, J. L. (2016). A Carotenoid-Deficient Mutant in *Pantoea* sp. YR343, a Bacteria Isolated from the Rhizosphere of *Populus deltoides*, Is Defective in Root Colonization. *Frontiers in Microbiology*, 7, 491. <http://doi.org/10.3389/fmicb.2016.00491>

Copyright © 2016 Bible, Fletcher, Pelletier, Schadt, Jawdy, Weston, Engle, Tschaplinski, Masyuko, Polisetti, Bohn, Coutinho, Doktycz and Morrell-Falvey.

## The Lipid Bilayer

Biological membranes are complex, heterogeneous, and two-dimensional assemblies possessing distinct regions with unique biophysical composition and properties [1]. Common to all cells, biological membranes primarily define boundaries, a basic feature important for the existence of life [2]. Membranes are responsible for maintaining a constant internal environment, even in the presence of environmental fluctuations. Besides being instrumental in protecting cells, membranes are also considered organizational sites where metabolism and signaling events occur [3]. In addition, membranes contain channels and receptors that allow specific small molecules, such as water, nutrients, and metabolic products, to flow into and out of the cell [4]. Membranes also aid in cellular self-recognition and adhesion, which are important to the defense system. Thus, studying the properties of membranes is vital for understanding cells both on a single cell level and on an organismal level (Figure 1.1A).

Danielli and Harvey were the first to show that membranes consist of lipids and proteins [5]. In 1972, Singer and Nicholson proposed the Fluid Mosaic model, which describes the structure of the membrane as a homogenous bilayer of lipids in proteins and other macromolecules are embedded [6]. In the following years, Mouritsen and Bloom established the Mattress model, in which mismatching between the proteins and lipids creates regions or domain that are non-homogenous in nature [7]. Both the fluid mosaic model and the mattress model describe membranes as dynamic structures. This dynamic property is crucial for cellular activity and several biological functions.

The structural similarity of all bio-membranes is due to the polar lipids that form the lipid bilayer, while the functional diversity is due to the proteins that are anchored in the bilayer [8]. Generally, most membranes contain approximately 40% of their dry weight as lipid and 60% as protein [9]. Lipids are water-insoluble organic substances that are amphipathic in nature with a hydrophobic tail and a hydrophilic head group within a molecule. Because of this amphipathic nature, lipids are capable of forming bilayers spontaneously [10]. Lipids are classified into three main categories based on their structure: phospholipids, glycolipids, and sterols [11]. The lipid composition in a membrane depends on the type of cell, but in general most membranes possess amphipathic phospholipids. The hydrophobic nature of lipid tails is attributed due to the presence of two non-polar hydrocarbon chains typically consisting of 16-18 carbon molecules. These fatty acid chains can be either both saturated, both unsaturated (containing double bonds) or one saturated and the other unsaturated. The head group attached to a phosphate moiety makes the polar region of the lipid. Choline, ethanolamine, serine, or glycerol can make up the polar head group [12, 13]. Each head group possess a unique charge density and curvature that contributes to the overall structure of the membrane. If the cross-sectional area of the head group is similar to the

cross-sectional area of the fatty acyl chains, these lipids impart zero curvature (example: phosphatidylcholine/serine). If the cross-sectional area between the lipid head group and tail is different, the phospholipid can impart either positive (example: phosphatidylinositol) or negative curvature (example: phosphatidylethanolamine). Positive curvature is imparted when the head group is larger when compared to the acyl chains and negative curvature is when the tails are relatively larger than the head groups creating an inverted conical shape [14, 15] (Figure 1.1).

Approximately, 20-30% of all genes in most genomes encode for membrane proteins [16]. In general, two distinct structures are commonly found in membrane proteins:  $\alpha$ -helix bundle and  $\beta$ -barrel proteins that are formed due to intra-molecular hydrogen bonding of amino acid residues [17, 18]. Membrane functions, such as transport, signaling, and enzymatic activities, are attributed to proteins. Proteins found in membranes can be classified as peripheral or integral membrane proteins. Peripheral membrane proteins adhere temporarily to biological membranes and can, therefore, be isolated relatively easily using mild conditions. These proteins do not possess transmembrane domains but can anchor to the lipid bilayer either by ionic or hydrophobic interactions or using a lipid anchor such as Glycosylphosphatidylinositol-anchored (GPI)- anchored proteins [19, 20]. Integral membrane proteins span the lipid bilayer (once or more than once) with their transmembrane helices [21].

Studying lipid-protein interactions are essential to the understanding of the organizational principles of all biological membranes. Functioning of several proteins such as G-protein coupled receptors (GPCR) requires activation by specific lipids [22]. It has also been shown that interactions between lipid headgroup and proteins regulate the conformational transitions, further regulating functioning of the protein [23]. Proteins in turn regulate the phase behavior of the membrane, influencing the mobility of lipid species. Thus, different lipid molecules can interact dynamically, forming transient or stable structures which are used by proteins as a platform for carrying out their function or for interaction with other proteins [24, 25].

### **Distribution and role of sterols in cell membranes**

Apart from the lipids previously mentioned, sterols a subgroup of amphipathic lipids are also found in most eukaryotic and a few prokaryotic membranes [28]. These molecules are synthesized by complex pathways that are regulated independently of lipid biosynthesis [29]. Sterol biosynthetic pathways contain many steps and energetically expensive. For example, cholesterol biosynthesis from Acetyl-CoA requires 30 enzymatically catalyzed steps [30].

Among the sterols, cholesterol is abundant in higher eukaryotic organisms with 90% of the synthesized cholesterol found in the membranes, while the remaining 10% is found in circulating lipoproteins [31]. In general, cholesterol is the precursor for the synthesis of hormones and other biologically-relevant molecules [32-34]. In membranes, cholesterol can also modulate membrane biophysical properties and play other membrane associated roles such as ion permeation and signal transduction [35-37]. Other sterol analogs such as lanosterol and ergosterol have also shown to be an important for structural, functional and dynamic membrane properties. Lanosterol, a biosynthetic precursor of cholesterol is found in prokaryotic membranes [30]. Ergosterol is found in membranes of yeast, fungi and protozoans [38]. In plants, stigmasterol and sitosterol are biologically-important sterols [39].

In some prokaryotic membranes, additional sterol analogs, including hopanoids and carotenoids, have also been identified. Recent studies have shown that hopanoids interact with lipids in the outer membranes of bacteria to form highly ordered regions similar to cholesterol-sphingolipid interaction in eukaryotes [40]. Several studies have also shown that carotenoids, such as zeaxanthin, can rigidify the fluid phase of membranes, thereby limiting oxygen penetration and protecting the lipid bilayer from oxidative degradation [41]. The importance of carotenoids in bacterial membranes will be discussed in detail below.

### **Membrane phase transition**

An important feature of all biological membranes is their thermotropic phase transition. Phase transition is the property of lipids to transform from one phase of a system to another [42]. Every lipid species is characterized by a transition temperature,  $T_t$ . Lipids in the membrane can change from an ordered/gel state to a fluid/liquid crystalline state [43]. This property is important for overall maintenance of membrane structure and functioning. The fluid state is the most biologically relevant because at the body temperature, most of the membrane lipids have a higher phase transition contributing to the membrane fluid phase. The temperature at the which phase transition can occur is dependent on the composition of the fatty acid tail. Thus, in biology, phase transition is vital for a cell to respond to environmental changes and to regulate a vast number of biological functions occurring at the cell membrane. In prokaryotes, membrane fluidity is critical to survival under varying environmental conditions [44].

### **Membrane organization and lipid rafts**

Since the fluid mosaic model was first proposed by Singer and Nicholson, new experimental evidence has led to modified models of eukaryotic membrane organization.

One such model was proposed by Kia Simons and Elina Ikonen in 1997 [45] and is referred to the raft hypothesis. According to the raft hypothesis, sphingolipids and cholesterol preferentially associate to form micrometer-sized domain called “lipid rafts”. This interaction creates regions of the membrane that are characterized by order, possessing lipid with saturated fatty acyl tails [46, 47]. These assemblies are dynamic, allowing individual lipids to associate and dissociate independently whenever required. Another important component of the lipid rafts is proteins. Thus, lipids rafts are considered as a principle component of the lateral organization of plasma membrane lipids having functional roles in cell signaling and membrane trafficking [48]. In cell signaling, lipid rafts increase the focal concentration of receptors thereby accelerating the signaling process. In membrane trafficking, lipid rafts function as attachment platform for proteins [45].

The common biochemical feature used to identify lipid rafts is the presence of raft-resident proteins. GPI proteins and flotillins are commonly recovered in membrane fractions with cholesterol and glycosphingolipids. Both these proteins are considered as markers for lipid rafts [45, 48-51]. Lipid rafts are commonly isolated by using non-ionic detergents such as Triton-X. These membrane fractions are termed detergent-resistant membrane (DRM) fractions and are thought to represent lipid rafts *in vivo* [52-54]. It has been widely accepted that cholesterol can dynamically alter the lipid bilayers. Cholesterol inhibits the gel-liquid phase transition and promotes the liquid-ordered (*l<sub>o</sub>*) phase. When cholesterol associates with saturated lipids such as 1,2-dipalmitoyl-sn-glycero-3-phosphocholine (DPPC) and sphingomyelin, lipid rafts are formed. Thus, cholesterol is thought to be essential for the functioning of lipid rafts [55, 56] (Figure 1.2).

Several studies have linked the role of lipid rafts to signal transduction functioning. For example, in tyrosine kinase signaling, enzymes and scaffolds are recruited to specific sites of the plasma membrane which helps in signal enhancement [57]. Another evidence for lipid raft formation is eukaryotes us during immunoglobulin E (IgE) signaling. Fluorescence microscopy have demonstrated the formation of patches of gangliosides and GPI-anchored protein by fluorescence microscopy [58]. T-cell antigen receptor, Ras signaling are other examples that form lipid rafts to streamline the signaling events [59-62].

While studies have shown the existence of lipid rafts, certain obscurities also exist. For examples, the type of detergent used can introduce variation in the type of lipids identified these rafts. Brij96V, Tween 20 and Triton-X are common non-ionic detergents with varying ionic strengths used to isolate lipid rafts [64]. Among them only Triton-X have shown to enrich lipids that are thought to be commonly associated with lipid rafts [65]. Apart from possessing different lipid composition, DRMs isolated by different detergent also enrich different set of proteins. Altogether, different detergents extract DRMs of



varying lipid and protein compositions, thus emphasizing the need to redefine lipid rafts. Interestingly, some studies have shown that detergent treatment induces the formation of ordered regions in a homogenous fluid membrane [66]. Schütz et al., have also shown that the GPI-anchored proteins are not associated with lipid rafts thus, raising serious doubts on the original raft hypothesis [67, 68].

The existence of lipid rafts has traditionally been associated with eukaryotic membranes but studies in a few prokaryotes such as *Bacillus subtilis* have shown that bacteria can form functional membrane microdomains, even with lack of cholesterol. The formation of lipid rafts in prokaryotes can be explained by the presence of sterol analogs such as hopanoids and carotenoids [69]. Absence of polyisoprenoid (sterol) lipids in *B. subtilis* resulted in the loss of activity of KinC, a membrane-associated sensor kinase that triggers biofilm formation [70]. This leads to the hypothesis that prokaryotic sterols may play a role in the formation of membrane microdomains similar to cholesterol in eukaryotes. Flotillin (lipid raft marker) homologs have also been identified in prokaryotes. The activity of flotillin in eukaryotes is critical for the functioning of lipid raft associated cellular processes such as membrane trafficking and cell polarization. Prokaryotic flotillins also organize the membrane into domains enabling protein interactions and oligomerization [71-73]. Interestingly, it was found that the spirochete *Borrelia burgdorferi* does not possess sphingolipids but does possess cholesterol in its membranes which enables the formation of functional membrane microdomain (FMM) [74].

Even though the presence of lipid rafts is not clear, the concept of lateral membrane organization is present in all biological membranes. The property of membrane sub-compartmentalization (rafts) is what makes membranes function efficiently [75]. In order to mediate cellular processes, small regions of the membranes may interact and form large stable lipid rafts by specific protein-protein, protein-lipid and lipid-lipid interactions. Importantly, raft-like regions play a crucial role in membrane functioning by providing strength to the membranes and influencing membrane fluidity [76].

### **Membrane fluidity**

Fluidity is the quality of ease of movement, which indirectly correlates to viscosity [77]. Membrane fluidity is essential for microorganisms that need to adapt to changing environmental conditions. It also serves other functions such as: 1) allowing membrane proteins to rapidly diffuse in the bilayer; 2) allowing membrane protein and lipids to diffuse from the site of synthesis; 3) enabling membrane fusion; and 4) ensuring equal distribution of membrane molecules between daughter cells during cell division [78].

Temperature, lipid head groups, lipid tail length, degree of unsaturation of the lipid tails, and the presence of sterols influence membrane fluidity. The tight and regular packing of

the phospholipid tails makes the membranes more viscous and less fluid [79]. At high temperatures, membranes become fluid and the opposite happens in low temperatures. Cholesterol is an important bidirectional regulator of membrane fluidity [80-82]. At high temperatures, cholesterol can stabilize the membrane and raise its melting point. However, cholesterol can intercalate between the phospholipid tails and prevent them from clustering together at low temperatures. Lipid head groups are also known to influence membrane fluidity. For example, phosphatidylethanolamine (PE) has a smaller head group with conical geometry. Therefore, PE lipids can be tightly packed together and therefore has shown to reduce membrane fluidity [83].

### **Carotenoids- properties and functions**

Sterols are hallmarks of eukaryotic membranes. They are associated with lateral organization of the plasma membranes and have been shown to important various signaling and membrane trafficking events [84]. It has been well known, that cholesterol is not found in prokaryotes but there is increasing evidence of presence of other sterol analogs such as hopanoids and carotenoids, which may possess similar functional attributes similar to cholesterol.

Microorganisms do not have cholesterol but functional and structural analogs such as hopanoids, carotenoids, isoarborinol and other triterpenes are more widespread in distribution. Hopanoids are pentacyclic triterpenoids that contain a hopane backbone and are structurally related to cholesterol. Studies on bacteriohopanetetrol have shown similar structural orientation similar to cholesterol in eukaryotic membranes [85]. Simons et al., have also shown that hopanoids determine order of bacterial outer membranes and deletion of hopanoids leads to defects in energy-dependent multidrug efflux [40]. The properties and functions of carotenoids will be explained in detail below.

The most striking feature of carotenoids is the presence of a conjugated system representing alternating double and single bonds. This conjugated system is responsible for the various properties exhibited by carotenoids. They contain 40 carbon atoms per molecule with variable numbers of hydrogen atoms [86]. The first steps in the formation of carotenoids belongs to the mevalonate pathway [87]. The first C-40 carotenoid phytoene is produced by the condensation of two molecules of C-20 geranylgeranyl diphosphate (GGPP). Desaturation and isomerization of phytoene produces lycopene—a red nonpolar carotenoid. Lycopene is then cyclized to produce  $\beta$ -carotene—another nonpolar carotenoid. Hydroxylation of carotene rings generates zeaxanthin—a yellow polar carotenoid [88]. Carotenoids are lipophilic compounds and, thus, are usually found in the lipid bilayer or cell membranes in prokaryotes. Carotenoids possess several conjugated double bonds, which enables them to form geometrical isomers. For example,

theoretically  $\beta$ -carotene can form 272 isomers whereas  $\alpha$ -carotene can form 512 isomers [89].

Shape, size, and hydrophobicity determine the positioning of carotenoids in the membranes. Nonpolar carotenoids, such as  $\beta$ -carotene, are not bound by any orientation constraints and, thus, lie in the hydrophobic core of the membranes. On the other hand, xanthophylls or polar carotenoids, such as zeaxanthin, can span the lipid bilayer and attach to the opposite sides of the membrane due to the presence of the oxygen moiety in their rings [90]. Thus, structural details define the precise orientation that the carotenoids can adopt within the lipid bilayer. Altogether, carotenoids can further influence membrane fluidity of biomembranes [91].

Carotenoids have several independent biological functions in different organisms. For example, retinal, a carotenoid derivative, acts as a visual pigment in all animals. Apart from visual functions, they also possess antioxidant properties which protect from several diseases, including erythropoietic protoporphyria and age-related macular degeneration [92, 93]. In invertebrates, carotenoids protect the egg from defensive action of proteases. In prokaryotes, carotenoids provide photoprotection and are important components to the photosynthetic apparatus in blue-green algae where they play important roles in light harvesting [94]. They also provide distinct coloration to plants and animals. From an industrial perspective, carotenoids are nutritional components used for prevention of human diseases. Thus, pharmaceutical and nutraceutical industries have invested resources to identify new sources and applications of carotenoid molecules [95] (Figure 1.3).

### **Role of carotenoids in membrane fluidity**

As mentioned previously, carotenoids reside in membranes and, thus, play important roles in membrane reinforcement. Membrane fluidity results in ease of movement, which indirectly correlates to viscosity. Membrane viscosity or fluidity is essential for microorganisms that need to adapt to harsh environmental conditions [96] [78]. Several physiological functions, such as protein/enzyme and lipid insertion and diffusion, regulation of conformational changes in the proteins, and diffusion of small molecules across the membranes, are controlled by fluidity [80] [97]. Changes in temperature, osmolarity, or oxidative stress can cause fluctuations in the fluidity of cell membranes, which, in turn, activates other regulatory reactions that ultimately leads to bacterial acclimation.

Cholesterol is an important modulator of membrane fluidity. In contrast to eukaryotes, prokaryotes lack cholesterol and sphingolipids, which are considered essential for membrane organization. Bacterial hopanoids and carotenoids, however, have structural

similarities to that of eukaryotic sterols (cholesterol) [41]. In *Staphylococcus aureus*, it was shown that carotenoids alter membrane fluidity and, in turn, make the bacteria more susceptible to anti-microbial peptides [98]. Thus, carotenoids are thought to be important modulators of membrane biophysical properties.

Although molecular dynamic studies indicate a role of carotenoids in membrane organization, the experimental evidence is still lacking to determine if the computational results may be extrapolated to natural membrane systems. The biophysical role of carotenoids has not yet been evaluated in bacterial membranes. To understand the role of carotenoids in membrane organization, we aimed to study a plant associated bacteria, *Pantoea* sp. YR343 that possesses the carotenoid zeaxanthin in its membranes.

### **Plant-microbe interaction**

Plant-microbe interactions are essential to the functioning of terrestrial ecosystems. The interactions between plants and microorganisms occur on many different levels and in various ways [99]. Virtually all parts of the plants—from the roots to the leaves—interact with microbes at a certain stage of plant growth. These interactions can be beneficial (e.g., nitrogen fixation) or detrimental (e.g., pathogenesis) [100]. Plants not only provide a sheltered space for the microbes to colonize but also a source of nutrients. In turn, the microbes secrete compounds that benefit plant growth and development and may also defend the plant from other pathogenic microorganisms [101]. Thus, soil microbes shape the plant habitat by enhancing plant productivity and ecosystem function.

The root-rhizosphere interface of *Populus* is a perfect model to study a variety of associations between bacteria and plant host. *Populus* is a genus of deciduous flowering plants commonly found in the northern hemisphere. *Populus* is the first tree genome to be fully sequenced and is, therefore, considered a model organism for studying woody perennials [102-105]. *Populus* trees have gained attention as a potential bioenergy feedstock for cellulose-derived biofuels. With important features such as fast growth, abundance, and being a keystone species, *Populus* has become an ideal model to study a variety of plant-microbe interactions [106]. Microbes found in the rhizosphere (area surrounding the roots) and endosphere (inside the root) have gained attention due to their role in phytoremediation and, importantly, as plant-growth promoting bacteria [107].

By studying the *Populus* microbiome, we aim to understand the molecular mechanisms responsible for the interactions between microbes and the plant roots. The futuristic goal would be to also study other plant species, which would ultimately help in improving crop yield, plant growth and development, and aid in bioenergy production.

### ***Pantoea* sp. YR343**

*Pantoea* is one of the several classes of bacteria identified from the rhizosphere of *P. deltoides*. The *Pantoea* genus encompasses at least 20 species of gram-negative bacteria. This class consists of yellow-pigmented, rod-shaped, and motile bacteria associated with plants, animals, and humans [108-110]. The first members were recognized to be plant pathogens that cause wilting, galls, and necrosis in agriculturally relevant crops [111]. *P.spetica*, *P. calida*, *P. ananatis* and *P. agglomerans* have been isolated from human wounds, blood and fractures [112]. Some *Pantoea* isolates also produce antimicrobials (BlightBan C9-1) that can help control fire blight of apple and pear trees. Since then, *Pantoea* has also been explored for its antimicrobial production and bioremediation potential [113, 114]. It can also fix atmospheric nitrogen in plant roots under nitrogen-limiting conditions. Most importantly, *Pantoea* is genetically tractable, which makes it an ideal group for exploring its role in plant growth and development [115].

The genus *Pantoea* is comprised of both pathogenic and non-pathogenic microbes. Strains, such as *P. ananatis* and *P. stewartii*, are common pathogens of maize and corn, respectively, whereas other strains, such as *P. agglomerans*, can promote plant growth by enhancing root architecture. A notable study candidate known to promote plant growth is *Pantoea* sp. YR343. *Pantoea* sp. YR343, a gram-negative gamma proteobacterium, is a robust plant root colonizer able to solubilize phosphate, produce biofilms, and secrete the plant phytohormone indole-3 acetic acid (IAA). Moreover, *Pantoea* sp. YR343 is genetically tractable, making it an ideal system for studying the molecular mechanisms that promote plant root colonization.

A characteristic feature of *Pantoea* sp. YR343 is the presence of the lipophilic carotenoid pigment zeaxanthin in its membrane, which gives it a distinct yellow color (fig 5A). The best-known function of carotenoids is its protective role against reactive oxygen species attributed to the conjugated double bond system. However, some carotenoids are also known to span the phospholipid bilayer of the membrane and, thus, are postulated to provide rigidity and promote membrane fluidity. Even though extensive research has shed light on the importance of carotenoids in photosynthesis and as a potent antioxidant, research on membrane biophysical properties in bacterial membranes is lacking.

### **$\Delta$ *crtB*, a carotenoid deficient strain of *Pantoea* sp. YR343**

The distinct yellow color colonies of *Pantoea* sp. YR343 is due to the presence of zeaxanthin, a polar carotenoid in the membrane [115, 116]. The carotenoid biosynthesis pathway has been described in *Pantoea* and includes six enzymes: geranyl geranyl diphosphate synthase CrtE, phytoene synthase CrtB, phytoene desaturase CrtI, lycopene cyclase CrtY,  $\beta$ -carotene hydroxylase CrtZ, and the zeaxanthin glucosyltransferase CrtX

[117, 118] (Figure 1.3A). Phytoene synthase (CrtB) is the first rate-limiting enzyme that converts geranylgeranyl pyrophosphate to phytoene, which is an important precursor for carotenoid production [119]. It has been shown that bacteria that are unable to produce carotenoids are more susceptible to environmental stress factors than their parent (wildtype) strains. To explore other important functions of carotenoids, especially its role in membrane organization, our lab successfully created a mutant strain deficient in phytoene synthase ( $\Delta crtB$ ). A clean deletion of the gene phytoene synthase was generated using a homologous recombination technique. As expected, the  $\Delta crtB$  mutant was unable to produce any carotenoids, which was confirmed by studying their spectroscopic signatures [116].

Initial tests revealed that the  $\Delta crtB$  mutant cells were more susceptible to oxidative stress with hydrogen peroxide. Surprisingly—apart from the expected loss of antioxidant potential—other unexpected phenotypes, such as defects in biofilm and pellicle formation, IAA secretion, and reduced root colonization were observed in the  $\Delta crtB$  mutant (Figure 1.4). Ultimately, why does the loss of carotenoids induce various phenotypic defects?

Although molecular dynamic studies indicate a role of carotenoids in membrane organization, the experimental evidence is still lacking to determine if the computational results may be extrapolated to natural membrane systems [120]. Since the structural properties of carotenoids (isoprenoids) resemble those of cholesterol, we hypothesize that the phenotypic defects observed in the  $\Delta crtB$  mutant are due to the changes in both lipid and protein composition, which modulate the biophysical properties of the membrane and influence signaling and transport. We aim to understand the influence of carotenoids on structural and biological properties on cell membranes by looking at the lipidome, proteome, and transcriptome of the mutant strain that lacks the carotenoids. We will compare the results to that of the wildtype strain that has carotenoids in its membranes. With proteomics, we aim to understand if the lack of carotenoids influences membrane protein functioning and localization. Lipidomics will reveal if the membrane lipids compensate for the loss of carotenoids and, in turn, will help us identify the role of carotenoids in membrane fluidity. Finally, we can analyze how the transcriptome changes with absence of carotenoid production with transcriptomics. Membrane biophysical property (fluidity) will also be investigated using atomic force microscopy and fluorescence anisotropy.

To understand how natural systems, differ from artificial system we also aim to use vesicles/liposomes made up of lipids extracted from wildtype and  $\Delta crtB$  cells. Research to understand membrane biophysical properties has been extensively carried out in artificial systems called vesicles. Vesicles are small artificial vesicles possessing one or several bilayers [121]. Thus, vesicles are considered biological models for *in vitro* studies.

Vesicles have also been commonly used to study the effects of carotenoids on membrane phase transition, polarity, anisotropy, and fluidity [122]. Even though vesicles provide insights, it does not accurately represent what happens in living cells. Cells are complex structures that not only possess cell membranes but also other structures such as lipopolysaccharide (LPS) that can change the physiological and structural properties of membranes. To understand the effects of LPS on membrane fluidity, biophysical studies on spheroplasts (cells that lack the outer membranes/LPS) were also carried out.

## References

1. Sezgin, E., et al., The mystery of membrane organization: composition, regulation and roles of lipid rafts. *Nature Reviews Molecular Cell Biology*, 2017. 18(6): p. 361.
2. Vereb, G., et al., Dynamic, yet structured: The cell membrane three decades after the Singer–Nicolson model. *Proceedings of the National Academy of Sciences of the United States of America*, 2003. 100(14): p. 8053-8058.
3. Bernardino de la Serna, J., et al., There Is No Simple Model of the Plasma Membrane Organization. *Frontiers in Cell and Developmental Biology*, 2016. 4(106).
4. Harrison, R. and G.G. Lunt, Membrane Function, in *Biological Membranes: Their Structure and Function*. 1980, Springer Netherlands: Dordrecht. p. 9-15.
5. Escriba, P.V., et al., Membranes: a meeting point for lipids, proteins and therapies. *J Cell Mol Med*, 2008. 12(3): p. 829-75.
6. Singer, S.J. and G.L. Nicolson, The fluid mosaic model of the structure of cell membranes. *Science*, 1972. 175(4023): p. 720-731.
7. Mouritsen, O. and M. Bloom, Models of lipid-protein interactions in membranes. *Annual review of biophysics and biomolecular structure*, 1993. 22(1): p. 145-171.
8. Chattopadhyay, A., *Membrane Organization and Dynamics*. Vol. 20. 2017: Springer.
9. Harrison, R., *Biological membranes: their structure and function*. 2013: Springer Science & Business Media.
10. Feigenson, G.W., Phase behavior of lipid mixtures. *Nature chemical biology*, 2006. 2(11): p. 560.
11. Bretscher, M.S., Membrane structure: some general principles. *Science*, 1973. 181(4100): p. 622-629.
12. Zambrano, F., S. Fleischer, and B. Fleischer, Lipid composition of the Golgi apparatus of rat kidney and liver in comparison with other subcellular organelles. *Biochimica et Biophysica Acta (BBA)-Lipids and Lipid Metabolism*, 1975. 380(3): p. 357-369.
13. Roelofsen, B., G.V. Meer, and J.A. Opdenkamp, The lipids of red cell membranes: Compositional, structural and functional aspects. *Scandinavian Journal of Clinical and Laboratory Investigation*, 1981. 41(sup156): p. 111-115.
14. Bigay, J. and B. Antony, Curvature, lipid packing, and electrostatics of membrane organelles: defining cellular territories in determining specificity. *Developmental cell*, 2012. 23(5): p. 886-895.
15. Kucerka, N., et al., Curvature effect on the structure of phospholipid bilayers. *Langmuir*, 2007. 23(3): p. 1292-1299.
16. Von Heijne, G., The membrane protein universe: what's out there and why bother? *Journal of internal medicine*, 2007. 261(6): p. 543-557.



17. Von Heijne, G., Membrane protein structure prediction: hydrophobicity analysis and the positive-inside rule. *Journal of molecular biology*, 1992. 225(2): p. 487-494.
18. Kleinschmidt, J.H., Folding of  $\beta$ -barrel membrane proteins in lipid bilayers—Unassisted and assisted folding and insertion. *Biochimica et Biophysica Acta (BBA)-Biomembranes*, 2015. 1848(9): p. 1927-1943.
19. Jung, H.R. and O.N. Jensen, Proteomic analysis of GPI-anchored membrane proteins. *Drug Discovery Today: Technologies*, 2006. 3(3): p. 339-346.
20. Singer, S.J., Some early history of membrane molecular biology. *Annu. Rev. Physiol.*, 2004. 66: p. 1-27.
21. Pollard, T.D., et al., *Cell Biology E-Book*. 2016: Elsevier Health Sciences.
22. Jensen, M.Ø. and O.G. Mouritsen, Lipids do influence protein function—the hydrophobic matching hypothesis revisited. *Biochimica et Biophysica Acta (BBA) - Biomembranes*, 2004. 1666(1): p. 205-226.
23. Martens, C., et al., Lipids modulate the conformational dynamics of a secondary multidrug transporter. *Nature Structural & Molecular Biology*, 2016. 23: p. 744.
24. Iburguren, M., D.J. López, and P.V. Escribá, The effect of natural and synthetic fatty acids on membrane structure, microdomain organization, cellular functions and human health. *Biochimica et Biophysica Acta (BBA)-Biomembranes*, 2014. 1838(6): p. 1518-1528.
25. Lee, A.G., *Lipid–protein interactions*. 2011, Portland Press Limited.
26. Shadiac, N., et al., Close allies in membrane protein research: Cell-free synthesis and nanotechnology. *Molecular membrane biology*, 2013. 30(3): p. 229-245.
27. Ariöz, C., *Exploring the Interplay of Lipids and Membrane Proteins*. 2014.
28. Bastiaanse, E.L., K.M. Höld, and A. Van der Laarse, The effect of membrane cholesterol content on ion transport processes in plasma membranes. *Cardiovascular research*, 1997. 33(2): p. 272-283.
29. Russell, D.W., Cholesterol biosynthesis and metabolism. *Cardiovascular drugs and therapy*, 1992. 6(2): p. 103-110.
30. Risley, J.M., Cholesterol biosynthesis: Lanosterol to cholesterol. *Journal of chemical education*, 2002. 79(3): p. 377.
31. Lange, Y. and B. Ramos, Analysis of the distribution of cholesterol in the intact cell. *Journal of Biological Chemistry*, 1983. 258(24): p. 15130-15134.
32. Schoonjans, K., et al., Sterols and gene expression: control of affluence. *Biochimica et Biophysica Acta (BBA)-Molecular and Cell Biology of Lipids*, 2000. 1529(1): p. 114-125.
33. Russell, D.W. and K.D. Setchell, Bile acid biosynthesis. *Biochemistry*, 1992. 31(20): p. 4737-4749.
34. Finegold, L.X., *Cholesterol in membrane models*. 1992: CRC Press.

35. Haines, T.H., Do sterols reduce proton and sodium leaks through lipid bilayers? *Progress in lipid research*, 2001. 40(4): p. 299-324.
36. Bloch, K., Cholesterol: evolution of structure and function, in *New Comprehensive Biochemistry*. 1991, Elsevier. p. 363-381.
37. Kusumi, A., et al., Protein-phospholipid-cholesterol interaction in the photolysis of invertebrate rhodopsin. *Biochemistry*, 1983. 22(5): p. 1165-1170.
38. Mercer, E.I., The biosynthesis of ergosterol. *Pesticide Science*, 1984. 15(2): p. 133-155.
39. Griebel, T. and J. Zeier, A role for  $\beta$ -sitosterol to stigmasterol conversion in plant-pathogen interactions. *The Plant Journal*, 2010. 63(2): p. 254-268.
40. Saenz, J.P., et al., Hopanoids as functional analogues of cholesterol in bacterial membranes. *Proc Natl Acad Sci U S A*, 2015. 112(38): p. 11971-6.
41. Ourisson, G., M. Rohmer, and K. Poralla, Prokaryotic hopanoids and other polyterpenoid sterol surrogates. *Annual Reviews in Microbiology*, 1987. 41(1): p. 301-333.
42. Koynova, R. and M. Caffrey, Phases and phase transitions of the phosphatidylcholines. *Biochimica et Biophysica Acta (BBA)-Reviews on Biomembranes*, 1998. 1376(1): p. 91-145.
43. Lee, A., Lipid phase transitions and phase diagrams I. Lipid phase transitions. *Biochimica et Biophysica Acta (BBA)-Reviews on Biomembranes*, 1977. 472(2): p. 237-281.
44. Melchior, D.L., Lipid phase transitions and regulation of membrane fluidity in prokaryotes, in *Current topics in membranes and transport*. 1982, Elsevier. p. 263-316.
45. Simons, K. and E. Ikonen, Functional rafts in cell membranes. *Nature*, 1997. 387(6633): p. 569.
46. Keller, S., et al., Red blood cell lipids form immiscible liquids. *Physical review letters*, 1998. 81(22): p. 5019.
47. Rietveld, A. and K. Simons, The differential miscibility of lipids as the basis for the formation of functional membrane rafts. *Biochimica et Biophysica Acta (BBA)-Reviews on Biomembranes*, 1998. 1376(3): p. 467-479.
48. Jacobson, K., O.G. Mouritsen, and R.G. Anderson, Lipid rafts: at a crossroad between cell biology and physics. *Nature cell biology*, 2007. 9(1): p. 7.
49. Moran, M. and M.C. Miceli, Engagement of GPI-linked CD48 contributes to TCR signals and cytoskeletal reorganization: a role for lipid rafts in T cell activation. *Immunity*, 1998. 9(6): p. 787-796.
50. Brown, D.A. and J.K. Rose, Sorting of GPI-anchored proteins to glycolipid-enriched membrane subdomains during transport to the apical cell surface. *Cell*, 1992. 68(3): p. 533-544.

51. Schulte, T., et al., Reggie-1 and reggie-2, two cell surface proteins expressed by retinal ganglion cells during axon regeneration. *Development*, 1997. 124(2): p. 577-587.
52. Schroeder, R.J., et al., Cholesterol and sphingolipid enhance the Triton X-100 insolubility of glycosylphosphatidylinositol-anchored proteins by promoting the formation of detergent-insoluble ordered membrane domains. *Journal of Biological Chemistry*, 1998. 273(2): p. 1150-1157.
53. Ahmed, S.N., D.A. Brown, and E. London, On the origin of sphingolipid/cholesterol-rich detergent-insoluble cell membranes: physiological concentrations of cholesterol and sphingolipid induce formation of a detergent-insoluble, liquid-ordered lipid phase in model membranes. *Biochemistry*, 1997. 36(36): p. 10944-10953.
54. Brown, D. and E. London, Functions of lipid rafts in biological membranes. *Annual review of cell and developmental biology*, 1998. 14(1): p. 111-136.
55. Thewalt, J.L. and M. Bloom, Phosphatidylcholine: cholesterol phase diagrams. *Biophysical journal*, 1992. 63(4): p. 1176-1181.
56. Ipsen, J.H., et al., Phase equilibria in the phosphatidylcholine-cholesterol system. *Biochimica et Biophysica Acta (BBA)-Biomembranes*, 1987. 905(1): p. 162-172.
57. Varshney, P., V. Yadav, and N. Saini, Lipid rafts in immune signalling: current progress and future perspective. *Immunology*, 2016. 149(1): p. 13-24.
58. Stauffer, T.P. and T. Meyer, Compartmentalized IgE receptor-mediated signal transduction in living cells. *J Cell Biol*, 1997. 139(6): p. 1447-54.
59. Prior, I.A., et al., Direct visualization of Ras proteins in spatially distinct cell surface microdomains. *The Journal of cell biology*, 2003. 160(2): p. 165-170.
60. Janes, P.W., S.C. Ley, and A.I. Magee, Aggregation of lipid rafts accompanies signaling via the T cell antigen receptor. *The Journal of cell biology*, 1999. 147(2): p. 447-461.
61. Schlessinger, J., Cell signaling by receptor tyrosine kinases. *Cell*, 2000. 103(2): p. 211-225.
62. Simons, K. and D. Toomre, Lipid rafts and signal transduction. *Nature reviews Molecular cell biology*, 2000. 1(1): p. 31.
63. Zhong, J., From simple to complex: investigating the effects of lipid composition and phase on the membrane interactions of biomolecules using in situ atomic force microscopy. *Integrative Biology*, 2011. 3(6): p. 632-644.
64. Schuck, S., et al., Resistance of cell membranes to different detergents. *Proceedings of the National Academy of Sciences*, 2003. 100(10): p. 5795-5800.
65. Jakop, U., et al., The solubilisation of boar sperm membranes by different detergents—a microscopic, MALDI-TOF MS, <sup>31</sup>P NMR and PAGE study on membrane lysis, extraction efficiency, lipid and protein composition. *Lipids in health and disease*, 2009. 8(1): p. 49.

66. Shaw, A.S., Lipid rafts: now you see them, now you don't. *Nature immunology*, 2006. 7(11): p. 1139.
67. Sevcsik, E., et al., GPI-anchored proteins do not reside in ordered domains in the live cell plasma membrane. *Nature communications*, 2015. 6: p. 6969.
68. BÜTIKOFER, P., et al., GPI-anchored proteins: now you see'em, now you don't. *The FASEB journal*, 2001. 15(2): p. 545-548.
69. Bramkamp, M. and D. Lopez, Exploring the existence of lipid rafts in bacteria. *Microbiol Mol Biol Rev*, 2015. 79(1): p. 81-100.
70. LeDeaux, J.R. and A.D. Grossman, Isolation and characterization of kinC, a gene that encodes a sensor kinase homologous to the sporulation sensor kinases KinA and KinB in *Bacillus subtilis*. *Journal of bacteriology*, 1995. 177(1): p. 166-175.
71. Lopez, D. and G. Koch, Exploring functional membrane microdomains in bacteria: an overview. *Current opinion in microbiology*, 2017. 36: p. 76-84.
72. Somani, V.K., et al., Identification of novel raft marker protein, FlotP in *Bacillus anthracis*. *Frontiers in microbiology*, 2016. 7: p. 169.
73. Schneider, J., et al., In vivo characterization of the scaffold activity of flotillin on the membrane kinase KinC of *Bacillus subtilis*. *Microbiology*, 2015. 161(9): p. 1871-1887.
74. LaRocca, T.J., et al., Cholesterol lipids of *Borrelia burgdorferi* form lipid rafts and are required for the bactericidal activity of a complement-independent antibody. *Cell host & microbe*, 2010. 8(4): p. 331-342.
75. Simons, K. and J.L. Sampaio, Membrane organization and lipid rafts. *Cold Spring Harbor perspectives in biology*, 2011. 3(10): p. a004697.
76. Lingwood, D. and K. Simons, Lipid rafts as a membrane-organizing principle. *Science*, 2010. 327(5961): p. 46-50.
77. Lands, W.E., Fluidity of membrane lipids, in *Membrane Fluidity*. 1980, Springer. p. 69-73.
78. Los, D.A. and N. Murata, Membrane fluidity and its roles in the perception of environmental signals. *Biochim Biophys Acta*, 2004. 1666(1-2): p. 142-57.
79. Shinitzky, M. and Y. Barenholz, Fluidity parameters of lipid regions determined by fluorescence polarization. *Biochimica et Biophysica Acta (BBA)-Reviews on Biomembranes*, 1978. 515(4): p. 367-394.
80. McMURCHIE, E.J. and J.K. Raison, Membrane lipid fluidity and its effect on the activation energy of membrane-associated enzymes. *Biochimica et Biophysica Acta (BBA)-Biomembranes*, 1979. 554(2): p. 364-374.
81. Chen, Q., et al., Excess membrane cholesterol alters human gallbladder muscle contractility and membrane fluidity. *Gastroenterology*, 1999. 116(3): p. 678-685.
82. Cho, W.-J., S. Trikha, and A.M. Jeremic, Cholesterol regulates assembly of human islet amyloid polypeptide on model membranes. *Journal of molecular biology*, 2009. 393(3): p. 765-775.

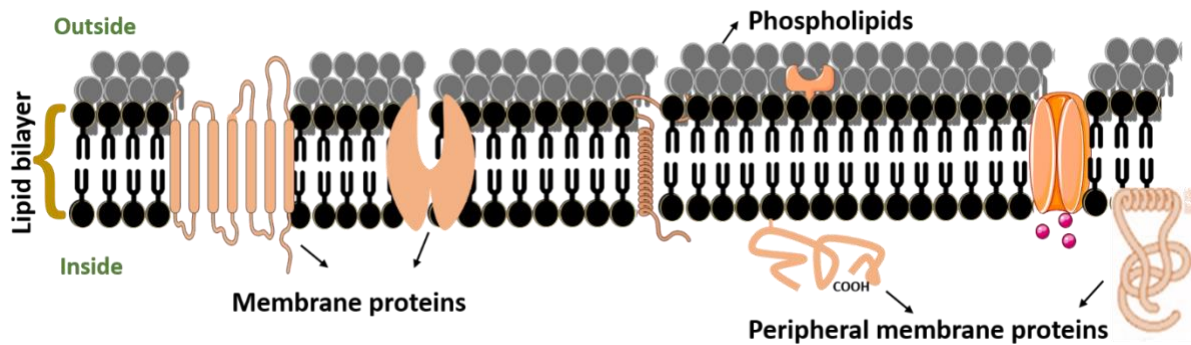
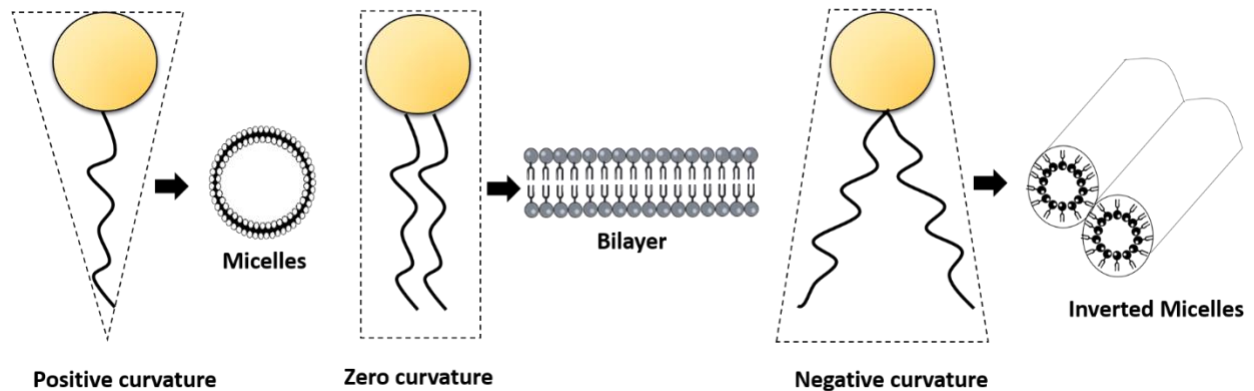
83. Dawaliby, R., et al., Phosphatidylethanolamine Is a Key Regulator of Membrane Fluidity in Eukaryotic Cells. *J Biol Chem*, 2016. 291(7): p. 3658-67.
84. Puri, V., et al., Cholesterol modulates membrane traffic along the endocytic pathway in sphingolipid-storage diseases. *Nature cell biology*, 1999. 1(6): p. 386.
85. Bisseret, P. and M. Rohmer, Bacterial sterol surrogates. Determination of the absolute configuration of bacteriohopanetetrol side chain by hemisynthesis of its diastereoisomers. *The Journal of Organic Chemistry*, 1989. 54(12): p. 2958-2964.
86. Britton, G., Structure and properties of carotenoids in relation to function. *The FASEB Journal*, 1995. 9(15): p. 1551-1558.
87. Martin, V.J., et al., Engineering a mevalonate pathway in *Escherichia coli* for production of terpenoids. *Nature biotechnology*, 2003. 21(7): p. 796.
88. Ruiz-Sola, M.Á. and M. Rodríguez-Concepción, Carotenoid Biosynthesis in *Arabidopsis*: A Colorful Pathway. *The Arabidopsis Book / American Society of Plant Biologists*, 2012. 10: p. e0158.
89. Olson, J.A. and N.I. Krinsky, Introduction: the colorful, fascinating world of the carotenoids: important physiologic modulators. *The FASEB Journal*, 1995. 9(15): p. 1547-1550.
90. Havaux, M., Carotenoids as membrane stabilizer in chloroplasts. *Trends Plant Sci* 3:147-151. Vol. 3. 1998. 147-151.
91. Kirti, K., et al., Colorful World of Microbes: Carotenoids and Their Applications. *Advances in Biology*, 2014. 2014: p. 1-13.
92. Sajilata, M., R. Singhal, and M. Kamat, The carotenoid pigment zeaxanthin—a review. *Comprehensive reviews in food science and food safety*, 2008. 7(1): p. 29-49.
93. Ibrahim, K., T.J. Hassan, and S.N. Jafarey, Plasma vitamin A and carotene in maternal and cord blood. *Asia-Oceania Journal of Obstetrics and Gynaecology*, 1991. 17(2): p. 159-164.
94. Vershinin, A., Biological functions of carotenoids-diversity and evolution. *Biofactors*, 1999. 10(2-3): p. 99-104.
95. Berman, J., et al., Nutritionally important carotenoids as consumer products. *Phytochemistry reviews*, 2015. 14(5): p. 727-743.
96. Chattopadhyay, M. and M. Jagannadham, Maintenance of membrane fluidity in Antarctic bacteria. *Polar biology*, 2001. 24(5): p. 386-388.
97. Lenaz, G., Lipid fluidity and membrane protein dynamics. *Bioscience reports*, 1987. 7(11): p. 823-837.
98. Mishra, N.N., et al., Carotenoid-related alteration of cell membrane fluidity impacts *Staphylococcus aureus* susceptibility to host defense peptides. *Antimicrob Agents Chemother*, 2011. 55(2): p. 526-31.

99. Berg, G., Plant–microbe interactions promoting plant growth and health: perspectives for controlled use of microorganisms in agriculture. *Applied microbiology and biotechnology*, 2009. 84(1): p. 11-18.
100. Stacey, G. and N.T. Keen, *Plant-microbe interactions*. 1996: Springer Science & Business Media.
101. Schirawski, J. and M.H. Perlin, *Plant–Microbe Interaction 2017—The Good, the Bad and the Diverse*. *International Journal of Molecular Sciences*, 2018. 19(5): p. 1374.
102. McKown, A.D., et al., Geographical and environmental gradients shape phenotypic trait variation and genetic structure in *Populus trichocarpa*. *New Phytologist*, 2014. 201(4): p. 1263-1276.
103. Gornall, J.L. and R.D. Guy, Geographic variation in ecophysiological traits of black cottonwood (*Populus trichocarpa*). *Botany*, 2007. 85(12): p. 1202-1213.
104. Tuskan, G.A., et al., The Genome of Black Cottonwood, *Populus trichocarpa* (Torr. & Gray). *Science*, 2006. 313(5793): p. 1596-1604.
105. Tuskan, G., et al. The populus genome: are there discernable difference between the genomes of perennial woody plants and herbaceous annuals? In *acta physiologiae plantarum*. 2004. Springer heidelberg tiergartenstrasse 17, d-69121 heidelberg, germany.
106. Gottel, N.R., et al., Distinct microbial communities within the endosphere and rhizosphere of *Populus deltoides* roots across contrasting soil types. *Applied and environmental microbiology*, 2011. 77(17): p. 5934-5944.
107. Shakya, M., et al., A multifactor analysis of fungal and bacterial community structure in the root microbiome of mature *Populus deltoides* trees. *PLoS One*, 2013. 8(10): p. e76382.
108. Brady, C., et al., Phylogeny and identification of *Pantoea* species associated with plants, humans and the natural environment based on multilocus sequence analysis (MLSA). *Systematic and Applied Microbiology*, 2008. 31(6-8): p. 447-460.
109. Ewing, W. and M. Fife, *Enterobacter agglomerans* (Beijerinck) comb. nov.(the herbicola-lathyri bacteria). *International Journal of Systematic and Evolutionary Microbiology*, 1972. 22(1): p. 4-11.
110. Muraschi, T.F., M. Friend, and D. Bolles, *Erwinia*-like microorganisms isolated from animal and human hosts. *Applied microbiology*, 1965. 13(2): p. 128-131.
111. Johnson, K. and V. Stockwell, Management of fire blight: a case study in microbial ecology. *Annual review of phytopathology*, 1998. 36(1): p. 227-248.
112. Brady, C.L., et al., Emended description of the genus *Pantoea*, description of four species from human clinical samples, *Pantoea septica* sp. nov., *Pantoea eucrina* sp. nov., *Pantoea brenneri* sp. nov. and *Pantoea conspicua* sp. nov., and transfer of *Pectobacterium cypripedii* (Hori 1911) Brenner et al. 1973 emend. Hauben et al.

- 1998 to the genus as *Pantoea cyripedii* comb. nov. International journal of systematic and evolutionary microbiology, 2010. 60(10): p. 2430-2440.
113. Hebishima, T., et al., Oral administration of immunopotentiator from *Pantoea agglomerans* 1 (IP-PA1) improves the survival of B16 melanoma-inoculated model mice. Experimental animals, 2011. 60(2): p. 101-109.
  114. Nakata, K., H. Inagawa, and G.-I. Soma, Lipopolysaccharide IP-PA1 from *Pantoea agglomerans* prevents suppression of macrophage function in stress-induced diseases. Anticancer research, 2011. 31(7): p. 2437-2440.
  115. Walterson, A.M. and J. Stavrinides, *Pantoea*: insights into a highly versatile and diverse genus within the Enterobacteriaceae. FEMS microbiology reviews, 2015. 39(6): p. 968-984.
  116. Bible, A.N., et al., A Carotenoid-Deficient Mutant in *Pantoea* sp. YR343, a Bacteria Isolated from the Rhizosphere of *Populus deltoides*, Is Defective in Root Colonization. Front Microbiol, 2016. 7: p. 491.
  117. Sedkova, N., et al., Diversity of carotenoid synthesis gene clusters from environmental Enterobacteriaceae strains. Applied and environmental microbiology, 2005. 71(12): p. 8141-8146.
  118. To, K.-Y., et al., Analysis of the gene cluster encoding carotenoid biosynthesis in *Erwinia herbicola* Eho13. Microbiology, 1994. 140(2): p. 331-339.
  119. Lindgren, L.O., K.G. Stålberg, and A.-S. Höglund, Seed-specific overexpression of an endogenous *Arabidopsis* phytoene synthase gene results in delayed germination and increased levels of carotenoids, chlorophyll, and abscisic acid. Plant physiology, 2003. 132(2): p. 779-785.
  120. Johnson, Q.R., et al., Effects of carotenoids on lipid bilayers. Phys Chem Chem Phys, 2018. 20(5): p. 3795-3804.
  121. Akbarzadeh, A., et al., Liposome: classification, preparation, and applications. Nanoscale Research Letters, 2013. 8(1): p. 102-102.
  122. Socaciu, C., R. Jessel, and H.A. Diehl, Competitive carotenoid and cholesterol incorporation into liposomes: effects on membrane phase transition, fluidity, polarity and anisotropy. Chemistry and Physics of Lipids, 2000. 106(1): p. 79-88.

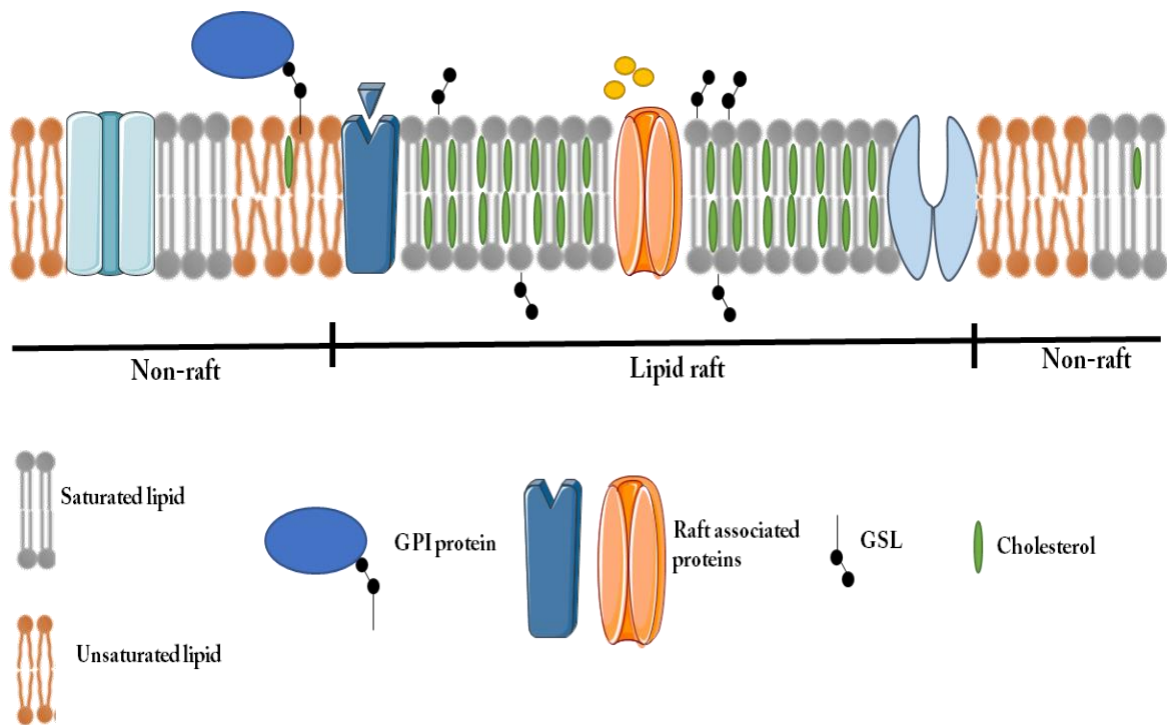
## Appendix



**A****B**

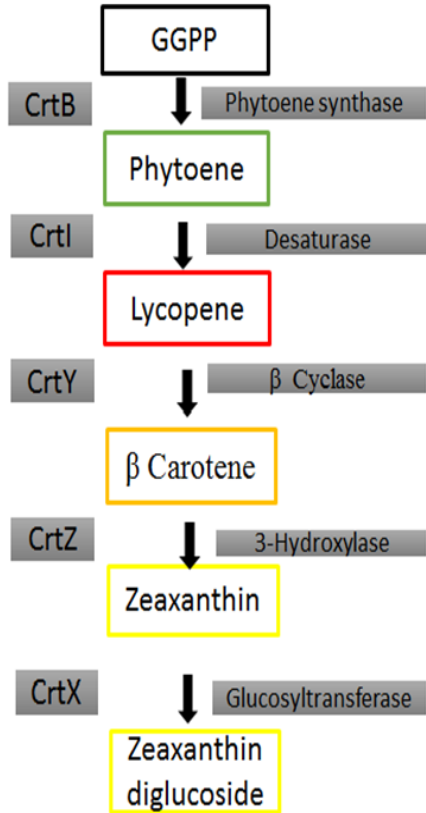
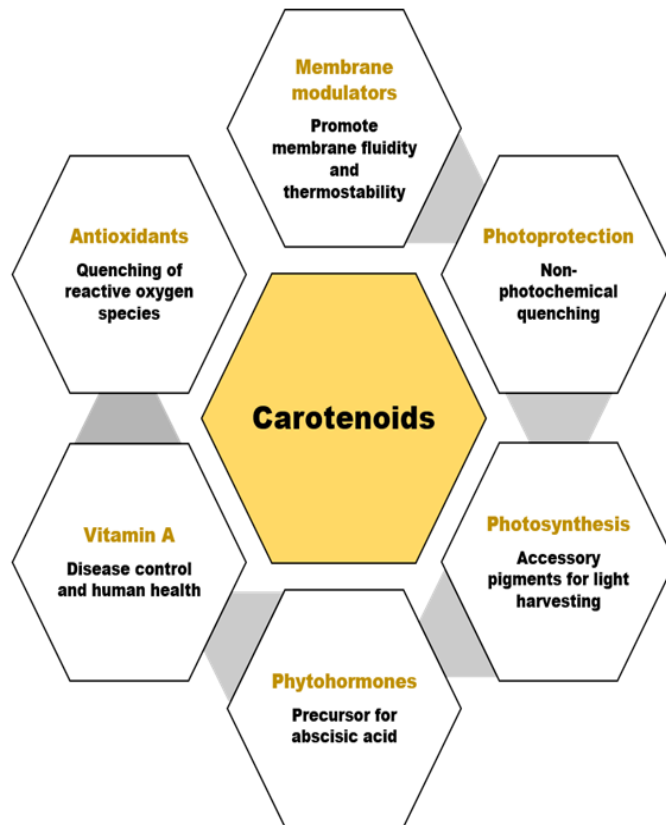
**Figure 1.1: Schematic representation of biological membranes with a heterogenous distribution of phospholipids and proteins**

A. Phospholipid bilayer constitutes the basic structure of all biological membranes. According to the fluid-mosaic model, proteins are embedded in a sea of lipids. Membrane proteins commonly associated with the lipid bilayer. Integral membrane proteins can insert into the membrane with their transmembrane helices, whereas peripheral proteins are commonly found attached to the cytosolic side of the lipid bilayer [adapted from 26]. B. Lipids with positive curvature tend to form micelles and with negative curvature they form inverted micelle structures. However, lipids with no curvature form bilayers when aligned [adapted from 27].



**Figure 1.2: A simplified model of lipid rafts in eukaryotic membranes**

Cholesterol, glycosphingolipids (GSL) and sphingomyelin (SM) are enriched in the outer leaflet of the lipid rafts whereas the inner leaflet contains saturated glycerophospholipids (GPL). The non-raft portion of the membranes contain unsaturated GPL. GPI-anchored proteins are commonly associated with lipid rafts [adapted from 63]

**A****B**

**Figure 1.3: Biosynthesis and functions of carotenoids**

A. Carotenoid biosynthesis has been well studied in *Pantoea*. The biosynthesis starts with the condensation of two molecules of GGPP to phytoene followed by a series of desaturation, cyclization and hydroxylation to produce the major carotenoid in *Pantoea* sp. YR343, Zeaxanthin.  
 B. Biologically important functions of carotenoids.

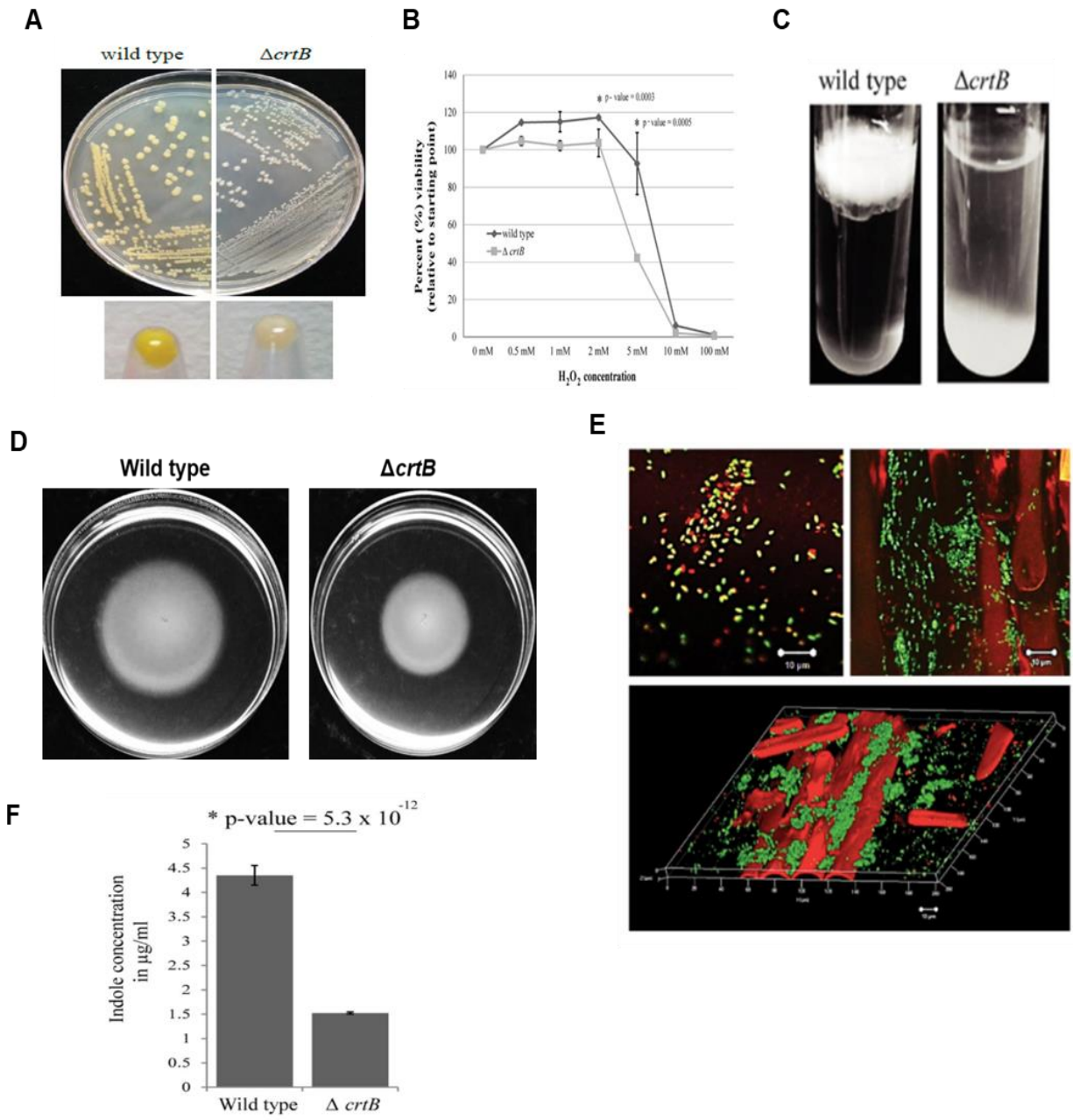


**Figure 1.4: Phenotypic defects associated with  $\Delta crtB$  mutant**

A. The loss of characteristic yellow color in the  $\Delta crtB$  mutant indicating the loss of carotenoid production. B. The  $\Delta crtB$  mutant was more susceptible to oxidative stress when compared to the wildtype. C. The  $\Delta crtB$  mutant could not form intact pellicles at the air-water interface. D. The  $\Delta crtB$  mutant was less motile when compared to the wildtype. E.  $\Delta crtB$  mutant could not colonize the roots as well as the wildtype. F. Reduced levels of IAA secretion in the  $\Delta crtB$  mutant [116].

## CHAPTER-2

**Deletion of carotenoids from membranes of *Pantoea sp.* YR343 results in altered lipid composition and changes in membrane biophysical properties**

## Abstract

Bacterial cell membranes are complex mixtures of lipids and proteins, the combination of which confers biophysical properties to the membrane and allows it to respond to environmental conditions. Carotenoids are sterol analogs that are also important for regulating membrane dynamics. The membrane of *Pantoea* sp. YR343 is characterized by the presence of the carotenoid zeaxanthin, which is best known for its role as an antioxidant. A carotenoid-deficient mutant of the plant-associated microbe *Pantoea* sp. YR343,  $\Delta crtB$ , displays defects in root colonization, reduced secretion of indole-3-acetic acid, and defects in pellicle/biofilm formation. Because these phenotypes may be the result of defects in membrane properties or organization, we examined the role of carotenoids in modulating membrane-related functions in this bacterial isolate. Here we demonstrate that the loss of carotenoids changes the membrane lipid composition in *Pantoea* sp. YR343 by increasing the amount of phosphatidylethanolamine and unsaturated fatty content in the  $\Delta crtB$  mutant membranes. These mutant cells displayed less fluid membranes in comparison to the wild type cells as measured by fluorescence anisotropy of whole cells. Studies with artificial systems, however, have shown that carotenoids impart membrane rigidifying properties. Thus, we examined membrane fluidity using spheroplasts and vesicles composed of lipids extracted from either wildtype or mutant cells. Interestingly, with the removal of the outer membrane and proteins,  $\Delta crtB$  vesicles were more fluid than vesicles made from lipids extracted from wildtype cells. In addition, carotenoids appeared to stabilize membrane fluidity during rapidly changing temperature changes. Taken together, these results suggest that *Pantoea* sp. YR343 compensates for the loss of carotenoids by changing lipid composition, which together with membrane proteins, reduces membrane fluidity. These changes may influence the abundance or function of membrane proteins that are responsible for the physiological defects observed in the  $\Delta crtB$  mutant cells.

## Introduction

Proteins and lipids are the two principal components of biological membranes [1, 2]. The relative proportions and heterogeneous distribution of proteins and lipids have important implications for sensing and responding to changing environments, molecular transport into and out of the cell, and for growth and division [3-5]. In bacteria, cell membranes act as a selective barrier and as sites of energy generation [6]. For example, the cell membranes of photosynthetic prokaryotes, such as cyanobacteria, harbor chromophores that are responsible for converting light energy to chemical energy [7, 8]. Bacterial membranes also contain enzymes, transporters, and scaffolding proteins important for membrane and cell wall biosynthesis, secretion, nutrient uptake, and cell division [9]. Indeed, bacterial membranes are exquisite multifunctional structures and the ability to dynamically alter their composition and organization is key to cellular survival.

In addition to proteins and lipids, eukaryotic membranes also contain cholesterol, a sterol molecule that plays a role in both the function and organization of the plasma membrane [10, 11]. For example, membrane fluidity can be modulated by temperature, length and degree of unsaturation of fatty acid chains, and cholesterol [12]. Cholesterol is a bidirectional regulator of membrane fluidity. At high temperatures, cholesterol increases the melting point of membranes thereby providing stability. At low temperatures, however, cholesterol prevents the clustering of phospholipids by intercalating between the lipid tails [13]. In addition, cholesterol can also regulate protein sorting into specific regions of membranes by thickening and stiffening the bilayers [14]. Furthermore, cholesterol is known to influence the functioning of membrane proteins such as GPCR, either by directly interacting with GPCR or indirectly by changing the membrane properties [13, 15, 16]. Thus, cholesterol can influence functioning of various cells by changing the biophysical properties of membranes.

Unlike eukaryotic cells, bacteria lack cholesterol. However, sterol analogs such as carotenoids and hopanoids are thought to serve similar functions in bacterial membranes [17, 18]. Carotenoids are polyisoprenoid, lipophilic pigments found in the cell membranes of plants, bacteria and algae [19]. Carotenoids are characterized by the presence of a conjugated double bond system with alternate double and single bonds [20]. The localization of carotenoids in the membrane is influenced by their shape, size, and hydrophobicity and provide insights into their potential role as membrane stabilizing agents. For example, nonpolar carotenes, such as  $\beta$ -carotene, are located in the hydrophobic core of the membrane. Conversely, polar xanthophylls, such as lutein and zeaxanthin, can span the lipid bilayer with their polar head groups, thereby anchoring opposite sides of the bilayer and resulting in limited orientational freedom [21].

In photosynthetic organisms, carotenoids play an important role in photosynthesis and photoprotection, whereas, in non-photosynthetic organisms, carotenoids play a role in reducing photooxidative damage [22, 23]. In plants and algae, carotenoids are located in specific pigment-protein complexes, serving as accessory pigments to the photosynthetic apparatus [7]. Carotenoids have been extensively studied for their antioxidant potential, which is mediated by a conjugated double bond system that provides a high reducing potential of carotenoid molecules [21]. In the purple photosynthetic bacterium, *Rhodobacter sphaeroides*, carotenoids have been known to protect cells from photodynamic damage by quenching bacteriochlorophyll a (BChl a), which is responsible for singlet oxygen causing damage [24, 25]. In *Staphylococcus aureus*, on the other hand, it has been shown that carotenoid related membrane alterations influence the susceptibility of the bacteria to host defense peptides [26].

The conjugated double bonds system of carotenoids is not only important for pigment properties but also influences membrane fluidity by increasing its rigidity and mechanical strength [27]. Molecular motion of lipids is important for the dynamic, structural, and functional properties of membranes. Previous studies using nuclear magnetic resonance (NMR), differential scanning calorimetry (DSC), and spin label electron spin paramagnetic resonance (EPR) suggest that carotenoids alter the dynamics of biological membranes, especially the fluidity of membranes, similar to that of cholesterol [28-32]. Fluorescence anisotropy measurements showed that polar carotenoids, such as zeaxanthin and lutein, effect the phase transition behavior of liposomes [33, 34].

In previous work, we constructed a mutant in *Pantoea* sp. YR343 that is defective in carotenoid production [35]. *Pantoea* sp. YR343 is a gram-negative gamma-proteobacteria isolated from the roots of *Populus deltoides* that displays plant-growth promoting properties, such as the production of the phytohormone indole-3-acetic acid and phosphate solubilization [35, 36]. *Pantoea* sp. YR343 has a characteristic yellow color due to the production of the carotenoid, zeaxanthin. Disruption of the gene encoding phytoene synthase (*crtB* PMI39\_03408), which catalyzes the first step in carotenoid biosynthesis, resulted in a mutant that is unable to produce carotenoids and is more susceptible to oxidative damage as expected. The  $\Delta$ *crtB* mutant, however, also displayed defects in plant root colonization, biofilm formation, and in indole-3-acetic acid secretion [35]. One possible explanation is that these defects may be the result of changes in membrane composition and organization due to the loss of carotenoids. Here, we investigate the effect of carotenoids on the biophysical properties of the membrane and its lipid content in *Pantoea* sp. YR343.

## Results

### ***Analysis of lipid head group and fatty acid composition***

To better understand the molecular basis for the phenotypes associated with loss of carotenoids in *Pantoea* sp. YR343, we examined the lipid composition of  $\Delta$ *crtB* mutant cells compared to wildtype. For these experiments, both mutant and wildtype cells were grown to stationary phase in Luria-Bertani (LB) medium and lipids were extracted as described in the Methods. Lipid head group analysis was carried out using Ultra Performance Liquid Chromatography-Mass Spectrometry (UPLC-MS) with external calibration. From these analyses, we found that four groups of phospholipids, including phosphatidylserine (PS), phosphatidylethanolamine (PE), phosphatidylglycerol (PG), and phosphatidic acid (PA), were detected in both wildtype and mutant cells, with PE being the most abundant in both strains (Figure 2.1A). From this analysis, however, we found that  $\Delta$ *crtB* mutant cells contained significantly more PE than wildtype cells. In contrast,



no significant differences in the concentrations of PG, PS, and PA were observed between wildtype and  $\Delta crtB$  mutant cells (Figure 2.1B). Among the detected head groups, we found that PE (32:1), PE (34:2) and PG (32:1) were significantly more abundant in the  $\Delta crtB$  mutant cells, whereas PE (33:1), PE (35:2), and PG (33:1) were significantly less abundant in  $\Delta crtB$  mutant cells (Figure 2.1B). Normalized  $\mu\text{M}$  concentration of all lipids detected are listed in Table 2.1.

Next, we examined the fatty acid profiles of wildtype and  $\Delta crtB$  cells by gas chromatography. A modified Bligh and Dyer method was used to extract lipids from both wildtype and mutant cells grown to stationary phase. Percentage composition of individual fatty acids were detected by Gas-chromatography-fatty acid methyl ester (GC-FAME) analysis. No differences in the saturated fatty acid composition was observed between the wildtype and mutant cells. Among the unsaturated fatty acids, however, C16:1 (palmitoleic acid) and C18:1 (vaccenic acid) were significantly less abundant in the mutant whereas C17:1 and C21:3 were detected in higher amounts (albeit not statistically significant) in the mutant vesicles (Table 2.2, Figure 2.1). Likewise, C19: cyclopropane fatty acid was found to be in higher amounts (but not significant) in the mutant vesicles (Figure 2.1). Percentage composition of total fatty acids detected in wildtype and  $\Delta crtB$  mutant cells are listed in Table 2.2.

### ***Elasticity and fluidity of membranes analyzed by Atomic force microscopy (AFM) and fluorescence anisotropy***

Because we observed differences in lipid profiles between wildtype and  $\Delta crtB$  mutant cells lacking carotenoids, we next asked whether these lipid profiles translated into differences in elasticity and membrane fluidity. The elasticity of wildtype and mutant cells grown in LB medium at 28°C or 45°C was measured using atomic force microscopy. Atomic force microscopy revealed that the morphology and topography of wildtype and mutant cells were very similar at both 28°C and at 45°C (Figure 2.3). At 28°C, the cell surface of both the wildtype and  $\Delta crtB$  mutant appeared to be rough, indicative of a stiff cell surface whereas at 45°C, cell topography was smooth indicating that increases in temperature induced a decrease in cell stiffness. Force distance curves were obtained by force volume mapping the surfaces of both wildtype and mutant cells (Figure 2.4A-B). The average Young's modulus for the wildtype and  $\Delta crtB$  mutant cells were  $2.12 \times 10^5$  Pa and  $5.67 \times 10^5$  Pa, respectively (Figure 2.4C). These data suggest that the  $\Delta crtB$  mutant cells were less elastic in comparison to the wildtype cells. Related to this, the  $\Delta crtB$  mutant cells had a wider distribution of Young's modulus values when compared to the wildtype at 28°C (Figure 2.4A). At higher temperatures, the Young's modulus would be expected to decrease as membranes become more fluid under these conditions. Indeed, the average Young's modulus measurement for wildtype and  $\Delta crtB$  mutant cells were  $1.4 \times 10^5$

Pa and  $2.84 \times 10^5$  Pa respectively (Figure 2.4C). The influence of temperature on elasticity was more dramatic in the mutant cells than in wildtype cells, as evidenced by the difference in elasticity values from 28°C to 45°C (Figure 2.4D).

To complement the results from these force measurements, we also performed fluorescence anisotropy using the 1,6-diphenyl-1,3,5-hexatriene (DPH) dye, an independent technique commonly used to determine membrane fluidity in intact cells. DPH polarization was measured at various temperatures between 25°C and 45°C in intact  $\Delta crtB$  mutant cells and compared to wildtype cells (Figure 2.5). The  $crtB$  mutant cells displayed higher polarization values indicating higher membrane rigidity in comparison to the wildtype cells at 25°C. Increasing the temperature from 25°C to 45°C resulted in reduced polarization in both wildtype and mutant cells, which is indicative of an increase in membrane fluidity. The  $\Delta crtB$  mutant cells displayed a linear decline in polarization with increasing temperature across the full range of 25-45°C. In comparison, wild type cells showed a large decrease in polarization upon heating from 28-35°C, but the polarization remained fairly stable upon further heating from 35-45°C (Figure 2.5). Taken together, the  $\Delta crtB$  cells displayed less fluid membranes at physiological temperature (28°C) when compared to the wildtype membranes.

### ***Fluorescence anisotropy measurement of spheroplasts***

The results from AFM and fluorescence anisotropy indicate that the cells lacking carotenoids displayed more rigid membranes than wildtype cells. These cells, however, are complex biological systems and contain other components that may influence these measurements. For this reason, we next examined the fluidity of membranes from wildtype or mutant cells in the absence of the cell wall by preparing spheroplasts. Using antibiotic treatment, filamentous cells of wildtype and  $\Delta crtB$  mutant cells were generated and then treated with lysozyme to form spheroplasts (Figure 2.6A). These spheroplasts from wildtype or mutant cells were then measured using fluorescence anisotropy. In this case, the removal of the outer membranes resulted in similar responses from both wildtype and  $\Delta crtB$  mutant cells (Figure 2.6B).

### ***Fluorescence anisotropy measurements of membrane vesicles***

In order to better understand the effects of carotenoids on lipids alone, we next prepared vesicles made from natural lipids extracted from either *Pantoea* sp. YR343 wildtype or  $\Delta crtB$  mutant cells using the Bligh and Dyer lipid extraction protocol. The resulting multilamellar vesicles were size extruded to 1 $\mu$ m, confirmed by dynamic light scattering (DLS). These results show that the average diameter for wildtype vesicles was 1.22  $\mu$ m and for the  $\Delta crtB$  mutant vesicles was 1.26  $\mu$ m (Figure 2.7A). The average polydispersity

index (PDI) for wildtype and mutant vesicles were 0.247 and 0.373 respectively (Figure 2.7B). We next performed spectral scans of the wildtype and  $\Delta crtB$  mutant vesicles to determine whether carotenoids were extracted during lipid extraction and vesicle generation. As expected, vesicles derived from lipids extracted from wildtype cells showed three peaks at 425 nm, 450 nm and 480 nm, which correspond to the spectra produced by the carotenoid, zeaxanthin (Figure 2.7C). In contrast, vesicles derived from lipids extracted from  $\Delta crtB$  mutant cells lacked these peaks, consistent with the loss of carotenoids described in this mutant (Figure 2.7C; [35]). To determine whether zeaxanthin formed aggregates in the wildtype natural extract vesicles, vesicles were dissolved in ethanol and examined by spectroscopy. These data indicate that zeaxanthin does not aggregate and is found in monomeric entities in the wildtype natural extract vesicles.

Fluorescence anisotropy was then used to examine the fluid properties of vesicles derived from wildtype and mutant extracts. As with whole cells, these experiments were carried out at a range of temperatures (25°C- 45°C) using DPH. Surprisingly, we found that the vesicles derived from  $\Delta crtB$  cells were more fluid than the vesicles derived from wildtype cells at 25°C (Figure 2.8). This result contrasts the fluorescence anisotropy results obtained with whole cells (Figure 2.8) in which  $\Delta crtB$  mutant cells displayed decreased membrane fluidity compared to wildtype cells. As was observed with the whole cell measurements, we found that membrane polarization decreased in a linear fashion with increasing temperature in both wildtype and mutant vesicles, as expected (Figure 2.8).

## Discussion

From the purification of carotene in the early 19th century by Wackenroder as part of his search for antihelminthic treatments [41], to the discovery of xanthophylls and luteins, the importance of carotenoids in plants, bacteria, animals and humans has long been appreciated [42]. For the most part, these studies have emphasized the importance of carotenoids in light harvesting and photoprotection [27, 42-44]. While less well-studied, a role for carotenoids in maintaining the mechanical properties of membranes, similar to cholesterol, was suggested many decades ago [45]. Since then, bacterial carotenoids have been shown to play a role in bacterial photosynthesis [46], the adaption of bacteria to low temperatures [47] [48], and in maintenance of membrane fluidity [49]. Here we have shown that loss of carotenoids in the  $\Delta crtB$  mutant cells leads to changes in membrane lipid composition, as well as changes in the membrane biophysical properties. Furthermore, artificial systems such as vesicles do not exactly mimic in vivo systems, as cells may employ different strategies to compensate for the loss of carotenoids.

Acclimatization to changing environmental conditions requires precise regulation of membrane fluidity [20]. Bacteria regulate the fluidity by modulating their membrane

phospholipids in response to temperature. At lower temperatures, membrane lipid bilayers undergo a reversible change of state from a liquid (fluid)-like state to an ordered (rigid) state. This temperature transition is a function of membrane lipid composition. Apart from lipids and proteins, eukaryotic membranes contain cholesterol, an important sterol that regulates membrane fluidity. This widely studied compound, however, is absent in most prokaryotic membranes. As described in this study, the cell membranes of *Pantoea* sp. YR343 are composed mainly of phospholipids, zeaxanthin, and proteins. Fatty acids are known to change the physical properties of cell membranes [50]. The degree of unsaturation of fatty acyl chains and their length and degree of branching determine the biophysical properties of the membrane. The ability of bacteria to respond to changes in temperature and oxidative stress by decreasing fatty acid chain length or by changing the degree of fatty acid unsaturation has been shown [51]. GC-FAME analysis of intact wildtype and mutant cells revealed differences in unsaturated fatty acid profiles, with palmitoleic acid and vaccenic acid being less abundant in the  $\Delta crtB$  mutant cell membranes. Since unsaturated fatty acids and carotenoids have opposing effects on membrane fluidity, with unsaturated fatty acids promoting fluidity [14] and carotenoids reducing membrane fluidity in model vesicles [20, 28, 52], it is possible that  $\Delta crtB$  mutant cells are compensating for the increase in membrane fluidity associated with the loss of carotenoids by decreasing the levels of palmitoleic acid and vaccenic acid.

It has been established that lipid geometry imparted by the lipid headgroups has a considerable effect on membrane phases [55]. To determine the lipid headgroup distribution between the wildtype and  $\Delta crtB$  mutant cells, we carried out lipidomics. Interestingly, the uncharged lipid PE was significantly more abundant in the  $\Delta crtB$  mutant cells compared to wildtype cells. It is well known that unsaturated PE lipids inherently assume a hexagonal conformation which, in turn, influences membrane curvature, an essential physical parameter required for membrane trafficking, cell division, and for modulating the distribution of membrane proteins. In insect and mammalian cells, it has been shown that the membrane fluidity is not only regulated by sterols but also by the amounts of PE lipid [56]. In bacterial species, PE has been shown to act as a lipid chaperone to help membrane protein folding and also aid in bacterial adhesion to promote the formation of biofilms [57]. Altogether, changes in both lipid head group and tail profile could change membrane organization, which in turn may affect protein localization and function, leading to the observed phenotypic defects in the  $\Delta crtB$  mutant cells.

It is well known that the phospholipid composition of the cell membrane influences membrane dynamics. Fluidity, the inverse of viscosity, is one of the principle attributes essential to homeoviscous adaptation. Previous results using artificial vesicles suggested that the addition of carotenoids to the lipid vesicles enhanced membrane rigidity. Surprisingly, this observation did not translate to the live cells as both fluorescence

anisotropy and AFM measurements indicated that the cells lacking carotenoids were more rigid/less elastic when compared to wildtype at 25°C. This discrepancy may be explained, at least in part, by the complexity of biological cells which contain many components beside lipids. As the temperature increased to 45°C, both wildtype and mutant cells became more fluid. However, the polarization values for wildtype cells remained constant from 35°C to 45°C, while they continued to decrease in mutant cells. This suggests that carotenoids help to stabilize membranes during dynamic environmental changes, which has important implications for cell survival. It has been observed that xanthophyll carotenoids, such as zeaxanthin and violaxanthin, possess thermostabilizing properties in chloroplasts (thylakoid membranes) to reduce lipid peroxidation [58-60]. Thus, the presence of carotenoids is important for protecting lipids from reactive oxygen species and for preventing cellular damage [61].

Vesicles, planar bilayers and lipid monolayers have been the model lipid systems used to understand complex properties of biological membranes to date [62]. While these systems provide valuable information on the physical chemistry of lipids, our data suggest that results from model lipid systems cannot be easily extrapolated to predict cellular behavior [63, 64]. Indeed, we observed that the effect of carotenoids on membrane fluidity was dramatically different depending on whether whole cells, spheroplasts, or natural-extract vesicles were measured, with whole cells and natural-extract vesicles having opposite results. This surprising result points to the importance of membrane proteins, in addition to lipids and carotenoids, for modulating membrane fluidity. Similarly, other studies have also shown that the removal of proteins and other cellular structures can change membrane properties, such as permeability and transition temperature ( $T_m$ ) values [65, 66]. Our current studies are aimed at characterizing the effect of carotenoids on membrane protein distribution and abundance. These studies illustrate both the challenges and importance of studying membrane dynamics in living systems.

## **Materials and methods**

### ***Bacterial strains and growth conditions***

*Pantoea* sp. YR343 wildtype and  $\Delta crtB$  cells were grown in Luria-Bertani medium (per 1 L, 10 g Bacto-tryptone, 10 g NaCl, 5 g yeast extract) at 28°C with shaking to an  $OD_{600}$  of 1 (stationary phase). Cultures were also grown in M9 medium (per 1 L: 6 g  $Na_2HPO_4$ , 3 g  $KH_2PO_4$ , 0.5 g NaCl, and 1 g  $NH_4Cl$ , plus 10 mL each of filter-sterilized 100 mM  $MgSO_4$ , 20% glucose, and 10 mM  $CaCl_2$ ). The  $\Delta crtB$  mutant was constructed as described in [35]. Cell viability was measured using the BacTiter-Glo™ Microbial cell viability assay (Promega) according to manufacturer's recommendations.

### ***Preparation of Pantoea sp. YR343 and $\Delta crtB$ mutant spheroplast***

Spheroplasts were generated by following the protocol described in Huang et al [68]. Briefly, *Pantoea* sp. YR343 wildtype and  $\Delta crtB$  mutant cells were grown overnight in LB medium at 28°C with shaking (250 RPM) to stationary phase. The cultures were then diluted (1:100) in LB medium and incubated in 28°C with shaking (250 RPM) to OD<sub>600</sub> of 0.5-0.7. Then, 0.5 mL of cells were diluted in 5 mL LB medium with carbenicillin (50 µg/mL) and cultures were grown for 2 hours in 28°C with shaking. After the cells reached an average length of ~30 µm in length (confirmed with confocal microscopy), 1 mL of cells were collected by centrifugation at 3000xg for 1 minute. The pellet was gently resuspended in 1 mL 800 mM sucrose. Spheroplasts were formed by adding the reagents in the following order: 30 µL 1 M Tris × HCl (pH 8.0), 5 µL 50 mg/mL lysozyme, 6 µL 5 mg/mL DNase, and 1.5 µL 0.5M EDTA-NaOH (pH 8.0). After 20 min incubation at room temperature, 100 µL of STOP solution (10 mM Tris × HCl at pH 8, 0.7 M sucrose, 20 mM MgCl<sub>2</sub>) was added to stabilize the spheroplasts. Spheroplast formation was confirmed by visualization under a confocal microscope. Spheroplasts were stored in liquid nitrogen for up to 2 weeks.

### ***Generation of natural extract vesicles***

*Pantoea* sp. YR343 wildtype and  $\Delta crtB$  cells were grown to stationary phase in LB medium and 10 mL of culture was harvested by centrifugation. The cells were washed with 1X phosphate buffered saline (PBS) and the pellets were frozen in liquid nitrogen. Gas chromatography-fatty acid methyl ester (GC-FAME) analysis was performed by Microbial ID, Inc. (Newark, DE). To analyze the fatty acid composition of vesicles made from wildtype or  $\Delta crtB$  extracts, lipids were first extracted from cell cultures using modified Bligh and Dyer method [69]. Briefly, wildtype and mutant cells (500 mL) were grown to stationary phase and harvested by centrifugation at 10,000 rpm for 10 min at 4°C. The cells were washed twice with sterile distilled water and resuspended in a final volume of 5 mL sterile water. Next, 18.75 mL of chloroform: methanol (1:2) was added to the cells and vortexed vigorously (2 min/sample). Next, 6.25 mL of chloroform, followed by 6.25 mL of distilled water was added to the mixture. The mixture was allowed to separate for 18 hours with intermittent shaking. After 18 hours, the bottom organic phase was recovered using a Pasteur pipette with positive pressure. The collected organic phase was dried under vacuum in a rotary evaporator followed by overnight drying in a vacuum oven. The dried films were rehydrated with buffer containing 10 mM MOPS, 100 mM NaCl and the final concentration of lipids adjusted to 10 mg/mL. The natural extract vesicles were extruded to 1 µm using a 1 µm membrane filter cutoff (T&T Scientific) and stored in -80°C till further use.

### ***Differential light scattering***

Samples for DLS were diluted to 100  $\mu$ M with buffer containing 10 mM MOPS, 100 mM NaCl and measured with Brookhaven BI-200SM system (Brookhaven Instruments, Holtsville, NY). Measurements were taken for a duration of 6 minutes.

### ***GC-FAME analysis***

100 mg of lipids extracted by modified Bligh and Dyer method were used for FAME extraction. Briefly, 1 mL of 1M HCl/MeOH was added to 100 mg of lipids and vortexed, followed by heating at 85°C for 1 hour. Then, 1 mL of water and 1 mL of hexane were added, and the samples were vortexed and centrifuged at 1600 rpm for 5 min. The upper organic phase was collected for GC-MS analysis. Agilent 7890A gas chromatograph with 7693A automatic liquid sampler, a HP-5 ms capillary column (30 m long  $\times$  0.25 mm inside diameter with a 0.25  $\mu$ m capillary film of 5% phenyl methylsilicone), and a 5975C mass-sensitive detector was used for GC-FAME analysis. 1  $\mu$ L of sample were introduced using splitless injection with an inlet temperature of 270°C with a 15s dwell time. The following program was used for FAME elution: 2 min at 60 °C; 20 °C/min to 170 °C; 5 °C/min to 240 °C; and 30 °C/min to 300 °C for 2 min. ChemStation Enhanced Data Analysis software and the NIST mass spectral database was used for peak assignment, integration, and mass spectral analysis.

### ***Lipidomic analysis***

Lipids were extracted using a modified version of a published protocol [70]. For these studies, 1 mL cell cultures were harvested by centrifugation, washed, and the cell pellet was frozen in liquid nitrogen. Then, the pellet was resuspended in 1 mL extraction buffer (95% EtOH, water, diethyl ether, pyridine, and 4.2N ammonium hydroxide (30:30:10:2:0.36)) and 100  $\mu$ L glass beads were added before vortexing. After vortexing, the sample was extracted for 20 min in a 60 °C water bath, then centrifuged for 10 min at 10,000 rpm. The supernatant was removed and added to a glass vial to dry under N<sub>2</sub>. The extraction was repeated, and the supernatant was added to the same glass vial for drying. The pellet was then extracted with 300  $\mu$ L water-saturated butanol and 150  $\mu$ L water, vortexed, and centrifuged at 10,000 rpm for 2 min. The top butanol phase was removed and placed in the same glass vial for drying. This step was repeated. After drying, the lipid extracts were resuspended in 300  $\mu$ L of 9:1 MeOH: CHCl<sub>3</sub> for mass spectroscopy analysis. Separations were performed using a Kinetex HILIC column (150 mm  $\times$  2.1 mm, 2.6  $\mu$ m) (Phenomenex, Torrance, CA, USA) connected to an Ultimate 3000 autosampler and UHPLC pump and an Exactive benchtop Orbitrap mass spectrometer (Thermo Fisher Scientific, San Jose, CA). Lipid extracts were ionized using an

electrospray ionization (ESI) probe. The UPLC-MS method ran for 35 min at a flow rate of 200  $\mu\text{L}/\text{min}$  with mobile phase A and B consisting of 10 mM aqueous ammonium formate, pH 3- and 10-mM ammonium formate, pH 3 in 93% (v/v) ACN, respectively. The gradient was as follows: 0% A for 1 min; increase to 19% A from 1 to 15 min, increase to 52% A from 15 to 15.1 min, maintain at 52% A from 15.1 to 25 min, decrease to 0% A from 25 to 25.1 min, maintain at 0% A from 25.1 to 35 min. The temperature of the column was maintained at 25°C and the temperature of the autosampler was maintained at 4°C. The same conditions were used for all UPLC-MS experiments. All samples were run with the same ESI settings in positive and negative mode for maximum lipidome coverage. The ESI settings were as follows: spray voltage, 4 kV; heated capillary, 350°C; sheath gas, 25 units; auxiliary gas, 10 units. The mass spectrometer (MS) was calibrated every 48 hours using the standard calibration mixture and protocol from ThermoFisher. MS data was collected with resolution of 140,000k and a scan range of 100-1500 m/z. The UPLC-MS data was evaluated using Maven software [71]. Lipids were identified by exact  $m/z$  values and retention times. Retention times were verified using lipid standards (Avanti Polar Lipids, Alabaster AL) from each class. External calibration curves were used to quantify phospholipid concentrations for phosphatidylserine (PS), phosphatidylethanolamine (PE), phosphatidylglycerol (PG), and phosphatidic acid (PA).

### ***Fluorescence anisotropy***

1,6-Diphenyl-1,3,5-hexatriene (DPH) (Sigma, D208000) was dissolved in dimethyl sulfoxide (DMSO) to a concentration of 750  $\mu\text{M}$ . Cells were grown overnight in LB medium and then diluted to  $\text{OD}_{600}$  of 0.05 in either M9 media or 1X Phosphate Buffered Saline (PBS) in the presence of 7  $\mu\text{M}$  DPH or DMSO as a control. The cells or spheroplasts were then incubated at 28°C for 45 min. After incubation, 100-200  $\mu\text{L}$  of sample was added to Corning™ 96-well solid black plates. Fluorescence anisotropy measurements were carried out in a POLARstar plate reader (BMG labtech) using a 355 nm excitation filter and two identical 430 nm emission filters, positioned 180° apart. Similarly, fluorescence anisotropy measurements for wildtype and  $\Delta crtB$  mutant natural extract vesicles were carried out in a lipid to dye ratio of 500:1. The final concentration of lipids used was 0.2 mg/ml and that of dye was 0.4 nM. Similar to the cells, the liposomes were incubated with the dye for 45 mins at 28°C prior to measurements. Anisotropy (mA units) and polarization (mP units) were calculated using the formulas: Polarization (mP):  $P = \frac{\text{Ch.A} - (\text{Ch.B})}{\text{Ch.A} + (\text{Ch.B})}$  and Anisotropy (mA):  $A = \frac{\text{Ch.A} - (\text{Ch.B})}{\text{Ch.A} + 2(\text{Ch.B})}$ .

### ***Atomic Force Microscopy***

Wildtype and  $\Delta crtB$  cells were grown in LB medium to an  $\text{OD}_{600}$  of 1 and 1 mL of each culture was harvested by centrifugation for 5 min at 5,000 rpm. The cell pellets were



resuspended in 500  $\mu\text{L}$  of sodium acetate buffer (18 mM sodium acetate, 1 mM  $\text{CaCl}_2$ , 1 mM  $\text{MnCl}_2$ , pH 5.2) and 100  $\mu\text{L}$  of each sample was placed on a gelatin coated mica disk for 5 min to dry. Each sample was then imaged in water using a 5500 PicoPlus atomic force microscopy (AFM) operating with the 1.20.2 operating system (Keysight Technologies Inc. Santa Rosa CA). The instrument was operated in contact mode using MLCT probes with spring constants of 0.01 and 0.03 N/m with a tip radius of 10 nm and Poisson ratio of 0.5. For both imaging and elasticity measurements, the applied force was kept at 3-5 nN. The force distance curves were measured with 8 X 8 points, with each point being an average of 3 force curves. These measurements were recorded on 2- $\mu\text{m}^2$  areas on the top of cells for an average of 7 different cells. This data was then converted to elasticity measurements using the Keysight software in PicoPlus 5500 AFM.

### ***Carotenoid incorporation yield***

Vesicles generated from lipids extracted from wildtype and mutant cultures were used to determine the extraction efficiency for carotenoids. 2 mg/mL of lipids were used for quantification. Vesicles were diluted in water and in ethanol: water ratio (1:9, v/v). UV-VIS spectrophotometer measurements were carried out in BioTek Synergy 2 microplate reader in triplicate in the range of 200-600nm with a scan rate of 1 nm/second.

## References

1. Osborn, M., Structure and biosynthesis of the bacterial cell wall. *Annual review of biochemistry*, 1969. 38(1): p. 501-538.
2. Goñi, F.M., The basic structure and dynamics of cell membranes: An update of the Singer–Nicolson model. *Biochimica et Biophysica Acta (BBA) - Biomembranes*, 2014. 1838(6): p. 1467-1476.
3. Salton, M.R., Structure and function of bacterial cell membranes. *Annu Rev Microbiol*, 1967. 21: p. 417-42.
4. Mactiger, N.A. and C.F. Fox, *Biochemistry of bacterial membranes*. *Annu Rev Biochem*, 1973. 42: p. 575-600.
5. Lombard, J., Once upon a time the cell membranes: 175 years of cell boundary research. *Biology Direct*, 2014. 9(1): p. 32.
6. Harold, F., Conservation and transformation of energy by bacterial membranes. *Bacteriological Reviews*, 1972. 36(2): p. 172.
7. Glazer, A.N., Structure and molecular organization of the photosynthetic accessory pigments of cyanobacteria and red algae. *Molecular and cellular biochemistry*, 1977. 18(2-3): p. 125-140.
8. Leverenz, R.L., et al., Structural and functional modularity of the orange carotenoid protein: distinct roles for the N-and C-terminal domains in cyanobacterial photoprotection. *The Plant Cell*, 2014: p. tpc. 113.118588.
9. Remaut, H. and R. Fronzes, *Bacterial Membranes: Structural and Molecular Biology*. 2014: Caister Academic Press.
10. Ikonen, E., Cellular cholesterol trafficking and compartmentalization. *Nature reviews Molecular cell biology*, 2008. 9(2): p. 125.
11. Wustner, D. and K. Solanko, How cholesterol interacts with proteins and lipids during its intracellular transport. *Biochim Biophys Acta*, 2015. 1848(9): p. 1908-26.
12. Los, D.A. and N. Murata, Membrane fluidity and its roles in the perception of environmental signals. *Biochim Biophys Acta*, 2004. 1666(1-2): p. 142-57.
13. de Meyer, F. and B. Smit, Effect of cholesterol on the structure of a phospholipid bilayer. *Proc Natl Acad Sci U S A*, 2009. 106(10): p. 3654-8.
14. Quinn, P.J., The fluidity of cell membranes and its regulation. *Progress in Biophysics and Molecular Biology*, 1981. 38: p. 1-104.
15. Cherezov, V., et al., High-resolution crystal structure of an engineered human  $\beta$ 2-adrenergic G protein–coupled receptor. *science*, 2007. 318(5854): p. 1258-1265.
16. Guixà-González, R., et al., Membrane cholesterol access into a G-protein-coupled receptor. *Nature Communications*, 2017. 8: p. 14505.
17. Saenz, J.P., et al., Hopanoids as functional analogues of cholesterol in bacterial membranes. *Proc Natl Acad Sci U S A*, 2015. 112(38): p. 11971-6.

18. Poger, D. and A.E. Mark, The relative effect of sterols and hopanoids on lipid bilayers: when comparable is not identical. *The Journal of Physical chemistry B*, 2013. 117(50): p. 16129-16140.
19. Alcaíno, J., M. Baeza, and V. Cifuentes, Carotenoid distribution in nature, in *Carotenoids in Nature*. 2016, Springer. p. 3-33.
20. Gruszecki, W.I. and K. Strzalka, Carotenoids as modulators of lipid membrane physical properties. *Biochim Biophys Acta*, 2005. 1740(2): p. 108-15.
21. Kirti, K., et al., *Colorful World of Microbes: Carotenoids and Their Applications*. *Advances in Biology*, 2014. 2014: p. 1-13.
22. Minhas, A.K., et al., A Review on the Assessment of Stress Conditions for Simultaneous Production of Microalgal Lipids and Carotenoids. *Front Microbiol*, 2016. 7: p. 546.
23. Takaichi, S., Carotenoids in algae: distributions, biosyntheses and functions. *Mar Drugs*, 2011. 9(6): p. 1101-18.
24. Glaeser, J. and G. Klug, Photo-oxidative stress in *Rhodobacter sphaeroides*: protective role of carotenoids and expression of selected genes. *Microbiology*, 2005. 151(Pt 6): p. 1927-38.
25. Ziegelhoffer, E.C. and T.J. Donohue, Bacterial responses to photo-oxidative stress. *Nat Rev Microbiol*, 2009. 7(12): p. 856-63.
26. Mishra, N.N., et al., Carotenoid-related alteration of cell membrane fluidity impacts *Staphylococcus aureus* susceptibility to host defense peptides. *Antimicrob Agents Chemother*, 2011. 55(2): p. 526-31.
27. Britton, G., Structure and properties of carotenoids in relation to function. *Faseb j*, 1995. 9(15): p. 1551-8.
28. Kostecka-Gugała, A., D. Latowski, and K. Strzałka, Thermotropic phase behaviour of  $\alpha$ -dipalmitoylphosphatidylcholine multibilayers is influenced to various extents by carotenoids containing different structural features-evidence from differential scanning calorimetry. *Biochimica et Biophysica Acta (BBA)-Biomembranes*, 2003. 1609(2): p. 193-202.
29. Gabrielska, J. and W.I. Gruszecki, Zeaxanthin (dihydroxy- $\beta$ -carotene) but not  $\beta$ -carotene rigidifies lipid membranes: a  $^1\text{H}$ -NMR study of carotenoid-egg phosphatidylcholine liposomes. *Biochimica et Biophysica Acta (BBA)-Biomembranes*, 1996. 1285(2): p. 167-174.
30. Jeżowska, I., et al., Effect of  $\beta$ -carotene on structural and dynamic properties of model phosphatidylcholine membranes. II. A  $^{31}\text{P}$ -NMR and  $^{13}\text{C}$ -NMR study. *Biochimica et Biophysica Acta (BBA)-Biomembranes*, 1994. 1194(1): p. 143-148.
31. Subczynski, W.K., E. Markowska, and J. Siewiewsiuk, Spin-label studies on phosphatidylcholine-polar carotenoid membranes: effects of alkyl-chain length and unsaturation. *Biochimica et Biophysica Acta (BBA)-Biomembranes*, 1993. 1150(2): p. 173-181.

32. Subczynski, W.K., et al., Effects of polar carotenoids on dimyristoylphosphatidylcholine membranes: a spin-label study. *Biochimica et Biophysica Acta (BBA)-Biomembranes*, 1992. 1105(1): p. 97-108.
33. Socaciu, C., R. Jessel, and H.A. Diehl, Competitive carotenoid and cholesterol incorporation into liposomes: effects on membrane phase transition, fluidity, polarity and anisotropy. *Chem Phys Lipids*, 2000. 106(1): p. 79-88.
34. Wisniewska, A., J. Widomska, and W.K. Subczynski, Carotenoid-membrane interactions in liposomes: effect of dipolar, monopolar, and nonpolar carotenoids. *Acta Biochim Pol*, 2006. 53(3): p. 475-84.
35. Bible, A.N., et al., A Carotenoid-Deficient Mutant in *Pantoea* sp. YR343, a Bacteria Isolated from the Rhizosphere of *Populus deltoides*, Is Defective in Root Colonization. *Front Microbiol*, 2016. 7: p. 491.
36. Estenson, K., et al., Characterization of Indole-3-acetic acid biosynthesis and the effects of this phytohormone on the proteome of the plant-associated microbe *Pantoea* sp. YR343. *Journal of proteome research*, 2018. 17(4): p. 1361-1374.
37. Wackenroder, H.W.F., The discovery and early history of carotene. *Bull. Hist. Chem*, 2009. 34(1): p. 33.
38. Krinsky, N.I., Antioxidant functions of carotenoids. *Free Radic Biol Med*, 1989. 7(6): p. 617-35.
39. Gust, D., et al., The Photochemistry of Carotenoids: Some Photosynthetic and Photomedical Aspectsa. *Annals of the New York Academy of Sciences*, 1993. 691(1): p. 32-47.
40. Frank, H.A., et al., *The Photochemistry of Carotenoids*. 1999: Dordrecht : Springer Netherlands.
41. Rohmer, M., P. Bouvier, and G. Ourisson, Molecular evolution of biomembranes: structural equivalents and phylogenetic precursors of sterols. *Proceedings of the National Academy of Sciences*, 1979. 76(2): p. 847-851.
42. Koyama, Y., et al., Singlet Excited States and the Light-Harvesting Function of Carotenoids in Bacterial Photosynthesis. *Photochemistry and photobiology*, 1996. 63(3): p. 243-256.
43. Fong, N., et al., Carotenoid accumulation in the psychrotrophic bacterium *Arthrobacter agilis* in response to thermal and salt stress. *Applied microbiology and biotechnology*, 2001. 56(5-6): p. 750-756.
44. Chintalapati, S., M.D. Kiran, and S. Shivaji, Role of membrane lipid fatty acids in cold adaptation. *Cell Mol Biol (Noisy-le-grand)*, 2004. 50(5): p. 631-42.
45. Chattopadhyay, M. and M. Jagannadham, Maintenance of membrane fluidity in Antarctic bacteria. *Polar biology*, 2001. 24(5): p. 386-388.
46. Yang, X., et al., Effects of fatty acid unsaturation numbers on membrane fluidity and  $\alpha$ -secretase-dependent amyloid precursor protein processing. *Neurochemistry international*, 2011. 58(3): p. 321-329.

47. Guerzoni, M.E., R. Lanciotti, and P.S. Cocconcelli, Alteration in cellular fatty acid composition as a response to salt, acid, oxidative and thermal stresses in *Lactobacillus helveticus*. *Microbiology*, 2001. 147(Pt 8): p. 2255-64.
48. Gabrielska, J. and W.I. Gruszecki, Zeaxanthin (dihydroxy- $\beta$ -carotene) but not  $\beta$ -carotene rigidities lipid membranes: A  $^1\text{H-NMR}$  study of carotenoid-egg phosphatidylcholine liposomes. *Biochimica et Biophysica Acta - Biomembranes*, 1996. 1285(2): p. 167-174.
49. Ernst, R., C.S. Ejsing, and B. Antonny, Homeoviscous Adaptation and the Regulation of Membrane Lipids. *Journal of Molecular Biology*, 2016. 428(24, Part A): p. 4776-4791.
50. Tiwari, K.B., C. Gatto, and B.J. Wilkinson, Interrelationships between Fatty Acid Composition, Staphyloxanthin Content, Fluidity, and Carbon Flow in the *Staphylococcus aureus* Membrane. *Molecules*, 2018. 23(5): p. 1201.
51. Mykytczuk, N.C.S., et al., Fluorescence polarization in studies of bacterial cytoplasmic membrane fluidity under environmental stress. *Progress in Biophysics and Molecular Biology*, 2007. 95(1): p. 60-82.
52. Dawaliby, R., et al., Phosphatidylethanolamine Is a Key Regulator of Membrane Fluidity in Eukaryotic Cells. *J Biol Chem*, 2016. 291(7): p. 3658-67.
53. Yu, C., et al., Phosphatidylethanolamine Deficiency Impairs *Escherichia coli* Adhesion by Downregulating Lipopolysaccharide Synthesis, Which is Reversible by High Galactose/Lactose Cultivation. *Cell Commun Adhes*, 2017. 23(1): p. 1-10.
54. Havaux, M., Carotenoids as membrane stabilizer in chloroplasts. *Trends Plant Sci* 3:147-151. Vol. 3. 1998. 147-151.
55. Tardy, F. and M. Havaux, Thylakoid membrane fluidity and thermostability during the operation of the xanthophyll cycle in higher-plant chloroplasts. *Biochimica et Biophysica Acta (BBA)-Biomembranes*, 1997. 1330(2): p. 179-193.
56. Havaux, M., et al., Thylakoid membrane stability to heat stress studied by flash spectroscopic measurements of the electrochromic shift in intact potato leaves: influence of the xanthophyll content. *Plant, Cell & Environment*, 1996. 19(12): p. 1359-1368.
57. McNulty, H.P., et al., Differential effects of carotenoids on lipid peroxidation due to membrane interactions: X-ray diffraction analysis. *Biochimica et Biophysica Acta (BBA)-Biomembranes*, 2007. 1768(1): p. 167-174.
58. Gennis, R.B., *Biomembranes : Molecular Structure and Function*, ed. SpringerLink. 1989: New York, NY : Springer New York : Imprint: Springer.
59. Cullis, P.R. and B. De Kruijff, Lipid polymorphism and the functional roles of lipids in biological membranes. *BBA - Reviews on Biomembranes*, 1979. 559(4): p. 399-420.

60. Cronan Jr, J.E. and E.P. Gelmann, Physical properties of membrane lipids: biological relevance and regulation. *Bacteriological Reviews*, 1975. 39(3): p. 232-256.
61. Reizer, J., N. Grossowicz, and Y. Barenholz, The effect of growth temperature on the thermotropic behavior of the membranes of a thermophilic *Bacillus*. Composition-structure-function relationships. *BBA - Biomembranes*, 1985. 815(2): p. 268-280.
62. Murga, M.L.F., et al., Permeability and Stability Properties of Membranes Formed by Lipids Extracted from *Lactobacillus acidophilus* Grown at Different Temperatures. *Archives of biochemistry and biophysics*, 1999. 364(1): p. 115-121.
63. Mika, J.T., et al., Measuring the viscosity of the *Escherichia coli* plasma membrane using molecular rotors. *Biophysical journal*, 2016. 111(7): p. 1528-1540.
64. Gierasch, L.M. and A. Gershenson, Post-reductionist protein science, or putting Humpty Dumpty back together again. *Nature chemical biology*, 2009. 5(11): p. 774.
65. Rojas, E.R., et al., The outer membrane is an essential load-bearing element in Gram-negative bacteria. *Nature*, 2018. 559(7715): p. 617.
66. Rottem, S. and L. Leive, Effect of variations in lipopolysaccharide on the fluidity of the outer membrane of *Escherichia coli*. *Journal of Biological Chemistry*, 1977. 252(6): p. 2077-2081.
67. Lenaz, G., Lipid fluidity and membrane protein dynamics. *Biosci Rep*, 1987. 7(11): p. 823-37.
68. Sun, Y., T.-L. Sun, and H.W. Huang, Physical properties of *Escherichia coli* spheroplast membranes. *Biophysical journal*, 2014. 107(9): p. 2082-2090.
69. Bligh, E.G. and W.J. Dyer, A rapid method of total lipid extraction and purification. *Can J Biochem Physiol*, 1959. 37(8): p. 911-7.
70. Guan, X.L., et al., Yeast lipid analysis and quantification by mass spectrometry. *Methods Enzymol*, 2010. 470: p. 369-91.
71. Melamud, E., L. Vastag, and J.D. Rabinowitz, Metabolomic analysis and visualization engine for LC-MS data. *Anal Chem*, 2010. 82(23): p. 9818-26.

## Appendix

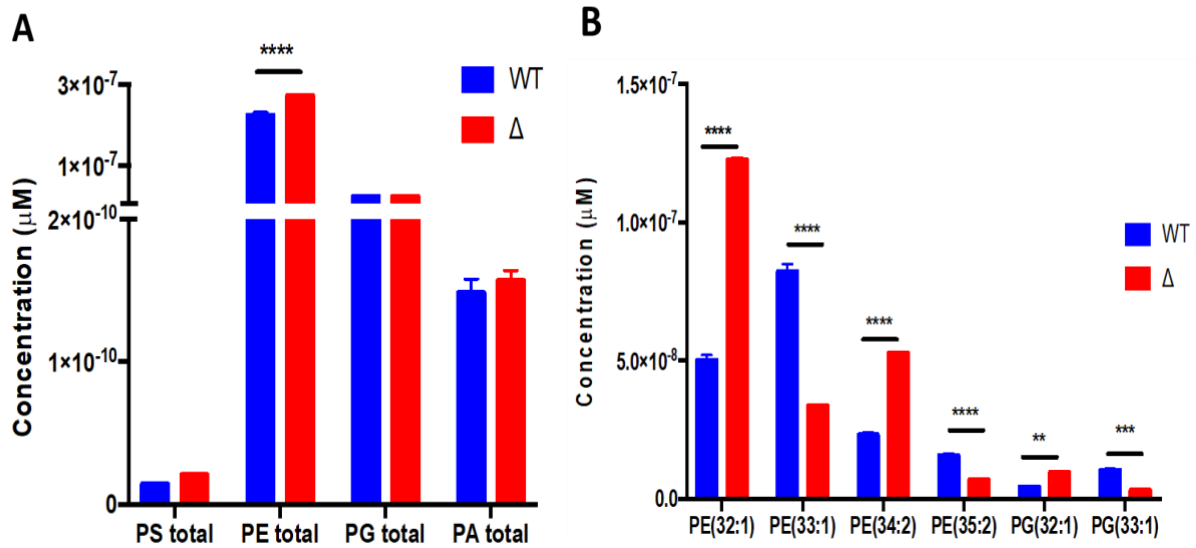


**Figure 2.1: *crtB* deletion causes changes in membrane lipid head group composition.**

Lipidomics analysis using Ultra performance liquid chromatograph mass spectrometry (UPLC-MS) of *Pantoea* sp. YR343 wildtype (blue) and  $\Delta crtB$  cells (red). A. Histogram showing the absolute concentration ( $\mu\text{M}$ ) of total lipids detected by class. PS- phosphatidylserine; PE- phosphatidylethanolamine; PG- phosphatidylglycerol and PA- phosphatidic acid. B. Histogram showing differences in the abundance of statistically significant lipid species between wildtype and mutant cells. Data represent means  $\pm$  SEMs of and representative of two independent experiments with  $n=3/\text{group}$ . Statistical significance was calculated by Two-way ANOVA with student t-test.  $P \leq 0.0001$  (\*\*\*\*),  $P \leq 0.001$  (\*\*\*) ,  $P \leq 0.01$  (\*\*),  $P \leq 0.05$  (\*)



**Table 2.1: Normalized  $\mu\text{M}$  concentration of all lipid head groups identified by lipidomics.**

Lipid head	Normalized $\mu\text{M}$ concentrations					
	YR343-1	YR343-2	YR343-3	$\Delta\text{crtB 1}$	$\Delta\text{crtB 2}$	$\Delta\text{crtB 3}$
PS(34:2)	3.2E-12	1.8E-12	2E-12	4.2E-12	3E-12	2.7E-12
PS(32:1)	1.1E-11	1.3E-11	1.2E-11	1.8E-11	1.8E-11	1.6E-11
PS total	1.4E-11	1.5E-11	1.3E-11	2.2E-11	2.1E-11	1.9E-11
PE(30:0)	2.9E-09	3.2E-09	3E-09	1.8E-09	1.7E-09	1.8E-09
PE(30:1)	1.1E-09	1.2E-09	1.1E-09	2.6E-09	2.6E-09	2.6E-09
PE(28:0)	3.4E-10	3.5E-10	3.2E-10	2.6E-10	2.6E-10	2.8E-10
PE(28:1)	4.3E-11	5.1E-11	4.3E-11	3.6E-10	3.7E-10	3.7E-10
PE(31:1)	2.1E-09	2.3E-09	2E-09	1.4E-09	1.4E-09	1.4E-09
PE(32:0)	2.8E-09	3E-09	2.7E-09	5.7E-10	5.8E-10	5.8E-10
PE(32:1)	4.8E-08	5.4E-08	4.8E-08	1.2E-07	1.2E-07	1.2E-07
PE(32:2)	3.2E-10	3.8E-10	3.2E-10	2.5E-09	2.5E-09	2.5E-09
PE(33:1)	7.9E-08	8.8E-08	8E-08	3.4E-08	3.3E-08	3.4E-08
PE(33:2)	1E-09	1.2E-09	1.1E-09	2.5E-09	2.5E-09	2.6E-09
PE(34:1)	2.8E-08	3.1E-08	2.9E-08	3.2E-08	3.1E-08	3.2E-08
PE(34:2)	2.3E-08	2.5E-08	2.2E-08	5.4E-08	5.2E-08	5.3E-08
PE(35:2)	1.5E-08	1.7E-08	1.6E-08	7.1E-09	6.9E-09	7.2E-09
PE(36:2)	1.1E-08	1.2E-08	1.1E-08	1.4E-08	1.3E-08	1.3E-08
PE(37:2)	9.4E-10	1.1E-09	9.9E-10	1.7E-10	1.9E-10	1.9E-10
PE total	2.2E-07	2.4E-07	2.2E-07	2.8E-07	2.7E-07	2.7E-07
PG(36:0)	3.6E-13	3.1E-13	3E-13	2.6E-13	4E-13	6E-13
PG(30:0)	5E-10	5.3E-10	4.5E-10	1.2E-10	1.1E-10	1.1E-10
PG(30:1)	8E-11	8.7E-11	7.6E-11	9.1E-11	8.9E-11	9.3E-11
PG(31:1)	2.4E-10	2.5E-10	2.1E-10	1E-10	1E-10	9.3E-11
PG(32:1)	4.5E-09	4.8E-09	4.2E-09	1E-08	9.7E-09	9.5E-09
PG(32:2)	1.9E-11	1.9E-11	1.7E-11	1.6E-10	1.6E-10	1.6E-10
PG(33:1)	1.1E-08	1.1E-08	9.7E-09	3.4E-09	3.3E-09	3.2E-09
PG(33:2)	6.1E-11	6.7E-11	5.2E-11	1.5E-10	1.5E-10	1.4E-10
PG(34:1)	4.6E-09	4.8E-09	4.2E-09	4.5E-09	4.4E-09	4.3E-09
PG(34:2)	1.2E-09	1.3E-09	1.2E-09	4.3E-09	4.2E-09	4.2E-09
PG(35:1)	4.6E-10	4.9E-10	4.2E-10	5E-11	5.4E-11	4.7E-11
PG(35:2)	1E-09	1.1E-09	9.2E-10	4.5E-10	4.4E-10	4.3E-10
PG(36:2)	9.2E-10	9.7E-10	8.3E-10	1.7E-09	1.7E-09	1.6E-09
PG(37:2)	1.4E-10	1.4E-10	1.3E-10	1.8E-11	1.9E-11	1.8E-11
PG total	2.4E-08	2.6E-08	2.2E-08	2.5E-08	2.4E-08	2.4E-08
PA(36:1)	1E-11	1.9E-12	9.6E-13	0	0	3.9E-13
PA(32:1)	5.9E-11	7E-11	6.4E-11	7.5E-11	7.5E-11	8E-11
PA(33:1)	2.5E-11	3E-11	2.4E-11	1.9E-12	2.2E-12	3.7E-12
PA(34:1)	2.1E-11	2.8E-11	2.5E-11	7.5E-12	7.8E-12	1.2E-11
PA(34:2)	2.1E-11	2.5E-11	2E-11	5.8E-11	5.9E-11	6.5E-11
PA(36:2)	7.5E-12	1.3E-11	1E-11	6.6E-12	7.6E-12	1E-11
PA total	1.3E-10	1.7E-10	1.4E-10	1.5E-10	1.5E-10	1.7E-10
Total	2.4E-07	2.7E-07	2.4E-07	3E-07	3E-07	3E-07

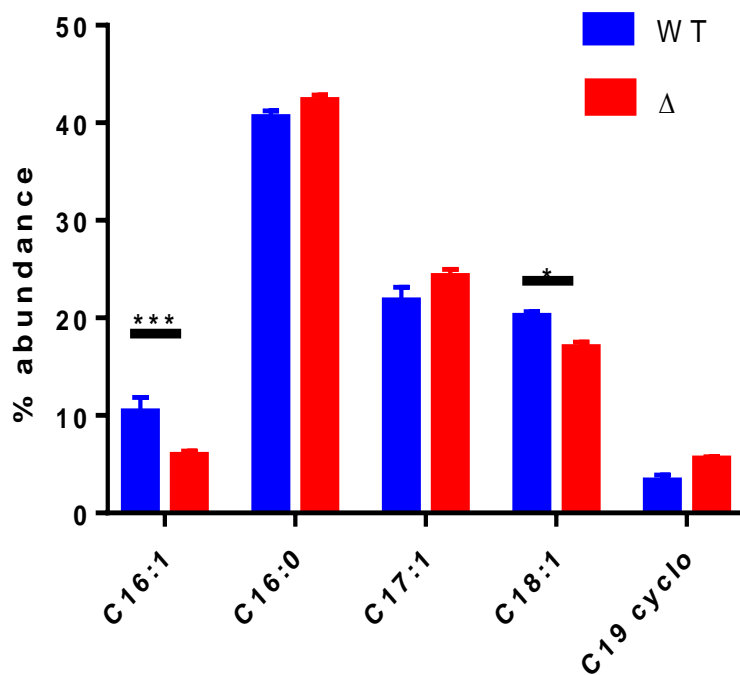


**Figure 2.2: Significant decrease in % abundance of unsaturated fatty acids (C16:1 and C18:1) in the  $\Delta crtB$  mutant cells.**

Gas chromatography mass spectrometry (GC-MS) identification of fatty acid methyl ester (FAME) profiles of *Pantoea* sp. YR343 wildtype and  $\Delta crtB$  mutant cells. Histograms showing difference in the abundance of FAME profiles between *Pantoea* sp. YR343 (blue) and  $\Delta crtB$  mutant cells (red). Data represent means  $\pm$  SEMs of and representative of two independent experiments with n=3/group. Statistical significance was calculated by Two-way ANOVA with student t-test.  $P \leq 0.0001$  (\*\*\*\*),  $P \leq 0.001$  (\*\*\*),  $P \leq 0.01$  (\*\*),  $P \leq 0.05$  (\*)

**Table 2.2: *crtB* deletion causes changes in membrane fatty acid composition.**

GC-FAME profiles of *Pantoea* sp. YR343 and  $\Delta crtB$  cells. Table representing the fatty acid percentage identified in *Pantoea* sp. YR343 and  $\Delta crtB$  cells.

Peak name	<i>Pantoea</i> sp. YR343			$\Delta crtB$		
	%	%	%	%	%	%
<b>C14:0</b>	0.568	0.432	0.26	0.545	0.47	0.478
<b>C16:1</b>	13.332	9.308	8.448	5.017	6.072	6.592
<b>C16:0</b>	41.633	39.248	40.718	43.358	41.358	42.148
<b>C17:1</b>	18.974	23.843	22.344	25.259	24.664	22.78
<b>C17:0</b>	1.372	2.13	1.968	0.58	0.649	0.49
<b>C18:1</b>	20.912	20.338	19.241	15.984	16.796	18.018
<b>C18:0</b>	0.891	0.786	0.897	1.018	0.967	0.925
<b>C19:1</b>	2.048	3.684	4.071	5.768	5.742	5.083
<b>cyclo</b>						
<b>C15:0</b>	0	0.359	0.252	0	0.264	0
<b>C15 Cyclo</b>	0	0.2	0		0.244	0.251
<b>C21:3</b>	0	0	0	1.893	1.837	1.849

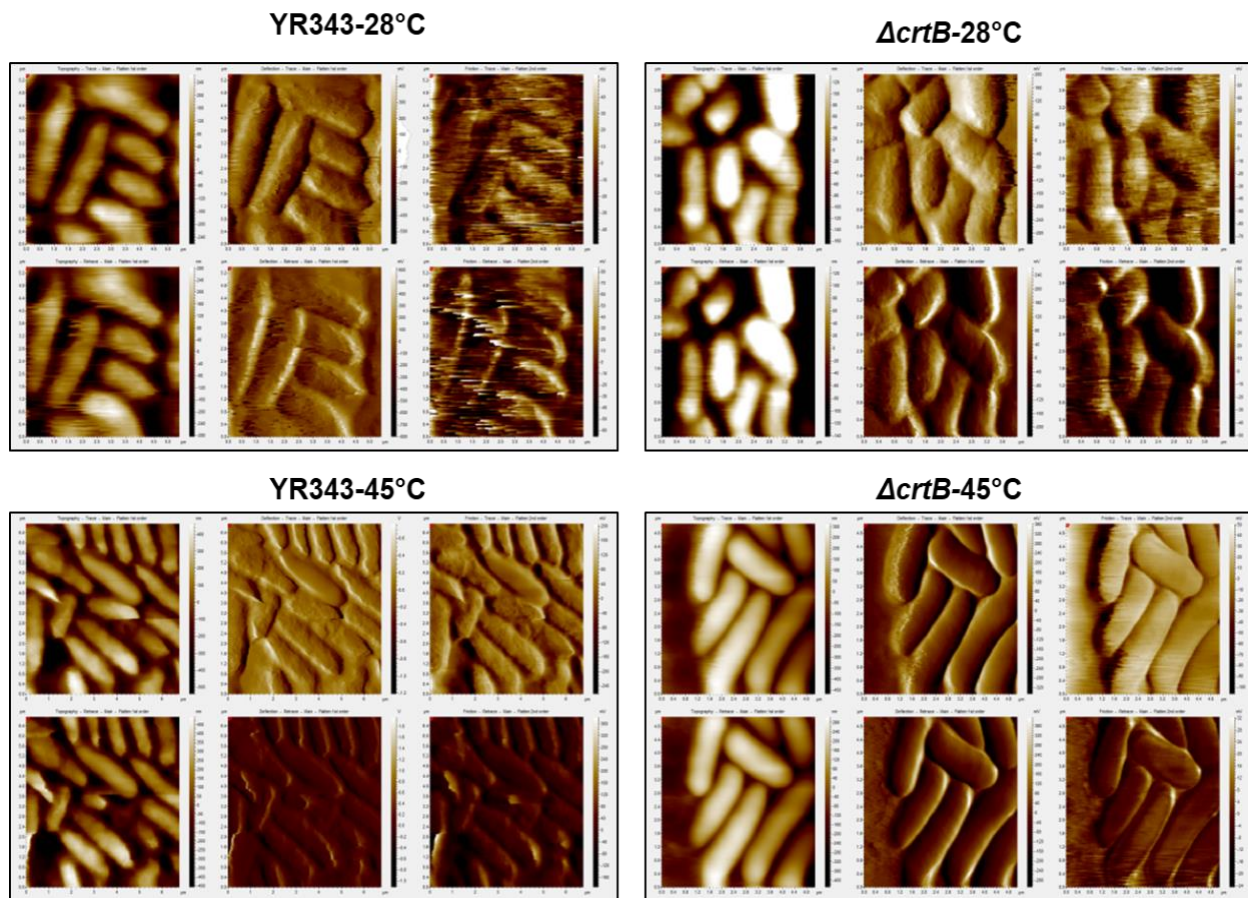


**Figure 2.3: Representative AFM deflection images of *Pantoea* sp. YR343 and  $\Delta crtB$  cells at 28°C and 45°C.**

For imaging with AFM, cells were mounted on mica surface covered in 0.1% 2500 gelatin. Sample was imaged using a 5500 PicoPlus AFM operating with the 1.20.2 operating system. (Keysight Technologies Inc. Santa Rosa CA. The instrument was operated in contact mode using MLCT probes with spring constants of 0.01 and 0.03 N/m with a tip radius of 10 nm and Poisson ratio of 0.5. For both imaging and elasticity measurements the applied force was kept at 3-5 nN. This technique has allowed imaging the cells in a liquid environment (distilled water) to detect changes in surface morphology of cells without disturbing the sample cell surface morphology.

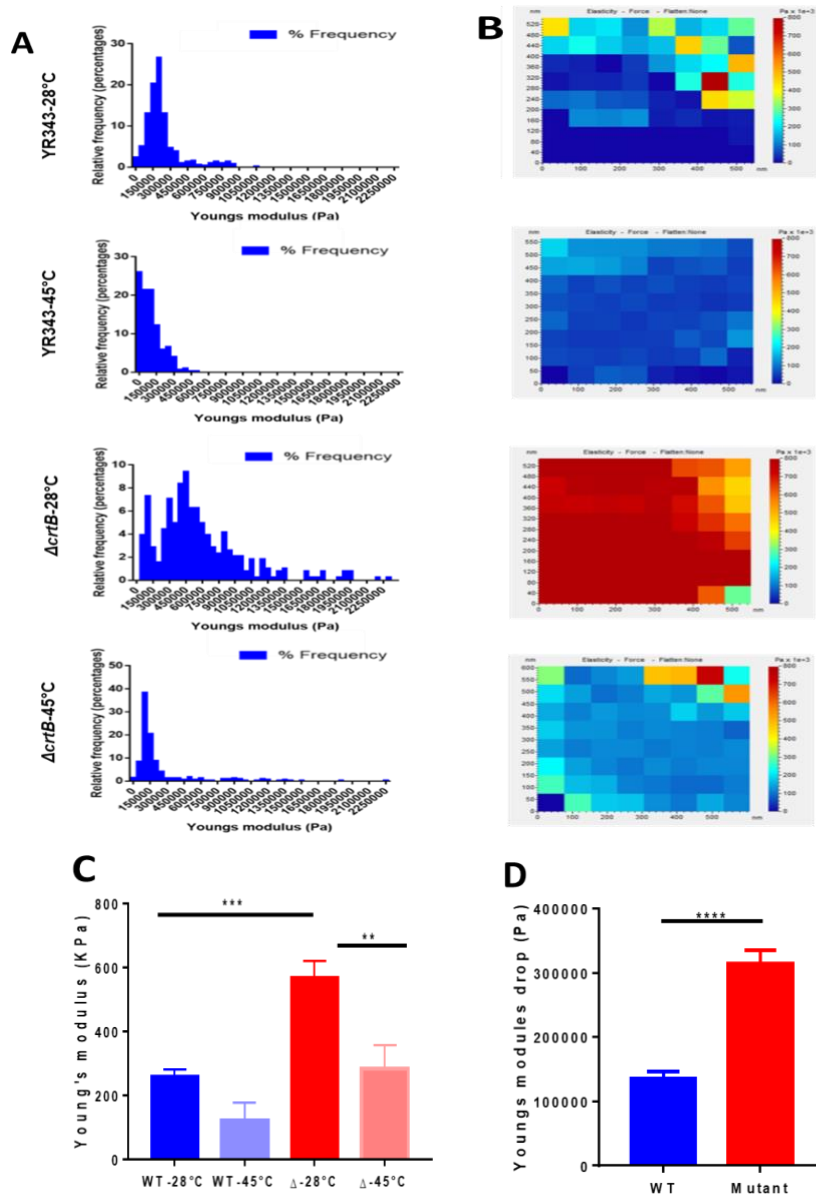


**Figure 2.4: Atomic force microscopy (AFM) reveals less elastic  $\Delta crtB$  mutant cell**

A. Histograms of frequency of AFM mechanical measurements- Young's modulus (in Pa) of *Pantoea sp.* YR343 and  $\Delta crtB$  cells at 28°C and 45°C. B. AFM sample force map results represented as a heat map. Force volume maps of the cell surface were taken by scanning 0.5 \* 0.5  $\mu\text{m}$  area on top of the cell and recording an array of 8 \* 8 points with each point being an average of force curves. C. Histograms showing difference in Young's modulus measurements of *Pantoea sp.* YR343 (blue) and  $\Delta crtB$  (red). D. Difference between Young's modulus at 28°C and 45°C. Data represent means  $\pm$  SEMs of and representative of two independent experiments with n=5/group. Statistical significance was calculated by Two-way ANOVA with student t-test.  $P \leq 0.0001$  (\*\*\*\*),  $P \leq 0.001$ (\*\*\*),  $P \leq 0.01$ (\*\*).

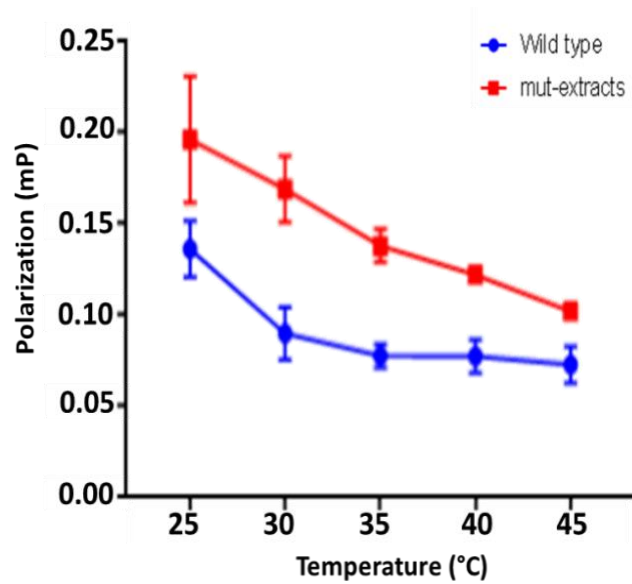


**Figure 2.5: Fluorescence anisotropy with DPH indicates a rigid  $\Delta crtB$  mutant membrane.**

Mean DPH anisotropy of *Pantoea* sp. YR343 wildtype (blue) and  $\Delta crtB$  cells (red) measured in 5°C increments from 25°C to 45°C at a fluorophore concentration of 7 $\mu$ M. Vertical bars denote standard error (SE) of the mean of three replicates.

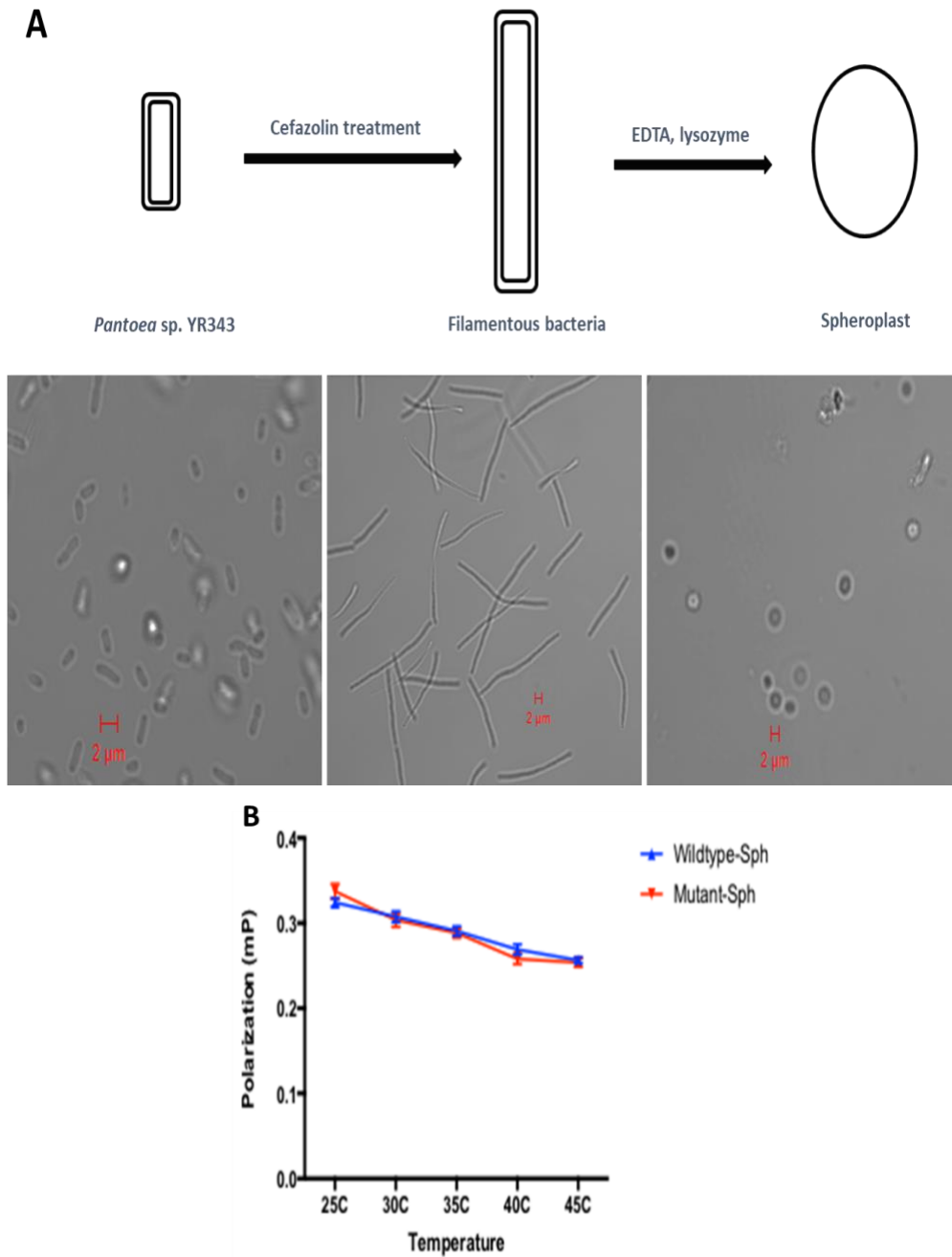


**Figure 2.6: Removal of outer membrane reveals no difference in fluorescence polarization between *Pantoea sp.* YR343 and  $\Delta crtB$  mutant spheroplast.**

A. Schematic and confocal images of spheroplast generation. B. Mean DPH anisotropy of *Pantoea sp.* YR343 and  $\Delta crtB$  spheroplast measured in 5°C increments from 25°C to 45°C at fluorophore concentration of 7μM. Data represent means ± SEMs of and representative of two independent experiments with n=5/group.

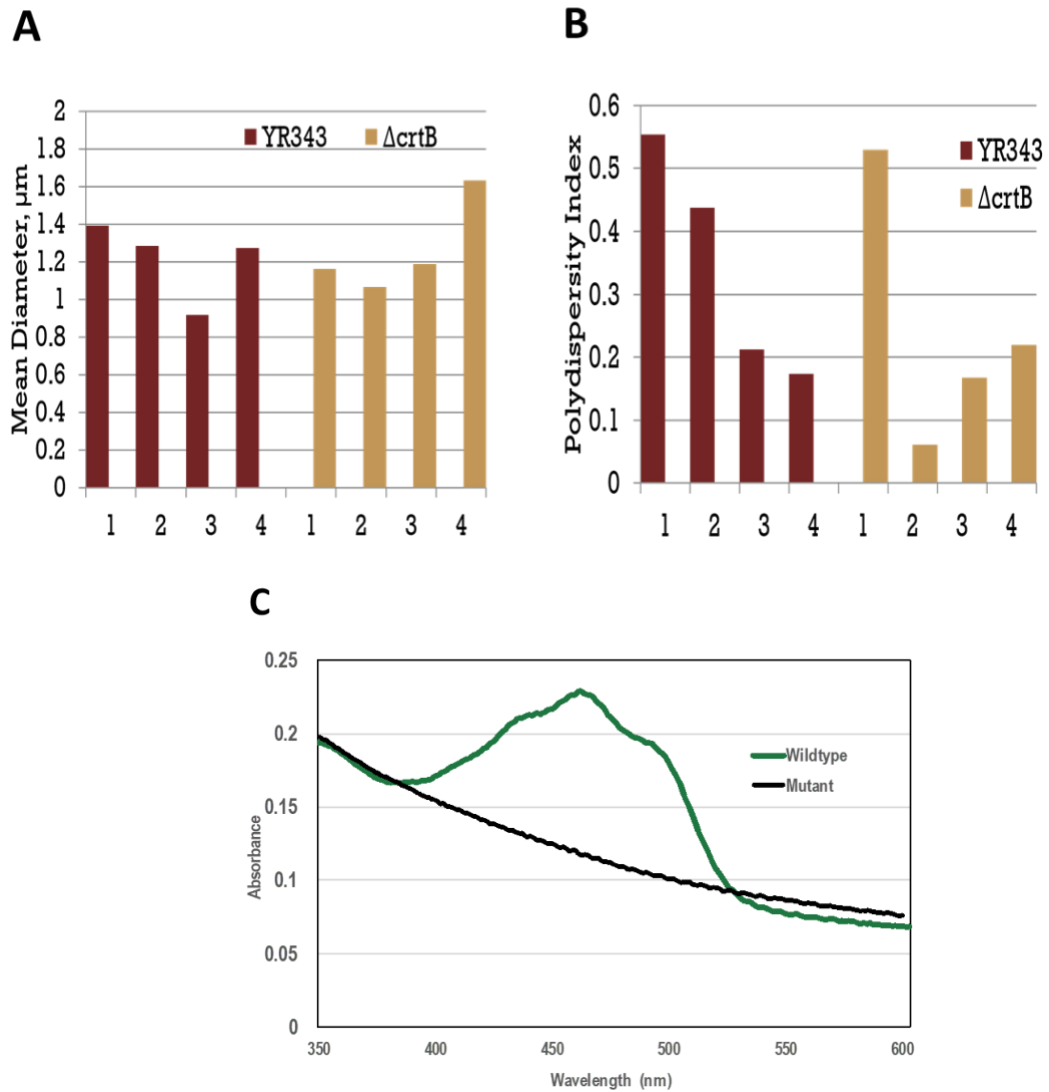


**Figure 2.7: Properties of extruded vesicles of *Pantoea* sp. YR343 and  $\Delta crtB$  mutant**

A. Diameter of extruded vesicles (4 biological replicates) of *Pantoea* sp. YR343 and  $\Delta crtB$  mutant. B. Polydispersity index measured by dynamic light scattering. C. Spectral scans (200-600nm) scans of *Pantoea* sp. YR343 and  $\Delta crtB$  vesicles



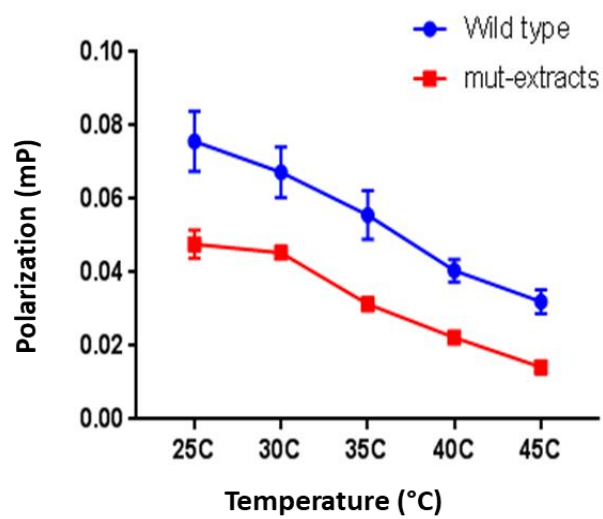


**Figure 2.8: Fluorescence anisotropy with DPH on natural extract vesicles indicates a fluid  $\Delta crtB$  mutant membrane.**

Mean DPH anisotropy of *Pantoea* sp. YR343 and  $\Delta crtB$  vesicles/liposomes measured in 5°C increments from 25°C to 45°C at fluorophore: lipid concentration of 1:500. Data represent means  $\pm$  SEMs of and representative of two independent experiments with n=5/group.

**CHAPTER-3**  
**Loss of carotenoids leads to changes in membrane protein classes in *Pantoea***  
**sp. YR343**

## Abstract

Membrane proteins found both at the inner membrane and outer membrane are involved in several distinct biological processes. They not only act as gatekeepers controlling the transport of molecules in and out of the cell but mainly play major roles in signal transduction, virulence, motility and cell-cell recognition. In eukaryotes, the stability and function of membrane proteins are controlled by certain lipids and sterols such as cholesterol. However, the role and importance of the prokaryotic alternatives of cholesterol such as carotenoids and hopanoids in maintain the integrity of the membrane proteins is yet to be established. We have previously shown that deletion of the carotenoid biosynthesis pathways leads to phenotypic defects such as defects in root colonization, secretion of IAA and inability to form biofilms along with the changes the membrane lipid composition and membrane biophysical properties. Using membrane and whole cell proteomics, we show that the deletion of carotenoid biosynthesis in *Pantoea* results in altered membrane protein distribution. Interestingly, lack of carotenoids impacted several membrane protein classes such as cell membrane biogenesis, cell motility and lipid biogenesis in the  $\Delta crtB$  mutant membranes. Several histidine kinase proteins that play major roles in signal transduction were also downregulated. We also studied different membrane fractions such as detergent resistant and sensitive membrane fractions to understand the role of carotenoids in membrane microdomain formation. Subsequently, the membrane protein composition in the detergent-resistant membrane fractions were significantly different between the wildtype. Thus, we hypothesize that the absence of zeaxanthin in the membranes of  $\Delta crtB$  mutant could not only lead to defects in membrane lipid distribution but also their protein distribution resulting in the altered physiological functions of the bacteria.

## Introduction

Membranes are not only physical boundaries that protect cells from harsh environmental conditions such as fluctuations in temperature, pH, and pressure, they also serve to compartmentalize essential cellular functions and facilitate the exchange of molecules and signals between two spaces [1, 2]. Biological membranes are primarily composed of proteins and lipids that are heterogeneously distributed throughout the membrane [3, 4]. In general, the membranes harbor lipids and membrane proteins that play vital roles in signaling, defense, metabolism, and molecular transport [5]. Thus, membranes serve as a central scaffold for cellular machinery regulating key physiological functions.

Membrane proteins account for 20-30% of the entire genetic complement of a bacterial cell [6, 7]. In gram negative bacteria, membrane proteins are found both at the interface of the cell surface and its environment as well as at the cytoplasmic membrane, where they are involved in several biological processes [8]. Membrane proteins are important for many cellular functions, including cell motility, chemotaxis, cyclic dimeric guanosine

monophosphate (c di-GMP) signaling, virulence, multidrug efflux and outer membrane biogenesis [9-11]. For example, OmpA is an important bacterial membrane protein that helps in adaptation to environmental stress and also serves as a virulence factor causing adherence, invasion and evasion of host defenses [12]. Most cellular processes are fulfilled by a complex network of multiple proteins including both transmembrane and membrane-associated proteins. Protein translocation across the membranes requires the complex interaction of several integral membrane proteins and a peripheral bound ATPase [13]. One well studied pathway in bacteria for protein translocation is the Sec-pathway, an integral membrane protein complex that mediates the transfer between the inner and outer membranes in gram negative bacteria [14]. Thus, membrane proteins with their diverse functions are critical for bacterial survival.

Apart from proteins and lipids, some bacterial membranes possess carotenoids that have several independent biological functions such as photoprotection, imparting coloration to plants, animals and bacteria and as a chromophore in photosynthesis. Carotenoid-protein interactions have been observed in both the plant and animal kingdoms. For example, astaxanthin, a polar carotenoid binds to the muscle protein in salmonid fish and is also known to associate with high-density lipoprotein which aides in the transport of carotenoids. In the photosynthetic apparatus of plants, algae and bacteria, carotenoids are found in the light-harvesting pigment-protein complexes. In bacterial membranes, it has been established that carotenoids reinforce membranes and control membrane thickness [15]. This property is essential for many key molecular processes, such as signal transduction, that involve the movement of proteins in the membrane. Therefore, changes in the structure and dynamics of a membrane due to carotenoids can further affect cellular events at the membrane.

The existence of membrane microdomains has traditionally been associated with eukaryotic membranes; but, studies in a few prokaryotes, such as *Bacillus subtilis*, have shown that bacteria can form functional membrane microdomains, even without cholesterol. The formation of these microdomains in prokaryotes can be explained by the presence of sterol analogs such as hopanoids and carotenoids [16]. Evidence supporting the role of such sterol analogs in microdomain formation was recently shown when the activity of a membrane-associated sensor kinase, KinC, was lost in the absence of poly isoprenoid (sterol) lipids in *B. subtilis* [17]. This leads to the hypothesis that prokaryotic sterols may play a role in the formation of membrane microdomains similar to that of cholesterol in eukaryotes. Flotillin (lipid raft marker) homologs have also been identified in prokaryotes. The activity of flotillin in eukaryotes is critical for the functioning of lipid raft associated cellular processes such as membrane trafficking and cell polarization [18-20]. Prokaryotic flotillins also organize the membrane into domains enabling protein interactions and oligomerization [21-23]. Even though the presence of such membrane

microdomains is not clear, the concept of lateral membrane organization is present in all biological membranes. The property of membrane sub-compartmentalization is what makes membranes function efficiently [24].

We have shown previously that *Pantoea* sp. YR343 is a robust root colonizer of Poplar trees and has several plant-growth promoting properties such as secretion of indole-3-acetic acid, phosphate solubilization and biofilm production [25]. *Pantoea* sp. YR343 produces the polar carotenoid, zeaxanthin [25], and a mutation in the phytoene synthase gene, *crtB*, resulted in a carotenoid deficient strain. The  $\Delta$ *crtB* mutant, as expected, was more susceptible to oxidative damage; but interestingly, it also displayed defects in plant root colonization, biofilm formation, and in indole-3-acetic acid secretion. To understand the roles of carotenoids in membrane organization and functioning, we examined how lipid distribution and membrane fluidity differed between the wild type and  $\Delta$ *crtB* mutant. Studies not only revealed differences in the lipid profile, but also the  $\Delta$ *crtB* mutant cell membranes displayed less fluid (rigid) properties in comparison to the wild type. From this study, it was evident that the loss of carotenoids from the membrane leads to changes in membrane organization and dynamics, in turn influencing functionality of cellular events.

Carotenoids impart structural constraints by restricting membrane thickness, which is crucial for protein insertion and functioning; hence, we hypothesized that physiological functions involving membrane proteins can be influenced by the presence or absence of carotenoids. In order to understand the relationship between the observed phenotypic defects in the  $\Delta$ *crtB* mutant cells and protein abundance and functioning, we used proteomics to investigate the differences in protein abundance, distribution and localization of proteins between the wild type and  $\Delta$ *crtB* mutant cells, and further focusing on membrane proteins and their distribution within membrane microdomains by analyzing detergent-resistant membrane (DRM) fractions, as well as detergent-sensitive membrane (DSM) fractions. The goal of this paper is to perform a comprehensive analysis of how carotenoids affects membrane protein distribution in *Pantoea* sp. YR343 and the carotenoid deficient strain,  $\Delta$ *crtB*.

## Results and Discussion

### ***Identification and quantification of protein abundances in Pantoea sp. YR343 and $\Delta$ crtB whole cells, membrane pellet, DRM and DSM samples***

The objective of this study was to establish a proteomic framework highlighting the similarities and differences between the protein profiles detected and quantified in *Pantoea* sp. YR343 (wildtype) and  $\Delta$ *crtB* cells. Whole cell, membrane pellet (MP), DRM

and DSM samples from *Pantoea* sp. YR343 and  $\Delta crtB$  collected during stationary phase were used for protein quantification. Overall, an average of 2153 and 2046 proteins, were identified for wildtype and  $\Delta crtB$  whole cells, with an average proteome coverage of 41.7% and 43.9% respectively. For the membrane fractions investigated, 1363 (27.8%) and 1270 (25.9%) proteins were identified for wildtype and  $\Delta crtB$  MP samples, 1311 (26.7%) and 1196 (24.4%) proteins were identified for the wildtype and  $\Delta crtB$  DRM samples and 645 (13.1%) and 653 (13.3%) proteins were identified for wildtype and  $\Delta crtB$  DSM samples (Figure 3.1A). A Venn diagram comparing the accession numbers of proteins identified in four different conditions are shown in Figure 3.1C, illustrating the intersections between proteomes. A total of 592 and 545 proteins were found in all the four samples of wildtype and  $\Delta crtB$  mutant samples, respectively.

Principle Component analysis (PCA) (Figure 3.1B) of the intensities measured indicated distinct groupings for proteins isolated from the whole cell, membrane pellet and DSM, in each of the wildtype and  $\Delta crtB$  biological replicates ( $n=3$ ) indicating reproducibility of both replicates and the two different samples (wildtype and  $\Delta crtB$  mutant) and ; whereas, a more scattered distribution of protein groupings was observed for the wildtype and  $\Delta crtB$  DRM samples. Major variance was observed in PC1 (discrete grouping of samples) with DSM samples and in PC2 (major variance) across the remaining factors. Sterols are vital components in the formation of membrane microdomains [21]; therefore, we hypothesized that the absence of carotenoids in the  $\Delta crtB$  mutant could be the main reason for the non-clustering of wildtype and  $\Delta crtB$  mutant DRM samples. We have previously shown that the loss of carotenoids in the  $\Delta crtB$  mutant leads to a decrease in membrane fluidity (Chapter 2). Proper functioning of proteins is regulated by bilayer material properties such as lipid curvature, bilayer thickness and elastic properties provided by sterols [37]. For example, mammalian 5-lipoxygenase (5-LO) binding and activity is regulated by membrane fluidity, binding and activity, thus suggesting that fluidity is a critical parameter for protein insertion and functioning [38]. In *Gloeobacter violaceus*, a cyanobacterium, the carotenoid composition influenced membrane organization by recruiting proteins/enzymes that are required for carotenoid metabolism, thereby displaying a different protein profile when compared to regions lacking carotenoids [39].

As previously mentioned lipids, proteins and sterols are critical for membrane organization and dynamics. Even though cholesterol is important for condensation of lipids in eukaryotes, [40] in prokaryotes carotenoids have also shown to possess similar functionality. Molecular dynamics simulations of zeaxanthin with 1,2-dimyristoyl-sn-glycero-3-phosphocholine (DMPC) bilayers, have shown that carotenoids can also influence the physical properties of bilayers [41]. In comparison to carotenoids, a single molecule of cholesterol can only span one leaflet of the lipid bilayer whereas a C40 carotenoid can span both the leaflets [42]. Cheng et al., have shown that zeaxanthin, through the process

of interdigitation or compression, can trigger the bilayer to become thinner [15]. Membrane thickness, charge distribution and material properties influence protein-lipid interactions [43]. It is well known that for the proper insertion and functioning of membrane proteins, bilayer thickness is a critical factor [44]. In turn, membrane thickness is modulated by phospholipid chain composition and sterol content [45]. Thus, the detection of fewer membrane proteins in the  $\Delta crtB$  mutant could be due to the loss of carotenoid in its membrane, disrupting the ability to control membrane thickness, in turn affecting protein insertion and functioning.

To test the enrichment of membrane proteins in each fraction, we used THMM software in order to identify proteins containing at least  $\geq 1$  transmembrane helix with a maximum number of transmembrane helices detected at 17. Approximately 24% of the proteome of *Pantoea* sp. YR343 consists of proteins with at least one transmembrane helix. Among all the proteins identified, wildtype and  $\Delta crtB$ -DSM samples had approximately 50% of proteins from the genome with transmembrane helix domains and the whole cell, MP and DRM fractions had at least  $>15\%$  of proteins with a transmembrane helix (Figure 3.2). In general, the proportion of membrane proteins to other cellular proteins is low and the limitations of solubility and separation could limit its detection and identification [46]. Interestingly,  $\Delta crtB$ \_DRM had fewer proteins with transmembrane helices when compared to wildtype\_DRM. One reasoning of the detection of few membrane proteins in the DRM fractions could be relatively low abundance of these microdomains. It is well known that microdomains are transient structures and the identification depends on the state of cellular activity [47].

Next, hierarchical clustering was used to assess the differences in expression levels of all proteins identified in the four fractions for wildtype and  $\Delta crtB$  cells (Figure 3.3). All wildtype and  $\Delta crtB$  samples clustered together. Whole cell and DSM samples for wildtype and  $\Delta crtB$  had very similar protein expression levels whereas the expression profile for the MP and DRM samples had interesting expression patterns. To identify significant proteins for each sample set, a p-value cutoff of  $\leq 0.05$  and a fold change (FC) of  $\geq 2$ , was used. In total, 240, 134, 297 and 71 proteins were significantly abundant in the whole cell, MP, DRM and DSM fractions, respectively, between wildtype and  $\Delta crtB$  cells represented as volcano plots (Figure 3.4). Out of these, 188 (in whole cell), 111 (in MP), 211 (in DRM) and 44 (in DSM), were significantly downregulated in the  $\Delta crtB$  mutant in comparison to the wildtype. In total, 21 proteins were found across all four fractions in both wild type and  $\Delta crtB$  cells.

## **Gene Ontology (GO) enrichment analysis**

To gain a deeper understanding of overall changes in protein expression between the wildtype and  $\Delta crtB$  mutant, functional *in silico* classification of proteins was achieved via GO analysis using BLAST2GO tool. Significant ( $p < 0.05$ ) enrichment in the categories of biological processes, cellular component and molecular function along with pairwise comparisons for whole cell, MP, DRM and DSM highlighting GO term enrichment for wildtype and  $\Delta crtB$  are listed in Table 3.1. Further, for each GO term, a functional group was identified, and related proteins were also listed.

Interestingly, in the whole cell pairwise comparisons, proteins belonging to lipid biosynthesis (GO:0008610), lipid metabolism (GO: 0006629) and oligosaccharide metabolism (GO:0009311) were downregulated in the  $\Delta crtB$  mutant. Some interesting proteins include lysophospholipase and the alpha-beta hydrolase superfamily that are important for glycerophospholipid metabolism [48]. Glycerophospholipids serve as the structural component of biological membranes and their alteration can affect physiology and adaptation [49]. Previously, we have reported that the  $\Delta crtB$  mutant possess more phosphatidylethanolamine (PE) head groups and more unsaturated fatty acids when compared to the wild type. This could be attributed due to the down regulation of lysophospholipase in the  $\Delta crtB$  mutant. Importantly, a regulator of protease activity HflC, stomatin/ prohibitin superfamily-ybbK (2511379369) was also down regulated in the  $\Delta crtB$  mutant. YbbK, belongs to the reggie (flotillin) superfamily, that has been widely studied in eukaryotic lipid rafts [50]. Flotillins are common eukaryotic raft marker proteins and recently, a homologous raft marker protein, FlotP, was identified in *Bacillus anthracis* membrane microdomains [22, 51]. Thus, this could mean that the absence of carotenoids in the  $\Delta crtB$  mutant may be responsible for the loss of formation of membrane microdomains, in turn affecting cellular functions such as protein signaling and transport.

Other proteins such as tyrosine kinase (2511379927), cardiolipin synthase (2511380815) and phytoene desaturase (2511381490) were also downregulated in the  $\Delta crtB$  mutant. Notably, four undecaprenyl phosphate proteins (Locus tag- PMI39\_03112, PMI39\_03113, PMI39\_03114, PMI39\_03115) in an operon involved in amino sugar and nucleotide sugar metabolism were downregulated in the  $\Delta crtB$  mutant [52]. Undecaprenyl phosphate is a 55-carbon polyisoprenoid lipid involved in bacterial cell wall biogenesis by functioning as a lipid carrier, trafficking sugar intermediates across the plasma membrane [53]. There is also growing evidence that polyisoprenoids increase membrane fluidity and ion permeability [35, 54-56]. The downregulation of this operon could possibly explain the observed decrease in membrane fluidity in the  $\Delta crtB$  mutant. It is well known that membrane fluidity is crucial for normal physiological functioning of cells such as signaling and transport.



DNA replication (GO:0006260) and regulation of catalytic activity (GO:0050790) were upregulated in the  $\Delta crtB$  mutant whole cell samples. Upregulation of the metabolic process- DNA replication and biological process- regulation of catalytic activity could be a possible compensatory mechanism to maintain DNA fidelity in the  $\Delta crtB$  mutant. Interestingly, two proteins involved in bacterial chemotaxis (PMI39\_02297 and PMI39\_01148) were upregulated in the  $\Delta crtB$  mutant. Chemotaxis is important for several biological processes such as biofilm formation, pathogenicity and survival of bacteria in their environment [57]. Methyl-accepting chemotaxis proteins (MCP) binding to ligands triggers downstream signaling, activating CheA, CheW and CheY proteins, which in turn interact with the flagellar protein FlhM to change the direction of flagellar rotation. Thus, protein involved in chemotaxis are critical in responding appropriately to environmental cues [58]. Upregulation of MCP proteins may be important for the  $\Delta crtB$  mutant to respond to changing concentrations of attractants and repellants in the environment. Interestingly, motility studies indicated that the  $\Delta crtB$  mutant was less motile when compared to the wildtype which could be due to the loss of functionality of one of the several proteins that make up the flagellar apparatus. This could indicate that the  $\Delta crtB$  mutant is compensating for the defects in flagella by upregulating other processes such as chemotaxis.

In the membrane pellet fractions, several proteins with functional significance ( $p \leq 0.05$  and  $FC \geq 2$ ) at the membrane were downregulated in the  $\Delta crtB$  mutant. In particular, proteins belonging to envelope (GO:0030313) and cell outer membrane (GO:0009279) as a part of the cellular component were downregulated in the  $\Delta crtB$  mutant. Similarly, a significant downregulation of several proteins involved in membrane biogenesis in the  $\Delta crtB$  mutant was observed. As carotenoids are an integral component of *Pantoea* sp. YR343 membranes, loss of carotenoids in the  $\Delta crtB$  mutant significantly affects other cellular functions at the membrane. Homeostasis is important for living organisms to maintain internal stability and it includes iron and metal homeostasis, membrane lipid homeostasis and pH homeostasis. Proteins involved in cellular homeostasis were significantly downregulated in the  $\Delta crtB$ \_DSM. For example, TonB (PMI39\_04701), an outer membrane receptor for ferrienterochelin and colicins, important for iron homeostasis was downregulated in  $\Delta crtB$ \_DSM. A *Burkholderia mallei tonB* mutant exhibited over secretion of siderophores and slower growth kinetics highlighting the importance of proteins involved in iron acquisition and metabolism [59].

Interestingly, significant upregulation of proteins belonging to processes involved in cytosol (GO:0005829), ribonucleotide binding (GO:0032553) and carboxylic acid metabolism and biosynthesis (GO:0019752 and GO:0046394) was observed in the  $\Delta crtB$  mutant.

Combining the results from the GO analysis, it can be concluded, in general, that proteins involved in membrane biogenesis, lipid metabolism, amino acids and sugar nucleotide metabolism, and iron homeostasis were significantly downregulated in the  $\Delta crtB$  mutant. Overall, the membrane of the  $\Delta crtB$  mutant is considerably affected by the loss of carotenoids. Membrane changes in turn can affect the insertion and functioning of several proteins leading to the observed phenotypic defects such as motility and biofilm formation, in turn causing defects in root colonization.

### **Functional classification by Cluster of orthologous groups (COGs)**

To identify specific proteins involved in a biological process/ function, COG classification was carried out next. COGs classify proteins on the basis of orthology, reflecting both one-to-many and many-to-many orthologous relationships as well as one-to-one relationships [60]. Among the significant proteins, transcription, carbohydrate transport, and metabolism categories were abundant in wildtype compared to the  $\Delta crtB$  whole cell sample; whereas, proteins belonging to cell wall/membrane/envelope biogenesis were abundant in both MP, DRM and DSM fractions (Figure 3.5). Next, COG categories (based on previous knowledge of phenotypic defects observed in the  $\Delta crtB$  mutant) were chosen and for each category, protein trends in the whole cell, membrane pellet, DRM and DSM fractions were recorded. As the  $\Delta crtB$  mutant displayed defects in root colonization, biofilm formation and increased membrane rigidity, we narrowed down the functional categories that could explain some of the observed defects. Next, transcriptomics analysis using KBase tools was used to identify differential expression of transcripts between the wildtype and  $\Delta crtB$  mutant samples. Only 5 transcripts were significantly ( $p$ -value  $\leq 0.05$  and  $FC \geq 2$ ) upregulated whereas, 879 transcripts significantly downregulated in the  $\Delta crtB$  mutant (Appendix B). Heat maps representing the differential expression profile of wildtype and  $\Delta crtB$  mutant are shown in Figure 3.6.

#### **a. Cell wall/membrane/envelope biogenesis**

Cell membranes are not only important for cell integrity but are also sites where several functions take place. Membrane fluidity is not only controlled by lipids and sterols, but also by membrane proteins. Insertion and functioning of proteins is only dependent on the biophysical state of the membrane, but interestingly, it has been shown that several proteins also mediate membrane fluidity. Proteins involved in cell wall/membrane/envelope biogenesis (M) in *Pantoea* sp. YR343 were collected from the JGI IMG database. In total, 270 proteins are involved in cell wall/membrane/envelope biogenesis. Among the significant proteins, 56 proteins belonging to this category were identified in at least one or more fractions. Table 3.2 lists all the significant proteins ( $p \leq 0.005$  and  $FC \geq 1$ ) involved in cell membrane biogenesis. Among all the proteins, six

undecaprenyl-phosphate (UDP) proteins belonging to peptidoglycan/lipopolysaccharide biosynthesis were found to be significantly downregulated in the  $\Delta crtB$  mutant. As previously mentioned UDP genes are involved in exopolysaccharide secretion, cationic antimicrobial peptide resistance, lipid A biogenesis and importantly in peptidoglycan synthesis [61]. Interestingly, UDP-3-O-[3-hydroxymyristoyl] glucosamine N-acyltransferase (PMI39\_03679) was found to be significantly upregulated in the mutant. Upregulation of this protein in the  $\Delta crtB$  mutant could be due to its involvement in biosynthesis of the essential amino acid lysine. Furthermore, most UDP proteins were detected in the DRM fraction. Transcript data for two of the most significant UDP proteins, undecaprenyl-phosphate 4-deoxy-4-formamido-L-arabinose transferase (PMI39\_03114) and UDP-4-amino-4-deoxy-L-arabinose-oxoglutarate aminotransferase (PMI39\_03115), also showed a downregulation at the transcript level in the  $\Delta crtB$  mutant (Appendix-B). Downregulation of UDP genes could probably explain the difference in the peptidoglycan layer of the  $\Delta crtB$  mutant in comparison to the wildtype. We also reported previously that the removal of the outer membrane, increased the fluidity of the  $\Delta crtB$  mutant membrane, thereby emphasizing its role in maintenance of membrane fluidity.

Outer membrane proteins (OMP) are important for transport of metabolites and toxins, membrane biogenesis and for bacterial resistance. The folding and insertion of several OMPs are carried out by BamA along with three lipoproteins: BamB, BamC and BamE forming the BAM machine (beta-barrel assembly). Lipoproteins are peripherally anchored membrane proteins involved in cell division, chemotaxis, signal transduction and envelope stability [62, 63]. [64]. Among the 4 Bam proteins, BamA (PMI39\_03681) and BamB (PMI39\_03586) were found to be downregulated in the  $\Delta crtB$  mutant. BamB was identified in both the membrane pellet and the DRM fraction. Studies have shown that BamB contains WD40 repeating units, thereby functioning as a scaffold protein in large multi-protein complexes. It was also shown that the Bam complex increases the efficiency of folding of membrane proteins such as OmpA and EspP [65]. Thus, the improper regulation and folding of OMP due to the downregulation of Bam complexes may explain some of the phenotypic defects observed in the  $\Delta crtB$  mutant.

Five proteins (dTDP-4-amino-4,6-dideoxygalactose transaminase (PMI39\_02354), outer membrane pore protein F (PMI39\_00526), UDP-3-O-[3-hydroxymyristoyl] glucosamine N-acyltransferase (PMI39\_03679), lipoprotein Spr (PMI39\_01917), periplasmic chaperone for outer membrane proteins Skp (PMI39\_03680)) were upregulated in the  $\Delta crtB$  mutant. Among these, skp protein is a multivalent periplasmic chaperon preventing misfolding and aggregation of OMPs during transit from the inner to the outer membranes [66]. Thus, the Skp and Bam machinery interaction is important for the transport and insertion of OMPs. Outer membrane protein F, a homotrimeric beta-barrel protein and a member of the bacterial porin superfamily, was found to be upregulated in the  $\Delta crtB$ \_DRM

fraction. These proteins are abundant and are involved in the transport of small metabolites [67].

Taken together, the downregulation of the above-mentioned proteins could explain the differences in membrane composition and biophysical property in the *ΔcrtB* mutant.

#### b. Cell motility (N)

In comparison to the wildtype, the *ΔcrtB* mutant displayed motility defects. Motility on swimming plates indicated that the *ΔcrtB* mutant was less motile when compared to the wildtype (Fig). To further confirm the, motility assay on microscope was conducted. The average mean speed (0.97μm/px) was 3.5μm/sec when compared to the wildtype (4.9 μm/px) (Fig). To explain the motility defect, we looked at the proteins involved in cell motility and how they differed between the wild type and *ΔcrtB* mutant. In total, 92 proteins in *Pantoea* sp. YR343 were found to be involved in cell motility (Table 3.3). Among the 28 proteins that form the flagellar complex, only 3 proteins: flagellar FliL (PMI39\_02182) and two flagellar hook-associated protein 2 (PMI39\_02605 and PMI39\_02159) were significantly downregulated in the *ΔcrtB* mutant. FliL protein has been reported to be important for cell motility. In *Salmonella* and *E. coli*, it was shown that FliL interacts closely with stators and the MS ring, ensuring delivery of higher torque, leading to increased motility. In the absence of FliL protein, single motors have been shown to rotate at lower speeds [68, 69]. Interestingly, flagella staining indicated that the *ΔcrtB* mutant had shorter flagella when compared to the wildtype (Figure 3.7). In summary, defects in the proteins that make up the flagellar apparatus could be the reason for the *ΔcrtB* mutant motility defects. Further, decreased motility affects other cellular functions such as root colonization and biofilm formation.

As previously discussed in GO categories, MCP undergo reversible methylation in response to changes in the concentration of attractants or repellents in their environment [70]. Interestingly, two MCP proteins- PMI39\_02297 and PMI39\_01148 were found to be upregulated in the *ΔcrtB*\_whole cell fraction; however, another MCP (PMI39\_02163), was found to be upregulated in the *ΔcrtB*\_DRM fraction. Proteins with Pas domains can sense redox potential and light important for global regulation of metabolism and development in prokaryotes [71, 72]. Overproduction of chemotaxis proteins could be a compensatory mechanism in the *ΔcrtB* mutant.

#### c. Lipid transport and metabolism (I)

We previously reported that the *ΔcrtB* mutant exhibited different membrane lipid head group and tail composition when compared to the wild type. 150 proteins are involved in

lipid transport and metabolism, among which 26 proteins were found to be significantly abundant in at least one fraction (Table 3.4). Choline dehydrogenase (PMI39\_02890) was significantly upregulated in all fractions of the  $\Delta crtB$  mutant. It has been shown that to adapt to changing environmental conditions, bacteria accumulate osmotic compounds such as potassium, glutamic acid, glutamine and betaine [73]. Choline dehydrogenase catalyzes the first step in glycine betaine synthesis to produce the final compound betaine, an effective osmoprotectant [74, 75]. Another choline dehydrogenase (PMI\_00318) was also upregulated in all fractions except DSM. Other proteins such as lysophospholipase, NAD(P) dependent dehydrogenases were also unregulated in the  $\Delta crtB$  mutant.

Cyclopropane-fatty-acyl-phospholipid synthase (PMI\_04767) and predicted lipid carrier protein YhbT, containing a SCP2 domain (PMI\_01503), were downregulated in the  $\Delta crtB$ \_DRM fractions. The physiological role of YhbT has not yet been identified, but it contains the sterol carrier protein 2 (SCP2), suggesting a role in lipid and sterol transport [76]. The absence of carotenoids in the  $\Delta crtB$  mutant reflects the downregulation of YhbT, indicating a possible interaction of carotenoids and YhbT.

#### d. Signal Transduction mechanism (T)

Bacterial signal transduction networks provide a holistic understanding of how bacteria sense and respond to both environmental and intracellular parameters. In *Pantoea* sp. YR343, 235 proteins are involved in signal transduction (Table 3.5). Among these, only 32 proteins were detected in at least in one fraction. The OmpR family is best characterized as regulator proteins of the “two-component system” [77]. Histidine kinases, along with their cognate response regulators, are involved in various physiological processes. In our data, we observed an upregulation of OmpR family proteins, including the phosphate regulon response regulator OmpR (PMI39\_03347) in the  $\Delta crtB$ \_DRM fractions. OmpR, along with its partner EnvZ (histidine kinase), are important for osmotic tolerance, virulence and motility in *Acinetobacter baumannii* [78-80]. Interestingly, two ompR proteins, with a sensor histidine kinase, BaeS (PMI\_01862) CpxA (PMI\_04406), having function in metal resistance and cell envelope protein folding respectively, were downregulated in the  $\Delta crtB$ \_DRM fractions. The two-component transcriptional regulator, LuxR (PMI39\_03635) was also upregulated in the  $\Delta crtB$ \_DRM fractions. In total, 23 different transcriptional regulators belonging to the LuxR family are found in *Pantoea* sp YR343.

The deletion of carotenoids in the  $\Delta crtB$  mutant leads to defects not only in the loss of antioxidant potential but also defects in the secretion of IAA, formation of pellicles/biofilms, motility defects, and altogether defects in efficient root colonization. In

this study, we have shown that the  $\Delta crtB$  mutant membrane proteome drastically changed when compared to the wildtype. Membranes thickness, composition and dynamics affects protein localization and functioning. As expected with the loss of carotenoids, we observe the loss of functioning of cellular processes taking place at the membrane such as lipid A biosynthesis involving the UDP biosynthetic pathway, functioning of the flagellar apparatus due to the reduced expression of FliL and loss of functioning of histidine kinases leading to defects in signal transduction. Another important observation was that the DRM fraction between the wildtype and  $\Delta crtB$  mutant were different, in that the DRM fraction represents membrane microdomains and the presence of cholesterol (in eukaryotes) or carotenoids, hopanoids (in prokaryotes) is vital. Absence of carotenoids may lead to unstable domain formation, or protein insertion and functioning may be affected due to changes in membrane thickness controlled by carotenoids. Another speculation for the observed increases and decreases in specific pathways could be a compensation mechanism to help bacteria survive in changing environmental conditions. Membranes are characterized by differing composition owing to the presence of unsaturated and saturated lipids of different chain length and branching, proteins and importantly sterols. The average thickness of eukaryotic cell membranes is 9Å, when saturated with cholesterol. Membrane thickness affects the functioning of several membrane proteins such as potassium channels, gramicidin A and rhodopsin [81, 82]. Recently, it was shown that carotenoids control membrane thickness either through the process of interdigitation and/or compression of lipid bilayers. Membrane thickness was also shown to be important for charged amino acids dictating the structure and activities of membrane proteins. The absence of zeaxanthin in the membranes of  $\Delta crtB$  mutant could lead to different membrane thickness, leading to defects in protein localization, insertion and functioning.

In conclusion, deletion of carotenoids from the membranes changes the membrane proteome, leading to the observed phenotypic defects.

## **Materials and methods**

### ***Bacterial strains and growth conditions***

*Pantoea sp.* YR343 and  $\Delta crtB$  cells were grown in Luria-Bertani broth (per 1 L, 10 g Bacto-tryptone, 10 g NaCl, 5 g yeast extract) medium at 28°C with shaking to OD<sub>600</sub> of 1 (stationary phase). The  $\Delta crtB$  mutant was constructed as described in [25].

*Isolation of whole cell, crude membrane fraction, detergent resistant membrane and detergent sensitive membrane fractions of Pantoea sp. YR343 and  $\Delta crtB$  cells*

To isolate different cell fractions, we used a modified version of the method described by Lopez [16]. Briefly, cells were grown in 500 mL of LB media overnight at 28°C with vigorous shaking. Cells were collected by centrifugation (8000\*RPM for 12mins) and washed thrice in phosphate buffered saline (PBS). Cells were collected at this stage for whole cell proteomic analysis and stored at -20°C. Next, Buffer H (20 mM 4-(2-hydroxyethyl)-1-piperazineethanesulfonic acid (HEPES [pH 8], 20 mM NaCl, 1 mM dithiothreitol [DTT], 1 mM phenylmethylsulfonyl fluoride [PMSF]), lysozyme (1 mg/ml), PMSF (100 µM), and DNase I was added to the washed cells. Cells were disrupted using French press followed by a short centrifugation to eliminate cell debris. The membrane fraction was precipitated by ultracentrifugation (100,000\*g for 1 hour at 4°C). The resulting cell pellet was resuspended in Buffer H+ 10% glycerol. At this stage, a fraction of the membrane pellet was collected.

To isolate DRM and DSM fractions, the membrane pellet was incubated for 30minutes at 4°C with lysis and separation buffer (CellLytic MEM protein extraction kit- Sigma Aldrich). After incubation, the membrane pellet was mixed 1:1 with 80% sucrose and carefully overlaid with 20%. Using a swinging bucket centrifuge, separation was carried out at 100,000\*g at 4°C for 16hours. The DRM and DSM fractions were collected and stored in -20°C for proteomic analysis.

### ***Protein extraction and digestion***

Cell pellets were suspended in sodium dodecyl sulfate (SDS) lysis buffer (2% in 100 mM of NH<sub>4</sub>HCO<sub>3</sub>, 10 mM DTT). Samples were physically disrupted by bead beating (0.15 mm) at 8k rpm for 5 min. Crude lysates were boiled 5 min at 90 °C. Cysteines were blocked by adjusting each sample to 30 mM IAA and incubated in the dark for 15 min at room temperature. Proteins were precipitated using a chloroform/methanol/water extraction. Dried protein pellets were resuspended in 2% SDC (100 mM NH<sub>4</sub>HCO<sub>3</sub>) and protein amounts were estimated by performing a BCA assay (Pierce Biotechnology). For each sample, an aliquot of ~500 ug of protein was digested via two aliquots of sequencing-grade trypsin (Promega, 1:75 [w:w]) at two different sample dilutions, (overnight) and subsequent 3 hr at 37 °C. The peptide mixture was adjusted to 0.5% FA to precipitate SDC. Hydrated ethyl acetate was added to each sample at a 1:1 [v:v] ratio three times to effectively remove SDC. Samples were then placed in a SpeedVac Concentrator (Thermo Fischer Scientific) to remove ethyl acetate and further concentrate the sample. The peptide-enriched flow through was quantified by BCA assay, desalted on RP-C18 stage tips (Pierce Biotechnology) and then stored at -80°C.LC-MS/MS analysis.

## **LC-MS/MS**

All samples were analyzed on a Q Exactive Plus mass spectrometer (Thermo Fischer Scientific) coupled with a Proxeon EASY-nLC 1200 liquid chromatography (LC) pump (Thermo Fisher Scientific). Peptides were separated on a 75  $\mu\text{m}$  inner diameter microcapillary column packed with 25 cm of Kinetex C18 resin (1.7  $\mu\text{m}$ , 100  $\text{\AA}$ , Phenomenex). For each sample, a 2  $\mu\text{g}$  aliquot was loaded in buffer A (0.1% formic acid, 2% acetonitrile) and eluted with a linear 150 min gradient of 2 – 20% of buffer B (0.1% formic acid, 80% acetonitrile), followed by an increase in buffer B to 30% for 10 min, another increase to 50% buffer for 10 min and concluding with a 10 min wash at 98% buffer A. The flow rate was kept at 200 nl/min. MS data was acquired with the Thermo Xcalibur software version 4.27.19, a topN method where N could be up to 15. Target values for the full scan MS spectra were  $1 \times 10^6$  charges in the 300 – 1,500 m/z range with a maximum injection time of 25 ms. Transient times corresponding to a resolution of 70,000 at m/z 200 were chosen. A 1.6 m/z isolation window and fragmentation of precursor ions was performed by higher-energy C-trap dissociation (HCD) with a normalized collision energy of 30 eV. MS/MS scans were performed at a resolution of 17,500 at m/z 200 with an ion target value of  $1 \times 10^6$  and a maximum injection time of 50 ms. Dynamic exclusion was set to 45 s to avoid repeated sequencing of peptides.

### ***Peptide identification and protein inference***

MS raw data files were searched against the *Pantoea sp.* YR343 FASTA database to which common contaminate proteins had been added. A decoy database, consisting of the reversed sequences of the target database, was appended to discern the false-discovery rate (FDR) at the spectral level. For standard database searching, the peptide fragmentation spectra (MS/MS) were analyzed by the Crux pipeline v3.0 [26]. The MS/MS were searched using the Tide algorithm [27] and was configured to derive fully-tryptic peptides using default settings except for the following parameters: allowed clip nterm-methionine, a precursor mass tolerance of 10 parts per million (ppm), a static modification on cysteines (iodoacetamide; +57.0214 Da), and dynamic modifications on methionine (oxidation; 15.9949). The results were processed by Percolator [28] to estimate  $q$  values. Peptide spectrum matches (PSMs) and peptides were considered identified at a  $q$  value  $<0.01$ . Across the entire experimental dataset, proteins were required to have at least 2 distinct peptide sequences and 2 minimum spectra per protein.

### ***Protein quantification***

For label-free quantification, MS1-level precursor intensities were derived from MOFF [29] using the following parameters: 10 ppm mass tolerance, retention time window for extracted ion chromatogram was 3 min, time window to get the apex for MS/MS precursor



was 30 s. Protein intensity-based values, which were calculated by summing together quantified peptides, normalized by dividing by protein length and then LOESS and median central tendency procedures were performed on log<sub>2</sub>-transformed. Using the freely available software Perseus (<http://www.perseus-framework.org>) [30], missing values were replaced by random numbers drawn from a normal distribution (width = 0.3 and downshift = 2.8).

### ***Statistical Analysis for differential abundances***

For this study, we performed ANOVA with post-hoc Tukey's test to identify differential protein abundances across the wildtype *Pantoea* sp. YR343 dataset set comparisons or  $\Delta crtB$  mutant dataset comparisons and protein abundances were considered to have a significant change in abundance for p-values <0.05 and at least one absolute value of log<sub>2</sub> fold-change difference >1. To identify differential protein abundances between wildtype and Delta fractions, we performed a Student's t-test for the pairwise comparisons. A protein was categorized as having a significant abundance difference if it passed a significance threshold requiring a p-value <0.05 and absolute value of log<sub>2</sub> fold-change difference >1. Hierarchical clustering (one-way; Fast Ward method) was performed to identify differential abundance patterns.

### ***Gene Ontology Enrichment***

Gene ontology (GO) term annotation was performed using Blast2GO [31] with a blastp E-value hit filter of  $1 \times 10^{-5}$ , an annotation cutoff value of 55 and a GO weight of 5. Using the Cytoscape [32] plugin ClueGO [33], observed GO biological processes were subjected to the right-sided hypergeometric enrichment test at medium network specificity selection and p-value correction was performed using the Holm-Bonferroni step-down method (Holm, 1979). For each cluster, we required a minimum of 3 and a maximum of 8 selected GO tree levels, and each cluster was set to include a minimum of 3- 4% of genes associated with each term. The GO terms at adjusted p<0.05 were considered significantly enriched.

### ***RNA extraction, sequencing and analysis***

Wild type and  $\Delta crtB$  cells were grown to stationary phase ( $OD_{600} = 1$ ). RNA was extracted using RNeasy mini kit (QIAGEN, Valencia, CA) kit following manufacturer's instructions and quantified using nanodrop. Sequencing was carried out by GENEWIZ Next Generation Sequencing Services. Transcript analysis was carried out using KBase[34] (<https://kbase.us/>) . KBase and its tools were used to generate the sample set, align and

assemble reads to the genome, and identify differentially abundant genes between wild type and  $\Delta crtB$ .

### ***Motility assays***

To compare the swimming motility function of *Pantoea* sp. YR343 and  $\Delta crtB$  cells, cells were grown overnight with shaking (250rpm) in LB medium. Swimming motility was examined on LB containing 0.3% w/v agar. 5 $\mu$ l of cells were spotted in the center of the plate and incubated at 28°C [35]. Live cell imaging of bacterial motility was measured by Nikon eclipse Ti-U inverted microscope. Cells from motility plates were inoculated in R2A media overnight at 28°C with shaking (250rpm). Next day cells were reinoculated in R2A media and grown to an OD<sub>600</sub> of 0.5. 20 $\mu$ l of cells were placed on a coverslip and 10s videos were captured using NIS-Elements imaging software. Trajectories and velocities (pixels/frame) of *Pantoea* sp. YR343 and  $\Delta crtB$  cells were calculated with the “TrackMate” plugin (<https://imagej.net/TrackMate>).

### ***Flagella staining***

Flagella staining was carried out using protocol adapted from Turner et al [36]. Briefly, *Pantoea* sp. YR343 and  $\Delta crtB$  cells from swimming plates were inoculated overnight in R2A medium at 28°C with shaking (250rpm). Next day, cells were diluted 1:10 in fresh R2A medium and grown to OD<sub>600</sub> of 0.5. Motility of the culture was confirmed using a confocal microscope. Cells were collected by centrifugation (2000\*g, 3 mins) and washed three times in buffer (0.01 M KPO<sub>4</sub>, 0.067 M NaCl, 10<sup>-4</sup> M (Ethylenediaminetetraacetic acid (EDTA) [pH 7.0]). Alexa Fluor 594 carboxylic acid succinimidyl ester (ThermoFisher Scientific) was added to the concentrated bacterial suspension and incubated in the dark for 1 hour. Cells were then washed three times with buffer containing Brij 35 (10<sup>-4</sup>%) and 0.4% glucose. Concentrated cells were then placed on an agarose pad (1% agarose in phosphate buffered saline) and imaged using a Zeiss LSM 710 confocal microscope with a TRITC filter.

## References

1. Konings, W.N., et al., The cell membrane plays a crucial role in survival of bacteria and archaea in extreme environments. *Antonie Van Leeuwenhoek*, 2002. 81(1-4): p. 61-72.
2. Siliakus, M.F., J. van der Oost, and S.W. Kengen, Adaptations of archaeal and bacterial membranes to variations in temperature, pH and pressure. *Extremophiles*, 2017. 21(4): p. 651-670.
3. Mato, J.M., Asymmetry in Membrane Phospholipids, in *Phospholipid Metabolism in Cellular Signaling*. 2017, CRC Press. p. 33-41.
4. Op den Kamp, J.A., Lipid asymmetry in membranes. *Annual review of biochemistry*, 1979. 48(1): p. 47-71.
5. Gennis, R.B., *Biomembranes: molecular structure and function*. 2013: Springer Science & Business Media.
6. Schlegel, S., et al., Revolutionizing membrane protein overexpression in bacteria. *Microb Biotechnol*, 2010. 3(4): p. 403-11.
7. Wallin, E. and G. von Heijne, Genome-wide analysis of integral membrane proteins from eubacterial, archaean, and eukaryotic organisms. *Protein Sci*, 1998. 7(4): p. 1029-38.
8. Silhavy, T.J., D. Kahne, and S. Walker, The bacterial cell envelope. *Cold Spring Harb Perspect Biol*, 2010. 2(5): p. a000414.
9. Dirienzo, J.M., K. Nakamura, and M. Inouye, The outer membrane proteins of Gram-negative bacteria: biosynthesis, assembly, and functions. *Annual review of biochemistry*, 1978. 47(1): p. 481-532.
10. Koebnik, R., K.P. Locher, and P. Van Gelder, Structure and function of bacterial outer membrane proteins: barrels in a nutshell. *Molecular microbiology*, 2000. 37(2): p. 239-253.
11. Koronakis, V., et al., Crystal structure of the bacterial membrane protein TolC central to multidrug efflux and protein export. *Nature*, 2000. 405(6789): p. 914.
12. Confer, A.W. and S. Ayalew, The OmpA family of proteins: roles in bacterial pathogenesis and immunity. *Vet Microbiol*, 2013. 163(3-4): p. 207-22.
13. Fekkes, P. and A.J.M. Driessen, Protein Targeting to the Bacterial Cytoplasmic Membrane. *Microbiology and Molecular Biology Reviews*, 1999. 63(1): p. 161-173.
14. Beckwith, J., The Sec-dependent pathway. *Res Microbiol*, 2013. 164(6): p. 497-504.
15. Johnson, Q.R., et al., Effects of carotenoids on lipid bilayers. *Physical Chemistry Chemical Physics*, 2018. 20(5): p. 3795-3804.
16. Bramkamp, M. and D. Lopez, Exploring the existence of lipid rafts in bacteria. *Microbiol Mol Biol Rev*, 2015. 79(1): p. 81-100.

17. LeDeaux, J.R. and A.D. Grossman, Isolation and characterization of kinC, a gene that encodes a sensor kinase homologous to the sporulation sensor kinases KinA and KinB in *Bacillus subtilis*. *Journal of bacteriology*, 1995. 177(1): p. 166-175.
18. Dermine, J.-F., et al., Flotillin-1-enriched lipid raft domains accumulate on maturing phagosomes. *Journal of Biological Chemistry*, 2001.
19. Olsson, S. and R. Sundler, The role of lipid rafts in LPS-induced signaling in a macrophage cell line. *Molecular immunology*, 2006. 43(6): p. 607-612.
20. Solomon, S., et al., The lipid raft microdomain-associated protein reggie-1/flotillin-2 is expressed in human B cells and localized at the plasma membrane and centrosome in PBMCs. *Immunobiology*, 2002. 205(1): p. 108-119.
21. Lopez, D. and G. Koch, Exploring functional membrane microdomains in bacteria: an overview. *Current opinion in microbiology*, 2017. 36: p. 76-84.
22. Somani, V.K., et al., Identification of novel raft marker protein, FlotP in *Bacillus anthracis*. *Frontiers in microbiology*, 2016. 7: p. 169.
23. Schneider, J., et al., In vivo characterization of the scaffold activity of flotillin on the membrane kinase KinC of *Bacillus subtilis*. *Microbiology*, 2015. 161(9): p. 1871-1887.
24. Simons, K. and J.L. Sampaio, Membrane organization and lipid rafts. *Cold Spring Harbor perspectives in biology*, 2011. 3(10): p. a004697.
25. Bible, A.N., et al., A Carotenoid-Deficient Mutant in *Pantoea* sp. YR343, a Bacteria Isolated from the Rhizosphere of *Populus deltoides*, Is Defective in Root Colonization. *Front Microbiol*, 2016. 7: p. 491.
26. McIlwain, S., et al., Crux: rapid open source protein tandem mass spectrometry analysis. *J Proteome Res*, 2014. 13(10): p. 4488-91.
27. Diament, B.J. and W.S. Noble, Faster SEQUEST searching for peptide identification from tandem mass spectra. *J Proteome Res*, 2011. 10(9): p. 3871-9.
28. Kall, L., et al., Semi-supervised learning for peptide identification from shotgun proteomics datasets. *Nat Methods*, 2007. 4(11): p. 923-5.
29. Argentini, A., et al., moFF: a robust and automated approach to extract peptide ion intensities. *Nature Methods*, 2016. 13(12): p. 962-965.
30. Tyanova, S., et al., The Perseus computational platform for comprehensive analysis of (prote)omics data. *Nat Methods*, 2016. 13(9): p. 731-40.
31. Conesa, A., et al., Blast2GO: a universal tool for annotation, visualization and analysis in functional genomics research. *Bioinformatics*, 2005. 21(18): p. 3674-6.
32. Shannon, P., et al., Cytoscape: a software environment for integrated models of biomolecular interaction networks. *Genome Res*, 2003. 13(11): p. 2498-504.
33. Bindea, G., et al., ClueGO: a Cytoscape plug-in to decipher functionally grouped gene ontology and pathway annotation networks. *Bioinformatics*, 2009. 25(8): p. 1091-3.

34. Arkin, A.P., et al., KBase: The United States Department of Energy Systems Biology Knowledgebase. *Nature biotechnology*, 2018. 36(7).
35. Herrera, C.M., et al., *Pantoea stewartii* subsp. *stewartii* exhibits surface motility, which is a critical aspect of Stewart's wilt disease development on maize. *Mol Plant Microbe Interact*, 2008. 21(10): p. 1359-70.
36. Turner, L., W.S. Ryu, and H.C. Berg, Real-time imaging of fluorescent flagellar filaments. *Journal of bacteriology*, 2000. 182(10): p. 2793-2801.
37. Andersen, O.S. and I. Roger E. Koeppe, Bilayer Thickness and Membrane Protein Function: An Energetic Perspective. *Annual Review of Biophysics and Biomolecular Structure*, 2007. 36(1): p. 107-130.
38. Pande, A.H., S. Qin, and S.A. Tatulian, Membrane Fluidity Is a Key Modulator of Membrane Binding, Insertion, and Activity of 5-Lipoxygenase. *Biophysical Journal*, 2005. 88(6): p. 4084-4094.
39. Rexroth, S., et al., The Plasma Membrane of the Cyanobacterium *Gloeobacter violaceus* Contains Segregated Bioenergetic Domains. *The Plant Cell Online*, 2011.
40. de Meyer, F. and B. Smit, Effect of cholesterol on the structure of a phospholipid bilayer. *Proc Natl Acad Sci U S A*, 2009. 106(10): p. 3654-8.
41. Cerezo, J., et al., Conformational changes of  $\beta$ -carotene and zeaxanthin immersed in a model membrane through atomistic molecular dynamics simulations. *Physical Chemistry Chemical Physics*, 2013. 15(17): p. 6527-6538.
42. Havaux, M., Carotenoids as membrane stabilizer in chloroplasts. *Trends Plant Sci* 3:147-151. Vol. 3. 1998. 147-151.
43. McIntosh, T.J. and S.A. Simon, Bilayers as Protein Solvents: Role of Bilayer Structure and Elastic Properties. *The Journal of General Physiology*, 2007. 130(2): p. 225-227.
44. Li, L.B., I. Vorobyov, and T.W. Allen, The role of membrane thickness in charged protein-lipid interactions. *Biochimica et Biophysica Acta (BBA)-Biomembranes*, 2012. 1818(2): p. 135-145.
45. Andersen, O.S. and R.E. Koeppe, 2nd, Bilayer thickness and membrane protein function: an energetic perspective. *Annu Rev Biophys Biomol Struct*, 2007. 36: p. 107-30.
46. Tan, S., H.T. Tan, and M.C. Chung, Membrane proteins and membrane proteomics. *Proteomics*, 2008. 8(19): p. 3924-3932.
47. Matkó, J. and J. Szöllősi, Regulatory aspects of membrane microdomain (raft) dynamics in live cells, in *Membrane Microdomain Signaling*. 2005, Springer. p. 15-46.
48. Istivan, T.S. and P.J. Coloe, Phospholipase A in Gram-negative bacteria and its role in pathogenesis. *Microbiology*, 2006. 152(Pt 5): p. 1263-74.

49. Dalebroux, Z.D., Cues from the Membrane: Bacterial Glycerophospholipids. *Journal of Bacteriology*, 2017. 199(13).
50. Rivera-Milla, E., C.A. Stuermer, and E. Malaga-Trillo, Ancient origin of reggie (flotillin), reggie-like, and other lipid-raft proteins: convergent evolution of the SPFH domain. *Cell Mol Life Sci*, 2006. 63(3): p. 343-57.
51. Hinderhofer, M., et al., Evolution of prokaryotic SPFH proteins. *BMC Evolutionary Biology*, 2009. 9(1): p. 10.
52. Sanyal, S. and A.K. Menon, Flipping lipids: why an' what's the reason for? *ACS chemical biology*, 2009. 4(11): p. 895-909.
53. TouzÉ, T. and D. Mengin-Lecreulx, Undecaprenyl Phosphate Synthesis. *EcoSal Plus*, 2008.
54. Hartley, M.D. and B. Imperiali, At the membrane frontier: A prospectus on the remarkable evolutionary conservation of polyprenols and polyprenyl-phosphates. *Archives of Biochemistry and Biophysics*, 2012. 517(2): p. 83-97.
55. de Ropp, J.S. and F.A. Troy, <sup>2</sup>H NMR investigation of the organization and dynamics of polyisoprenols in membranes. *J Biol Chem*, 1985. 260(29): p. 15669-74.
56. Janas, T., et al., The effect of undecaprenol on bilayer lipid membranes. *Acta Biochim Pol*, 1994. 41(3): p. 351-8.
57. Wadhams, G.H. and J.P. Armitage, Making sense of it all: bacterial chemotaxis. *Nature Reviews Molecular Cell Biology*, 2004. 5: p. 1024.
58. Guttenplan, S.B. and D.B. Kearns, Regulation of flagellar motility during biofilm formation. *FEMS microbiology reviews*, 2013. 37(6): p. 849-871.
59. Andrews, S.C., A.K. Robinson, and F. Rodríguez-Quiñones, Bacterial iron homeostasis. *FEMS Microbiology Reviews*, 2003. 27(2-3): p. 215-237.
60. Tatusov, R.L., et al., The COG database: a tool for genome-scale analysis of protein functions and evolution. *Nucleic acids research*, 2000. 28(1): p. 33-36.
61. Touz, E.T. and D. Mengin-Lecreulx, Undecaprenyl Phosphate Synthesis. *EcoSal Plus*, 2008. 3(1).
62. Zückert, W.R., Secretion of Bacterial Lipoproteins: Through the Cytoplasmic Membrane, the Periplasm and Beyond. *Biochimica et biophysica acta*, 2014. 1843(8): p. 1509-1516.
63. Noinaj, N., J.W. Fairman, and S.K. Buchanan, The Crystal Structure of BamB Suggests Interactions with BamA and Its Role within the BAM Complex. *Journal of Molecular Biology*, 2011. 407(2): p. 248-260.
64. Malinverni, J.C. and T.J. Silhavy, Assembly of Outer Membrane  $\beta$ -Barrel Proteins: the Bam Complex. *EcoSal Plus*, 2011. 4(2): p. 10.1128/ecosalplus.4.3.8.
65. Hussain, S. and H.D. Bernstein, The Bam complex catalyzes efficient insertion of bacterial outer membrane proteins into membrane vesicles of variable lipid composition. *J Biol Chem*, 2018. 293(8): p. 2959-2973.

66. Schiffrin, B., et al., Skp is a multivalent chaperone of outer membrane proteins. *Nature structural & molecular biology*, 2016. 23(9): p. 786-793.
67. Visudtiphole, V., et al., Refolding of *Escherichia coli* outer membrane protein F in detergent creates LPS-free trimers and asymmetric dimers. *Biochemical Journal*, 2005. 392(Pt 2): p. 375-381.
68. Partridge, J.D., V. Nieto, and R.M. Harshey, A New Player at the Flagellar Motor: FliL Controls both Motor Output and Bias. *mBio*, 2015. 6(2).
69. Zhu, S., et al., FliL associates with the stator to support torque generation of the sodium-driven polar flagellar motor of *Vibrio*. *Molecular microbiology*, 2015. 98(1): p. 101-110.
70. Kehry, M. and F. Dahlquist, The methyl-accepting chemotaxis proteins of *Escherichia coli*. Identification of the multiple methylation sites on methyl-accepting chemotaxis protein I. *Journal of Biological Chemistry*, 1982. 257(17): p. 10378-10386.
71. Taylor, B.L. and I.B. Zhulin, PAS Domains: Internal Sensors of Oxygen, Redox Potential, and Light. *Microbiology and Molecular Biology Reviews*, 1999. 63(2): p. 479.
72. Repik, A., et al., PAS Domain Residues Involved in Signal Transduction by the Aer Redox Sensor of *Escherichia coli*. *Molecular microbiology*, 2000. 36(4): p. 806-816.
73. Poolman, B. and E. Glaesker, Regulation of compatible solute accumulation in bacteria. *Mol Microbiol*, 1998. 29(2): p. 397-407.
74. Wood, J.M., et al., Osmosensing and osmoregulatory compatible solute accumulation by bacteria. *Comparative Biochemistry and Physiology Part A: Molecular & Integrative Physiology*, 2001. 130(3): p. 437-460.
75. Tsuge, H., et al., A novel purification and some properties of rat liver mitochondrial choline dehydrogenase. *Biochim Biophys Acta*, 1980. 614(2): p. 274-84.
76. Arends, J., et al., In vivo trapping of FtsH substrates by label-free quantitative proteomics. *Proteomics*, 2016. 16(24): p. 3161-3172.
77. Lee, A.K., C.S. Detweiler, and S. Falkow, OmpR regulates the two-component system SsrA-SsrB in *Salmonella* pathogenicity island 2. *Journal of bacteriology*, 2000. 182(3): p. 771-781.
78. Tipton, K.A. and P.N. Rather, An ompR-envZ Two-Component System Ortholog Regulates Phase Variation, Osmotic Tolerance, Motility, and Virulence in *Acinetobacter baumannii* Strain AB5075. *Journal of Bacteriology*, 2017. 199(3).
79. Foo, Y.H., et al., Cytoplasmic sensing by the inner membrane histidine kinase EnvZ. *Prog Biophys Mol Biol*, 2015. 118(3): p. 119-29.
80. Mattison, K. and L.J. Kenney, Phosphorylation alters the interaction of the response regulator OmpR with its sensor kinase EnvZ. *J Biol Chem*, 2002. 277(13): p. 11143-8.

81. Soubias, O., et al., Lipid– rhodopsin hydrophobic mismatch alters rhodopsin helical content. *Journal of the American Chemical Society*, 2008. 130(37): p. 12465-12471.
82. Yuan, C., et al., Bilayer thickness modulates the conductance of the BK channel in model membranes. *Biophysical journal*, 2004. 86(6): p. 3620-3633.



## Appendix

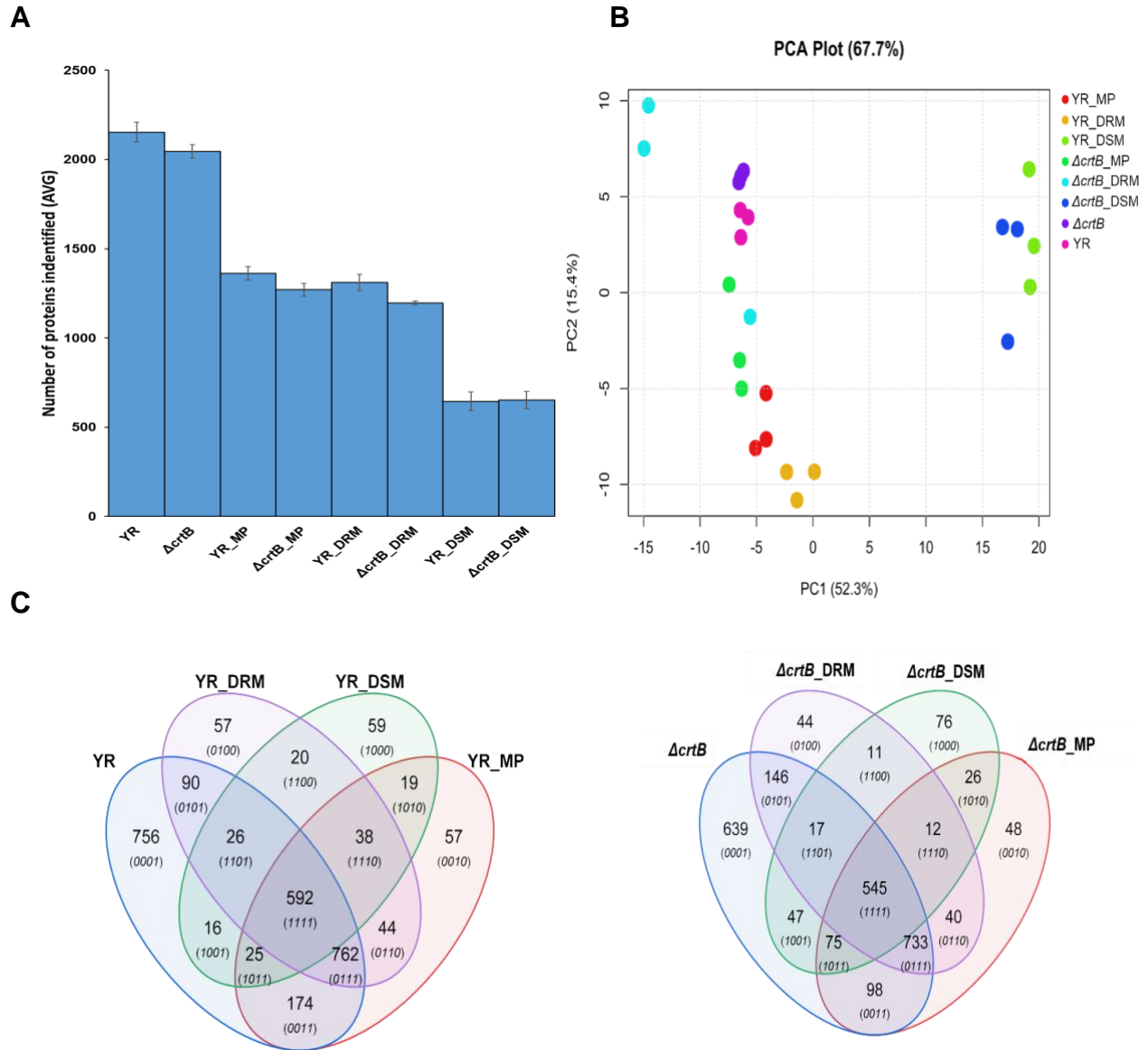


**Figure 3.1: Identification and analysis of the proteins identified in whole cell, membrane pellet, DRM and DSM fractions of *Pantoea* sp. YR343 and  $\Delta$ *crtB* mutant cells.**

A. Histogram representing the average no. of proteins identified for each sample from bottom-up proteomics. B. PCA plot of normalized abundance. The plot illustrates discrete grouping of biological replicates and major variance observed in PC1 with the DSM samples and in PC2 across the remaining factors. C. Venn diagram comparing accession numbers of protein identified in four different conditions illustrating the intersections between samples. The four ellipses represent the total number of hits from the four sample sets. The non-overlapping parts represents unique proteins for each sample.

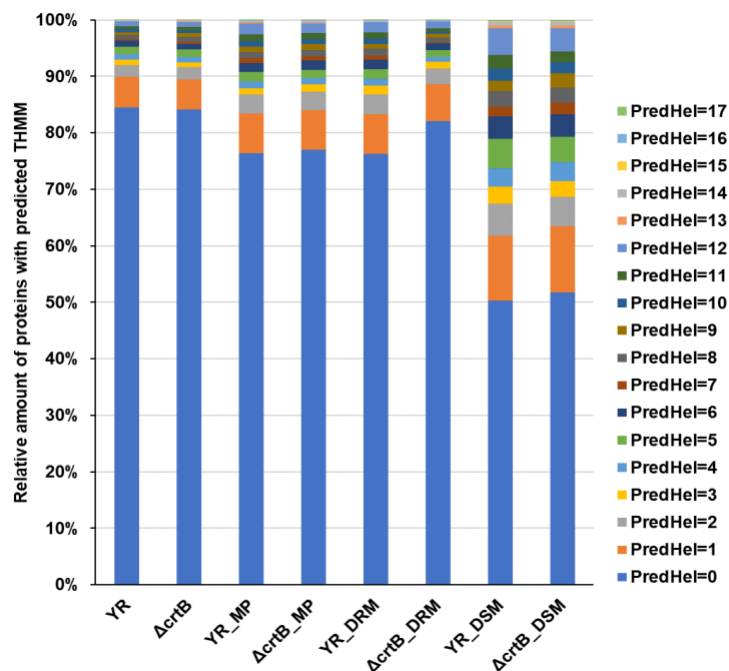


**Figure 3.2: Histogram representing the % of proteins with predicted transmembrane helix domains (THMM) for each sample.**

Proteins with predicted transmembrane helices were identified using THMM software. The membrane fraction samples contain a higher relative amount of proteins with predicted THMM domains, with DSM having the largest enrichment.

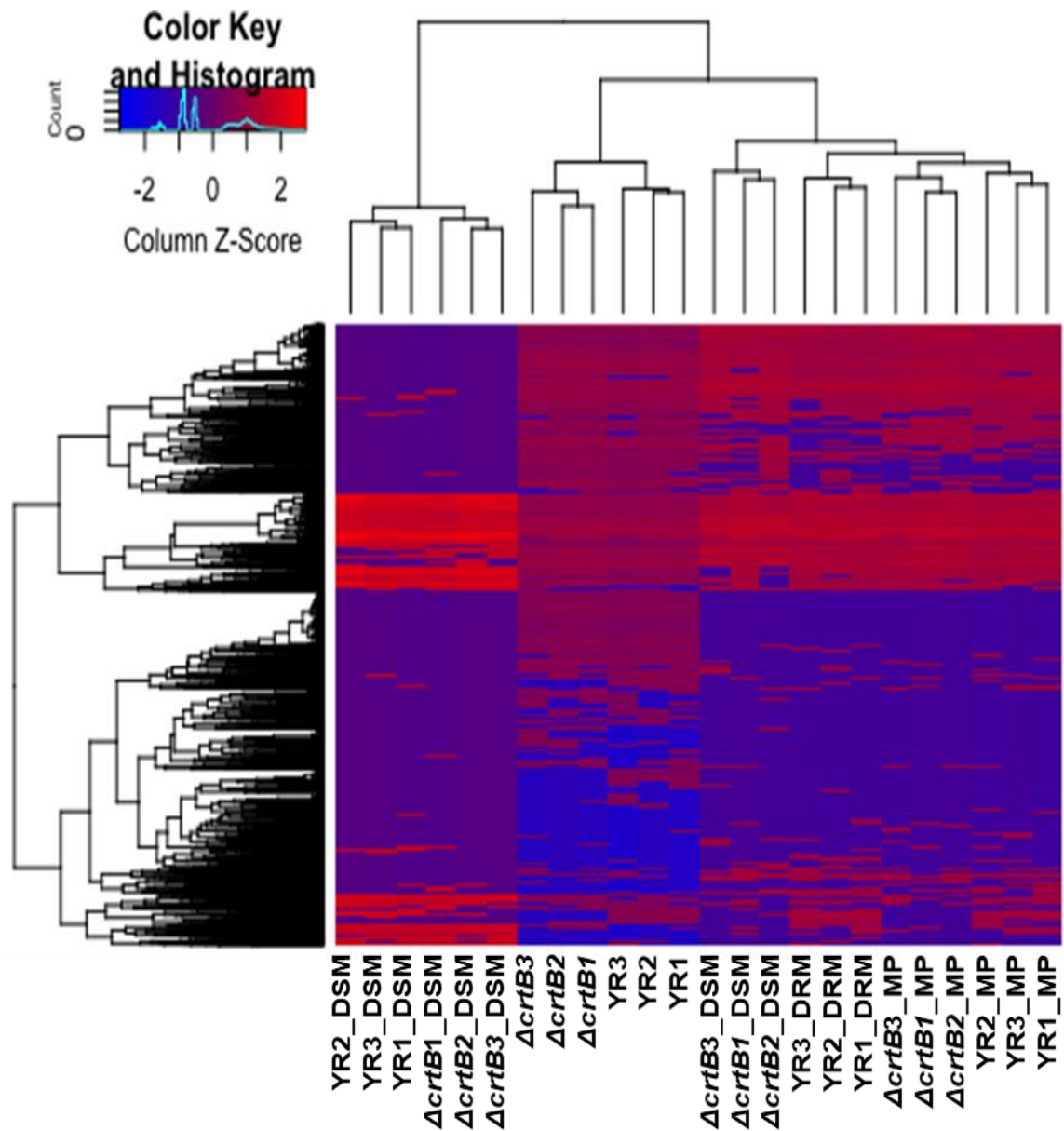


**Figure 3.3: Hierarchical clustering of all proteins identified in all four fractions of *Pantoea* sp. YR343 and  $\Delta crtB$  mutant.**

Heatmap of protein counts in *Pantoea* sp. YR343 and  $\Delta crtB$  mutant indicate fraction specific abundance of proteins and differential abundance of proteins between wildtype and  $\Delta crtB$  mutant.

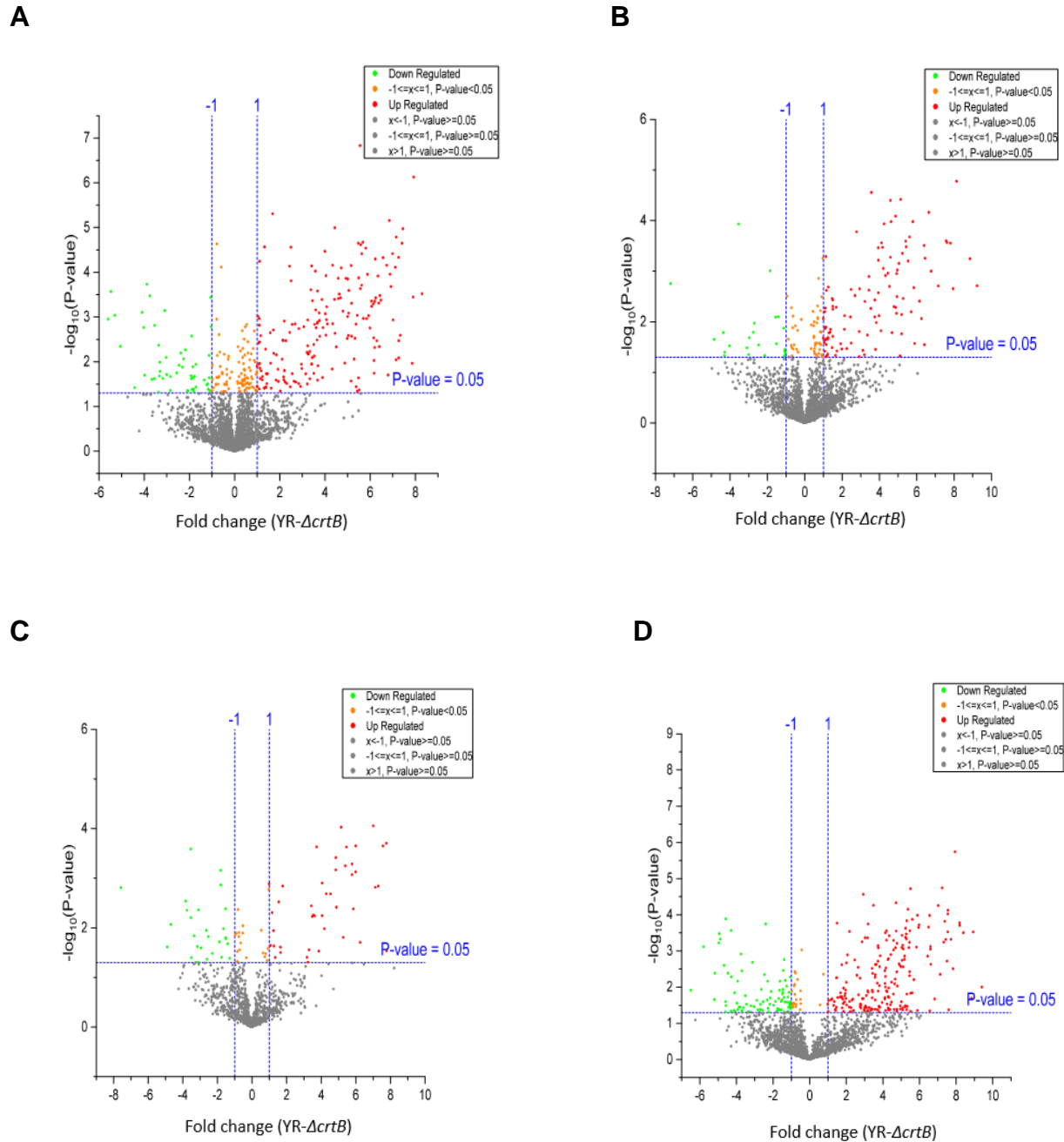


**Figure 3.4: Volcano plot illustrating significantly differentially abundant proteins.**

The  $-\log_{10}$  (Benjamini-Hochberg corrected P value) is plotted against the fold change are plotted to identify significantly different proteins. Significantly upregulated (green) and downregulated (red) proteins for A. Whole cells B. Membrane pellet C. DRM and D. DSM are shown.

**Table 3.1: Whole-genome gene ontology (GO) term annotation using Blast2GO software.**

Whole gene ontology was performed using Blast2GO with a blastp E-value hit filter of  $1 \times 10^{-3}$ , an annotation cutoff value of 55 and a GO weight of 5. Using ClueGO, observed GO biological process were subjected to the right-sided hypergeometric enrichment test at medium network specificity selection and p-value correction was performed using the Holm-Bonferroni step-down method.

<b>Whole-cell pairwise -- Down-regulated in <math>\Delta crtB</math></b>			
<b>GOID</b>	<b>GO Term</b>	<b>Ontology Source</b>	<b>No. of Genes</b>
GO:0044264	cellular polysaccharide metabolic process	GO_BiologicalProcess	12.00
GO:0009311	oligosaccharide metabolic process	GO_BiologicalProcess	9.00
GO:0006629	lipid metabolic process	GO_BiologicalProcess	23.00
GO:0008610	lipid biosynthetic process	GO_BiologicalProcess	17.00
GO:0016798	hydrolase activity, acting on glycosyl bonds	GO_MolecularFunction	9.00
GO:0004553	hydrolase activity, hydrolyzing O-glycosyl compounds	GO_MolecularFunction	9.00
GO:0015926	glucosidase activity	GO_MolecularFunction	5.00
GO:0090599	alpha-glucosidase activity	GO_MolecularFunction	3.00
GO:0016903	oxidoreductase activity, acting on the aldehyde or oxo group of donors	GO_MolecularFunction	9.00
GO:0019695	choline metabolic process	GO_BiologicalProcess	4.00
GO:0031455	glycine betaine metabolic process	GO_BiologicalProcess	4.00
GO:0006578	amino-acid betaine biosynthetic process	GO_BiologicalProcess	4.00
GO:0019285	glycine betaine biosynthetic process from choline	GO_BiologicalProcess	4.00
GO:0031456	glycine betaine biosynthetic process	GO_BiologicalProcess	4.00
GO:0008802	betaine-aldehyde dehydrogenase activity	GO_MolecularFunction	4.00

<b>Whole-cell pairwise -- Up-regulated in <math>\Delta crtB</math></b>			
<b>GOID</b>	<b>GO Term</b>	<b>Ontology Source</b>	<b>No. of Genes</b>
GO:0006260	DNA replication	GO_BiologicalProcess	4.00
GO:0050790	regulation of catalytic activity	GO_BiologicalProcess	5.00
GO:1901698	response to nitrogen compound	GO_BiologicalProcess	3.00

Table 3.1 continued

<b>MP pairwise -- Down-regulated in <math>\Delta crtB</math></b>			
<b>GOID</b>	<b>GO Term</b>	<b>Ontology Source</b>	<b>No. of Genes</b>
GO:0031241	periplasmic side of cell outer membrane	GO_CellularComponent	4.00
GO:0031975	envelope	GO_CellularComponent	21.00
GO:0030312	external encapsulating structure	GO_CellularComponent	16.00
GO:0030313	cell envelope	GO_CellularComponent	19.00
GO:0044462	external encapsulating structure part	GO_CellularComponent	12.00
GO:0009279	cell outer membrane	GO_CellularComponent	12.00
<b>DRM pairwise -- Down-regulated in <math>\Delta crtB</math></b>			
<b>GOID</b>	<b>GO Term</b>	<b>Ontology Source</b>	<b>No. of Genes</b>
GO:0048038	quinone binding	GO_MolecularFunction	8.00
GO:0071944	cell periphery	GO_CellularComponent	139.00
GO:0008104	protein localization	GO_BiologicalProcess	17.00
GO:1904659	glucose transmembrane transport	GO_BiologicalProcess	4.00
GO:0030001	metal ion transport	GO_BiologicalProcess	15.00
GO:0022804	active transmembrane transporter activity	GO_MolecularFunction	33.00
GO:0055085	transmembrane transport	GO_BiologicalProcess	49.00
GO:0031224	intrinsic component of membrane	GO_CellularComponent	104.00
GO:0005886	plasma membrane	GO_CellularComponent	120.00
GO:0016021	integral component of membrane	GO_CellularComponent	99.00
GO:0044459	plasma membrane part	GO_CellularComponent	73.00
GO:0031226	intrinsic component of plasma membrane	GO_CellularComponent	63.00
GO:0005887	integral component of plasma membrane	GO_CellularComponent	61.00
GO:0031975	envelope	GO_CellularComponent	31.00
GO:0098552	side of membrane	GO_CellularComponent	14.00
GO:0030312	external encapsulating structure	GO_CellularComponent	23.00
GO:0030313	cell envelope	GO_CellularComponent	26.00
GO:0044462	external encapsulating structure part	GO_CellularComponent	19.00
GO:0009279	cell outer membrane	GO_CellularComponent	19.00
GO:0031230	intrinsic component of cell outer membrane	GO_CellularComponent	7.00
GO:0031241	periplasmic side of cell outer membrane	GO_CellularComponent	7.00

Table 3.1 continued

<b>DRM pairwise -- Up-regulated in <math>\Delta crtB</math></b>			
<b>GOID</b>	<b>GO Term</b>	<b>Ontology Source</b>	<b>No. of Genes</b>
GO:0005829	cytosol	GO_CellularComponent	45.00
GO:0006090	pyruvate metabolic process	GO_BiologicalProcess	6.00
GO:0043168	anion binding	GO_MolecularFunction	28.00
GO:0032553	ribonucleotide binding	GO_MolecularFunction	21.00
GO:0030554	adenyl nucleotide binding	GO_MolecularFunction	18.00
GO:0032559	adenyl ribonucleotide binding	GO_MolecularFunction	18.00
GO:0006082	organic acid metabolic process	GO_BiologicalProcess	28.00
GO:0044283	small molecule biosynthetic process	GO_BiologicalProcess	22.00
GO:0016053	organic acid biosynthetic process	GO_BiologicalProcess	16.00
GO:0043436	oxoacid metabolic process	GO_BiologicalProcess	28.00
GO:1901566	organonitrogen compound biosynthetic process	GO_BiologicalProcess	25.00
GO:0019752	carboxylic acid metabolic process	GO_BiologicalProcess	27.00
GO:0046394	carboxylic acid biosynthetic process	GO_BiologicalProcess	16.00

<b>DSM pairwise -- Down-regulated in <math>\Delta crtB</math></b>			
<b>GOID</b>	<b>GO Term</b>	<b>Ontology Source</b>	<b>No. of Genes</b>
GO:1903509	liposaccharide metabolic process	GO_BiologicalProcess	4.00
GO:0030312	external encapsulating structure	GO_CellularComponent	10.00
GO:0015850	organic hydroxy compound transport	GO_BiologicalProcess	3.00
GO:0022838	substrate-specific channel activity	GO_MolecularFunction	3.00
GO:0019725	cellular homeostasis	GO_BiologicalProcess	3.00
GO:0048878	chemical homeostasis	GO_BiologicalProcess	3.00
GO:0005783	endoplasmic reticulum	GO_CellularComponent	3.00
GO:0046873	metal ion transmembrane transporter activity	GO_MolecularFunction	4.00
GO:0030001	metal ion transport	GO_BiologicalProcess	5.00
GO:0072511	divalent inorganic cation transport	GO_BiologicalProcess	3.00
GO:0000041	transition metal ion transport	GO_BiologicalProcess	4.00
GO:0070838	divalent metal ion transport	GO_BiologicalProcess	3.00



Table 3.1 continued

<b>DSM pairwise -- Up-regulated in <math>\Delta crtB</math></b>			
<b>GOID</b>	<b>GO Term</b>	<b>Ontology Source</b>	<b>No. of Genes</b>
GO:0045229	external encapsulating structure organization	GO_BiologicalProcess	3.00
GO:0015293	symporter activity	GO_MolecularFunction	3.00
GO:0022613	ribonucleoprotein complex biogenesis	GO_BiologicalProcess	6.00
GO:0003723	RNA binding	GO_MolecularFunction	8.00
GO:0042254	ribosome biogenesis	GO_BiologicalProcess	6.00
GO:0044446	intracellular organelle part	GO_CellularComponent	11.00
GO:0070925	organelle assembly	GO_BiologicalProcess	4.00
GO:0071826	ribonucleoprotein complex subunit organization	GO_BiologicalProcess	4.00
GO:0006518	peptide metabolic process	GO_BiologicalProcess	9.00
GO:0042273	ribosomal large subunit biogenesis	GO_BiologicalProcess	3.00
GO:0043232	intracellular non-membrane-bounded organelle	GO_CellularComponent	9.00
GO:0005840	ribosome	GO_CellularComponent	9.00
GO:0019843	rRNA binding	GO_MolecularFunction	7.00
GO:0022618	ribonucleoprotein complex assembly	GO_BiologicalProcess	4.00
GO:0034622	cellular protein-containing complex assembly	GO_BiologicalProcess	4.00
GO:0043604	amide biosynthetic process	GO_BiologicalProcess	9.00
GO:0043043	peptide biosynthetic process	GO_BiologicalProcess	9.00
GO:0044391	ribosomal subunit	GO_CellularComponent	9.00
GO:0006412	translation	GO_BiologicalProcess	9.00
GO:0042255	ribosome assembly	GO_BiologicalProcess	4.00
GO:0044445	cytosolic part	GO_CellularComponent	9.00
GO:0000027	ribosomal large subunit assembly	GO_BiologicalProcess	3.00
GO:0015934	large ribosomal subunit	GO_CellularComponent	8.00
GO:0022626	cytosolic ribosome	GO_CellularComponent	9.00
GO:0006364	rRNA processing	GO_BiologicalProcess	3.00
GO:0016072	rRNA metabolic process	GO_BiologicalProcess	3.00
GO:0022625	cytosolic large ribosomal subunit	GO_CellularComponent	8.00

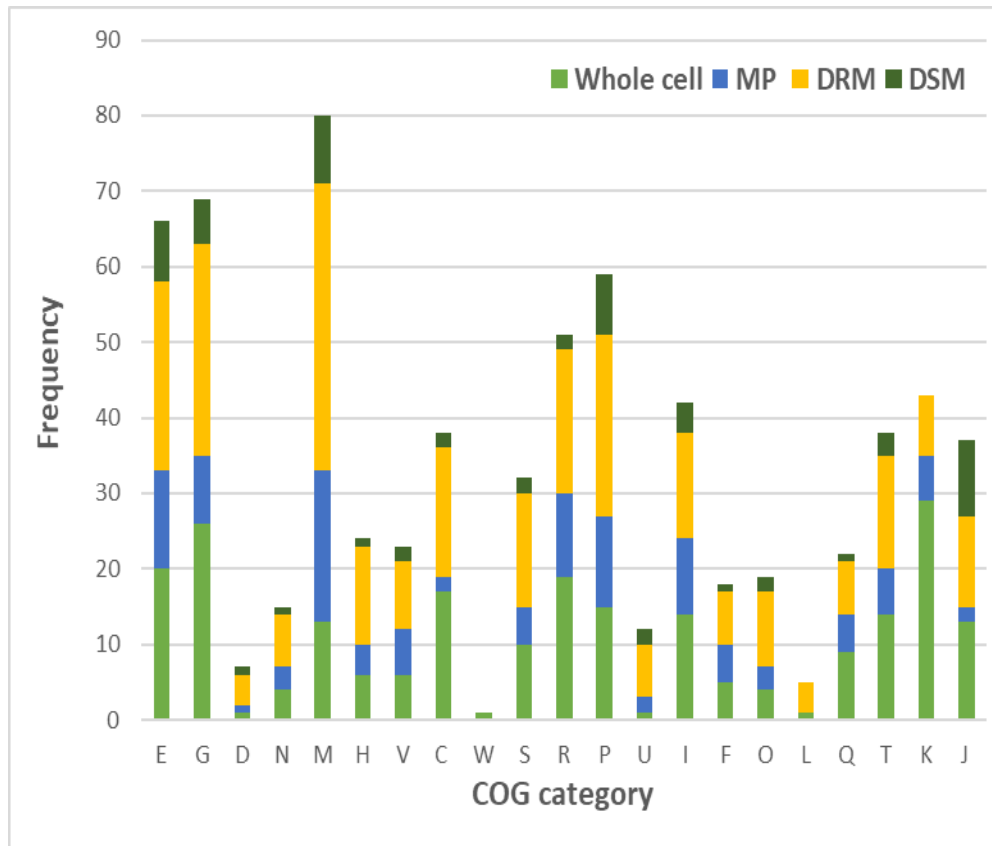


**Figure 3.5: Top orthologous groups for all significant proteins in whole cell, membrane pellet, DRM and DSM samples**

The functional classification of individual protein-coding gene was classified according to COG assignments. Following are the COG category labels: E- Amino acid transport and metabolism; G- Carbohydrate transport and metabolism; D-Cell cycle control, cell division, chromosome partitioning; N- Cell motility; M- Cell wall/membrane/envelope biogenesis; H- Coenzyme transport and metabolism; V- Defense mechanisms; C- Energy production and conversion; W- Extracellular structures; S- Function unknown R- General function prediction only; P- Inorganic ion transport and metabolism; U- Intracellular trafficking, secretion, and vesicular transport; I- Lipid transport and metabolism; F- Nucleotide transport and metabolism; O- Post-translational modification, protein turnover, and chaperones; L- Replication, recombination and repair; Q- Secondary metabolites biosynthesis, transport, and catabolism; T- Signal transduction mechanisms; K- Transcription; J - Translation, ribosomal structure and biogenesis

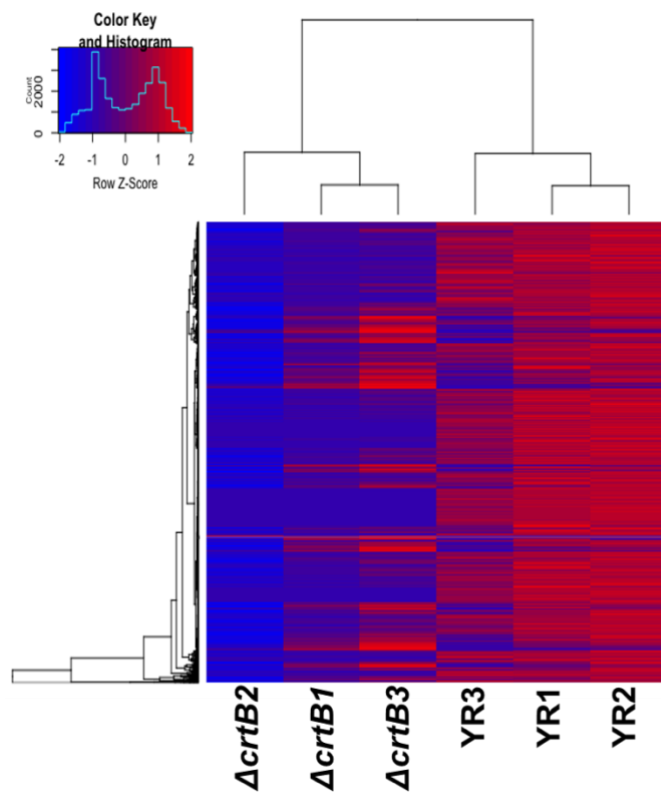


**Figure 3.6: Clustered heatmap of gene expression in *Pantoea* sp. YR343 and  $\Delta crtB$  mutant.**

Hierarchical clustering was performed using absolute gene counts. Genome wide gene signatures indicated low expression profiles in the  $\Delta crtB$  mutant compared to the wildtype.

**Table 3.2: List of significantly upregulated or downregulated proteins involved in cell wall/ membrane/ envelope biogenesis.**

Protein list from JGI for each COG category was matched with the proteomics dataset. The table represents proteins that were significantly different at least in one fraction in the wildtype or  $\Delta crtB$  mutant. TM/SP- proteins with transmembrane helices or signal peptide.

Cell wall/Membrane/envelope biogenesis							
Locus Tag	Gene Product Name	TM/SP	Whole cell	Membrane pellet	DRM	DSM	Transcriptomics
PMI39_01845	tyrosine-protein kinase Etk/Wzc	TM					
PMI39_04919	RND family efflux transporter, MFP subunit						
PMI39_01315	membrane fusion protein, multidrug efflux system	SP					
PMI39_03114	undecaprenyl-phosphate 4-deoxy-4-formamido-L-arabinose transferase	TM					
PMI39_04116	ADP-heptose:LPS heptosyltransferase						
PMI39_04793	undecaprenyl-phosphate galactose phosphotransferase	TM					
PMI39_00342	Nucleoside-diphosphate-sugar epimerase						
PMI39_03115	UDP-4-amino-4-deoxy-L-arabinose-oxoglutarate aminotransferase						
PMI39_04095	aspartate racemase						
PMI39_00324	4-hydroxy-tetrahydrodipicolinate synthase						
PMI39_02352	glucose-1-phosphate thymidyltransferase						
PMI39_02560	xylose isomerase						
PMI39_01126	hypothetical protein	SP					
PMI39_03339	penicillin-binding protein 1A	TM					
PMI39_03586	Beta-barrel assembly machine subunit BamB						
PMI39_01060	outer membrane protein	SP					
PMI39_03111	4-amino-4-deoxy-L-arabinose transferase	TM					
PMI39_04302	lipid A ethanolaminephosphotransferase	TM					

Table 3.2 continued

Locus Tag	Gene Product Name	TM/SP	Whole cell	Membrane pellet	DRM	DSM	Transcriptomics
PMI39_01643	membrane-bound lytic murein transglycosylase B	SP					
PMI39_01850	AsmA protein	TM					
PMI39_03681	Beta-barrel assembly machine subunit BamA	SP					
PMI39_00306	membrane fusion protein, macrolide-specific efflux system	TM					
PMI39_04772	N-acetylmuramoyl-L-alanine amidase						
PMI39_00593	D-alanyl-D-alanine carboxypeptidase (penicillin-binding protein 5/6)						
PMI39_00843	murein lipoprotein	SP					
PMI39_00870	hypothetical protein	SP					
PMI39_00927	membrane glycosyltransferase	TM					
PMI39_01154	autotransporter secretion outer membrane protein TamA	SP					
PMI39_01192	Apolipoprotein N-acyltransferase	TM					
PMI39_01206	rare lipoprotein A						
PMI39_01207	D-alanyl-D-alanine carboxypeptidase (penicillin-binding protein 5/6)	SP					
PMI39_01510	lipoprotein NlpI						
PMI39_01562	lipopolysaccharide export system ATP-binding protein						
PMI39_01583	apolipoprotein D and lipocalin family protein	SP					
PMI39_01648	lipoprotein NlpD	SP					
PMI39_01840	Glycosyltransferase involved in cell wall biosynthesis						
PMI39_01848	UDP-galactose-lipid carrier transferase	TM					
PMI39_01858	membrane fusion protein, multidrug efflux system	TM					
PMI39_02251	UDP-D-galactose:(glucosyl) LPS alpha-1,3-D-galactosyltransferase						
PMI39_02348	lipopolysaccharide biosynthesis protein WzzE	TM					
PMI39_02704	Lipopolysaccharide biosynthesis regulator YciM, contains six TPR domains and a predicted metal-binding C-terminal domain						

Table 3.2 continued

Locus Tag	Gene Product Name	TM/SP	Whole cell	Membrane pellet	DRM	DSM	Transcriptomics
PMI39_03032	membrane-bound lytic murein transglycosylase C						
PMI39_03220	outer membrane lipoprotein LolB	SP					
PMI39_03564	small conductance mechanosensitive channel	TM					
PMI39_03710	penicillin-binding protein 1B	TM					
PMI39_04013	Beta-barrel assembly machine subunit BamD	SP					
PMI39_04424	ADP-heptose:LPS heptosyltransferase	TM					
PMI39_04745	Membrane-bound inhibitor of C-type lysozyme						
PMI39_03971	Murein L,D-transpeptidase YafK	SP					
PMI39_01550	UDP-N-acetylglucosamine 1-carboxyvinyltransferase						
PMI39_01556	phospholipid/cholesterol/gamma-HCH transport system ATP-binding protein						
PMI39_00526	outer membrane pore protein F	TM+SP					
PMI39_01917	lipoprotein Spr	SP					
PMI39_03680	periplasmic chaperone for outer membrane proteins Skp	SP					
PMI39_02354	dTDP-4-amino-4,6-dideoxygalactose transaminase						
PMI39_03679	UDP-3-O-[3-hydroxymyristoyl] glucosamine N-acyltransferase						

↓ $\Delta crtB$
↑ $\Delta crtB$
Not significant
Not detected

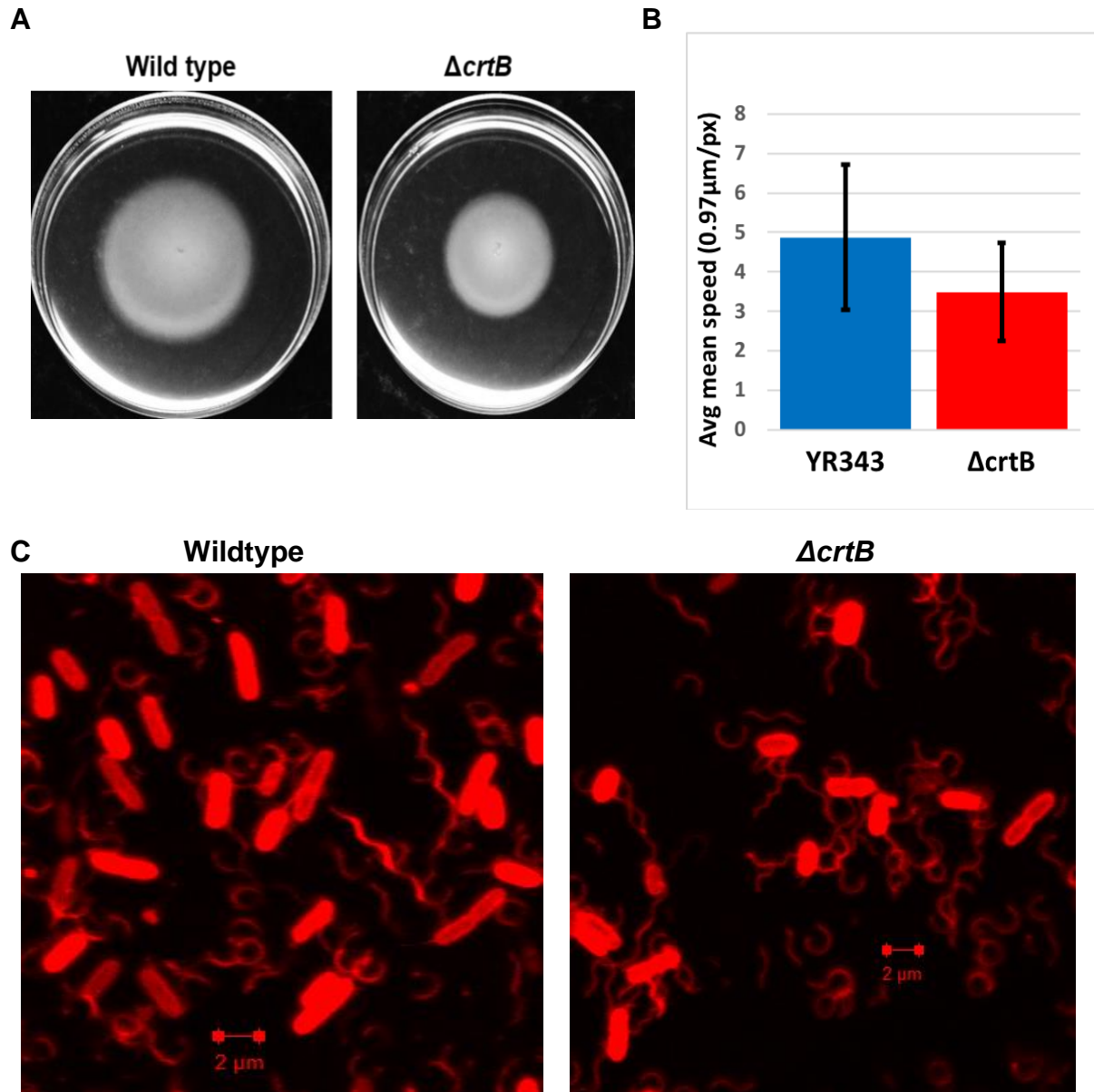


**Figure 3.7: Loss of carotenoids affects bacterial cell motility**

A. Swimming motility of wildtype and  $\Delta crtB$  mutant on LB plates with 0.3%. Cells were inoculated at the center of the plate from an overnight culture and photographed after 16hr incubation at 28°C B. Cells from motility plates were grown to  $OD_{600}$  of 0.5 and swimming motility videos of 10 biological replicates were collected and processed by ImageJ. C. Flagella staining with Alexa Fluor 594 carboxylic acid succinimidyl ester was carried out log-phase cells and imaged using confocal microscopy.

**Table 3.3: List of significantly upregulated or downregulated proteins involved in cell motility**



Protein list from JGI for each COG category was matched with the proteomics dataset. The table represents proteins that were significantly different at least in one fraction in the wildtype or  $\Delta crtB$  mutant. TM/SP- proteins with transmembrane helices or signal peptide.

Cell motility							
Locus tag	Gene name	TM/SP	Whole cell	Membrane pellet	DRM	DSM	Transcriptomics
PMI39_04109	Cellulose biosynthesis protein BcsQ						
PMI39_02605	flagellar hook-associated protein 2						
PMI39_02159	flagellar hook-associated protein 2						
PMI39_02182	flagellar FliL protein	TM					
PMI39_04337	methyl-accepting chemotaxis protein	TM					
PMI39_02618	methyl-accepting chemotaxis protein	TM					
PMI39_00776	methyl-accepting chemotaxis sensory transducer with TarH sensor	TM					
PMI39_00896	flagellar protein FlgJ						
PMI39_03117	leader peptidase (prepilin peptidase) / N-methyltransferase	TM					
PMI39_02510	major type 1 subunit fimbrin (pilin)						
PMI39_02163	methyl-accepting chemotaxis protein	TM					
PMI39_04071	Methyl-accepting chemotaxis protein	TM					
PMI39_02595	methyl-accepting chemotaxis protein-2, aspartate sensor receptor	TM					
PMI39_03890	methyl-accepting chemotaxis sensory transducer with Cache sensor	TM					
PMI39_02297	methyl-accepting chemotaxis sensory transducer with Pas/Pac sensor	TM					



Table 3.3 continued

Locus Tag	Gene Product Name	TM/SP	Whole cell	Membrane pellet	DRM	DSM	Transcriptomics
PMI39_01148	methyl-accepting chemotaxis sensory transducer with TarH sensor	TM					
PMI39_02512	outer membrane usher protein	SP					
PMI39_02513	Pilin (type 1 fimbria component protein)	SP					

 $\Delta crtB$
 $\Delta crtB$
Not significant
Not detected

**Table 3.4: List of significantly upregulated or downregulated proteins involved in lipid transport and metabolism.**

Protein list from JGI for each COG category was matched with the proteomics dataset. The table represents proteins that were significantly different at least in one fraction in the wildtype or  $\Delta crtB$  mutant. TM/SP- proteins with transmembrane helices or signal peptide.

Lipid transport and metabolism							
Locus tag	Gene Name	TM/SP	Whole cells	Membrane pellet	DRM	DSM	Transcriptomics
PMI39_00881	3-oxoacyl-[acyl-carrier-protein] synthase II						
PMI39_00789	NAD(P)-dependent dehydrogenase, short-chain alcohol dehydrogenase family						
PMI39_02975	3-hydroxyisobutyrate dehydrogenase						
PMI39_02976	Lysophospholipase, alpha-beta hydrolase superfamily						
PMI39_01503	Predicted lipid carrier protein YhbT, contains SCP2 domain						
PMI39_02402	acetyl-CoA acyltransferase						
PMI39_03583	4-hydroxy-3-methylbut-2-en-1-yl diphosphate synthase						
PMI39_04767	cyclopropane-fatty-acyl-phospholipid synthase						
PMI39_00695	putative cardiolipin synthase						
PMI39_03673	acetyl-CoA carboxylase carboxyltransferase subunit alpha						
PMI39_02890	choline dehydrogenase						
PMI39_03843	outer membrane lipase/esterase	TM+SP					
PMI39_00318	choline dehydrogenase						
PMI39_01261	Lysophospholipase, alpha-beta hydrolase superfamily						

Table 3.4 continued

Locus tag	Gene Name	TM/SP	Whole cells	Membrane pellet	DRM	DSM	Transcriptomics
PMI39_04227	NAD(P)-dependent dehydrogenase, short-chain alcohol dehydrogenase family						
PMI39_04693	NAD(P)-dependent dehydrogenase, short-chain alcohol dehydrogenase family						
PMI39_04916	Lysophospholipase, alpha-beta hydrolase superfamily	TM					
PMI39_00023	acetyl-CoA acyltransferase						
PMI39_02734	cardiolipin synthase	TM					
PMI39_01258	Phosphatidylglycerophosphate synthase	TM					
PMI39_02871	acyl-CoA thioester hydrolase						
PMI39_04133	NAD(P)-dependent dehydrogenase, short-chain alcohol dehydrogenase family						
PMI39_04906	L-fucose dehydrogenase						
PMI39_02456	L-lactate dehydrogenase (cytochrome)						
PMI39_03968	acyl-CoA dehydrogenase	TM					
PMI39_04547	diacylglycerol kinase (ATP)	TM					

↓ <i>ΔcrtB</i>
↑ <i>ΔcrtB</i>
Not significant
Not detected

**Table 3.5: List of significantly upregulated or downregulated proteins involved in signal transduction mechanism.**

Protein list from JGI for each COG category was matched with the proteomics dataset. The table represents proteins that were significantly different at least in one fraction in the wildtype or  $\Delta crtB$  mutant. TM/SP- proteins with transmembrane helices or signal peptide.

Signal transduction mechanisms							
Locus Tag	Gene name	TM/SP	Whole cell	Membrane pellet	DRM	DSM	Transcriptomics
PMI39_02445	amino acid ABC transporter substrate-binding protein, PAAT family	SP					
PMI39_00574	arginine transport system substrate-binding protein	SP					
PMI39_02695	carbon starvation protein	TM					
PMI39_00272	cell filamentation protein						
PMI39_00276	CRP/FNR family transcriptional regulator, cyclic AMP receptor protein						
PMI39_02334	diguanylate cyclase (GGDEF) domain-containing protein	TM					
PMI39_00427	DNA-binding response regulator, OmpR family, contains REC and winged-helix (wHTH) domain						
PMI39_03053	EAL domain, c-di-GMP-specific phosphodiesterase class I (or its enzymatically inactive variant)						
PMI39_02173	EAL domain, c-di-GMP-specific phosphodiesterase class I (or its enzymatically inactive variant)						
PMI39_00644	hypothetical protein						
PMI39_04647	lysine/arginine/ornithine transport system substrate-binding protein	SP					
PMI39_04337	methyl-accepting chemotaxis protein	TM					

Table 3.5 continued

Locus Tag	Gene name	TM/SP	Whole cell	Membrane pellet	DRM	DSM	Transcriptomics
PMI39_02618	methyl-accepting chemotaxis protein	TM					
PMI39_02163	methyl-accepting chemotaxis protein	TM					
PMI39_02297	methyl-accepting chemotaxis sensory transducer with Pas/Pac sensor	TM					
PMI39_00776	methyl-accepting chemotaxis sensory transducer with TarH sensor	TM					
PMI39_01148	methyl-accepting chemotaxis sensory transducer with TarH sensor	TM					
PMI39_04597	multi-sensor hybrid histidine kinase	TM					
PMI39_02678	phage shock protein C (PspC) family protein	TM					
PMI39_02138	phosphate starvation-inducible protein PhoH						
PMI39_04090	polar amino acid transport system substrate-binding protein	SP					
PMI39_04190	SOS-response transcriptional repressor LexA (RecA-mediated autopeptidase)						
PMI39_01240	tellurium resistance protein TerZ						
PMI39_03635	two component transcriptional regulator, LuxR family						
PMI39_02508	two component transcriptional regulator, LuxR family						
PMI39_04141	two component transcriptional regulator, LuxR family						
PMI39_02514	two-component system, NarL family, response regulator EvgA						
PMI39_03347	two-component system, OmpR family, phosphate regulon response regulator OmpR						
PMI39_02823	two-component system, OmpR family, response regulator QseB						

Table 3.5 continued

Locus Tag	Gene name	TM/SP	Whole cell	Membrane pellet	DRM	DSM	Transcriptomics
PMI39_01862	two-component system, OmpR family, sensor histidine kinase BaeS	TM					
PMI39_04406	two-component system, OmpR family, sensor histidine kinase CpxA	TM					

↓ <i>ΔcrtB</i>
↑ <i>ΔcrtB</i>
Not significant
Not detected

**CHAPTER-4**  
**Conclusions and Future Directions**

Membranes are vital components of life and represents the boundary between the cell and its environment. Importantly, they are sites where several cellular events occur. The ability to dynamically alter membrane organization and composition is key to cellular survival [1, 2]. Eukaryotes can form lipid rafts/domains where proteins, lipids and sterols cluster to promote cellular functions, such as signaling or transport. These raft-like regions play a crucial role by providing strength to the membranes and influencing membrane fluidity [3, 4]. Even though bacteria lack cholesterol, there is increasing evidence that bacterial membranes are also organized into subdomains [5, 6]. The role of carotenoids in membrane organization has not been evaluated in bacterial systems. Our goal is to use a combination of biological and physical science approaches to understand importance of carotenoids in bacterial membrane organization. To study this, we are investigating the role of carotenoids in *Pantoea sp.* YR343, a bacterium isolated from the rhizosphere of poplar trees and  $\Delta crtB$  mutant, that cannot produce any carotenoids.

In this dissertation, we presented findings that help understand the importance of carotenoids in bacterial membrane organization. Previous studies on understanding how carotenoids modulate membrane fluidity was limited to the use of molecular dynamic simulations and artificial systems such as vesicles/liposomes, single lipid and mixed lipid systems. Even though they shed some valuable light in characterizing membrane biophysical properties, they still lack on what truly occurs in native biological cells. To understand the effects of carotenoids we used a carotenoid deficient strain,  $\Delta crtB$ . The  $\Delta crtB$  mutant was not only more susceptible to oxidative stress but surprising displayed other phenotypic defects such as loss of secretion of indole 3-acetic acid, defects in plant root colonization and defects in pellicle formation [7]. We used a combination of biophysical, molecular and OMICS to understand the global effects of loss of bacterial carotenoids. Our aims were to systematically understand the carotenoid-membrane dynamics by studying membrane composition and properties of intact cells, spheroplast and natural-extract vesicles. We also studied how the membrane protein distribution changed between the wildtype and  $\Delta crtB$  mutant. Understanding the proteome of the  $\Delta crtB$  mutant could also give us clues to how the bacteria adapt to changing environmental conditions especially with the lack of carotenoids.

Using lipidomics, we recorded that the membranes of the  $\Delta crtB$  mutant were enriched for phosphatidylethanolamine and unsaturated fatty acids, a possible compensation required for the  $\Delta crtB$  mutant survival and adaptation. With this in mind, our next goal was to determine the membrane biophysical properties. Interestingly, the  $\Delta crtB$  mutant cells displayed less fluid/elastic properties. This observation was confirmed by two independent techniques. As previously stated maintained of membrane fluidity is essential for the proper functioning of several cellular processes. Atomic force microscopy and fluorescence anisotropy revealed that the carotenoids can also act as thermostable



agents and therefore the  $\Delta crtB$  mutant at higher temperatures could not control fluidity. Studies on understanding the membrane fluidity properties in *E. coli* have revealed that the outer membrane is a load bearing element and can also influence membrane fluidity [8]. To test, if the outer membrane of *Pantoea* sp. YR343 and  $\Delta crtB$  mutant also influenced membrane fluidity, we generated spheroplast (cells lacking the outer membrane). Studies on spheroplast revealed no difference in membrane fluid properties between *Pantoea* sp. YR343 and  $\Delta crtB$  mutant, indicating that the outer membranes are also important for maintaining membrane fluidity. Previous studies have focused on using artificial systems such as single lipid vesicles, where they have noted that zeaxanthin, a polar carotenoid makes the membranes fluid. These systems do not accurately represent of what happens *in vivo*. In nature, a bacterial membrane possesses a diversity of phospholipids. To understand the effects of carotenoids on mixed systems, we generated vesicles from lipids extracted from the wildtype and  $\Delta crtB$  mutant. Interestingly, studies on natural extract vesicles showed that the  $\Delta crtB$  mutant vesicles were more fluid when compared to the wildtype, concluding that carotenoids make the membrane more fluid. Overall, proving that artificial systems do not accurately represent of what takes places in a living cell. Thus carotenoids similar to cholesterol can have both membrane fluidizing and rigidizing important for providing mechanical strength, maintain lipid order and protecting bacteria from thermal stress.

Plant-microbe interactions are essential to the functioning of terrestrial ecosystem. Bacteria aid in plant growth and development by secreting plant phytohormones (such as IAA), solubilize phosphate and form biofilms. Importantly, these characteristic properties are lost in the  $\Delta crtB$  mutant. Membranes are the sites where several important cellular functions such as transport and signaling events takes place. Membrane proteins are vital to the survival of organisms. They are important for cell adhesion, signal transduction, membrane biogenesis etc. To correlate the observed phenotypic defects  $\Delta crtB$  mutant with the membrane proteins, we carried out cellular and membrane proteomics. Interestingly, several important classes of proteins belonging to cell motility, secondary metabolites, cell membrane biogenesis and lipid metabolism were significantly downregulated in the  $\Delta crtB$  mutant. Proteins important for chemotaxis were upregulated in the  $\Delta crtB$  mutant, indicating that the  $\Delta crtB$  mutant is compensating for the defects in flagella function. As previously mentioned in the introduction, we also aimed at looking at the possibility of formation of bacterial membrane domains. The DRM fraction which is considered to be the membrane microdomain had significantly less protein identified for the  $\Delta crtB$  mutant. We can conclude that the elimination of carotenoids in the membranes, causes a global effect on distribution and organization of membrane proteins and lipids leading to several phenotypic defects.

It is evident that carotenoids are important for bacterial membrane organization that in turn control plant root colonization. This dissertation helped understand the role of zeaxanthin, a polar carotenoid found in the membranes of *Pantoea* sp. YR343. The carotenoid biosynthetic pathway has been well studied in *Pantoea*. By deleting other enzymes in this pathway, we can modulate the production of carotenoids in *Pantoea* and construct strains that produce lycopene or  $\beta$ -carotene as end products. These strains will be valuable in understanding how different carotenoids insert into the membrane and their effect on structural, functional and system properties. Increasing our understanding about bacterial carotenoids and their role in membrane organization would greatly fill the gaps between natural and artificial systems.

Carotenoid gene expression has not been well studied. Importantly, at what growth stage is carotenoids been produced has not been reported. Using qPCR, reporter constructs and interactive imaging, we can monitor the environmental conditions that promote carotenoid gene expression. By creating reporter constructs in which the promoter from a gene of interest is used to drive GFP expression, can characterize both the temporal and spatial patterns of gene expression. This technique can be applied to any gene of interest and will allow us to correlate observable phenotypes to gene regulation which can be further interpreted by multi-scale simulations. Collectively, these experiments will determine the effect of different carotenoids on membrane structure, how different carotenoids insert into the membrane, how they influence molecular transport and signaling and how these processes relate to the involved molecular networks.

It is well known that carotenoids confer resistance to reactive oxygen species (ROS). As ROS is critical to promote inflammation, carotenoids can be incorporated to sites of inflammation which would in turn quench ROS and reduce inflammation. Another area of interest would be to understand how microbes regulate the synthesis of different carotenoids for use under different environmental conditions. The better knowledge of pigment properties and their biosynthesis can be useful in drug discovery, as several pathogenic bacteria such as *Mycobacterium* species produce carotenoids.

Increasing our understanding about structural and functional properties of carotenoids has multiscale applications from nutraceuticals, to vaccine development and importantly in bacterial colonization.

## References

1. Remaut, H. and R. Fronzes, *Bacterial Membranes: Structural and Molecular Biology*. 2014: Caister Academic Press.
2. Harrison, R., *Biological membranes: their structure and function*. 2013: Springer Science & Business Media.
3. Simons, K. and D. Toomre, Lipid rafts and signal transduction. *Nature reviews Molecular cell biology*, 2000. 1(1): p. 31.
4. Lingwood, D. and K. Simons, Lipid rafts as a membrane-organizing principle. *Science*, 2010. 327(5961): p. 46-50.
5. Bramkamp, M. and D. Lopez, Exploring the existence of lipid rafts in bacteria. *Microbiol Mol Biol Rev*, 2015. 79(1): p. 81-100.
6. Saenz, J.P., et al., Hopanoids as functional analogues of cholesterol in bacterial membranes. *Proc Natl Acad Sci U S A*, 2015. 112(38): p. 11971-6.
7. Bible, A.N., et al., A Carotenoid-Deficient Mutant in *Pantoea* sp. YR343, a Bacteria Isolated from the Rhizosphere of *Populus deltoides*, Is Defective in Root Colonization. *Front Microbiol*, 2016. 7: p. 491.
8. Rojas, E.R., et al., The outer membrane is an essential load-bearing element in Gram-negative bacteria. *Nature*, 2018. 559(7715): p. 617.

## APPENDIX

Appendix-A  
Molecular Toolbox of *Pantoea* sp. YR343

The appendix represents the different molecular tools that were used to generate clean-deletion or insertional mutants of different gene products in *Pantoea* sp. YR343. We have also established the use of integrated vector for localization studies that is very useful in circumventing copy number issues. Table A.1 list the primer sequences that were used in the following study.

### **Generation of marker-free gene deletion in *Pantoea* sp. YR343**

To generate clean deletion of genes of interest (GOI) in *Pantoea* sp. YR343, we used a vector containing *Bacillus subtilis sacB* coupled with pK18 vector containing antibiotic resistance [1, 2]. The pK18mobsacB vector contains a lacZ fragment, mobilizable sacB gene with a DGC1089 promoter, a multiple cloning site (MCP) and kanamycin resistant marker. To create a marker-less mutant, 1kb base pair fragments from upstream and downstream of the gene of interest were amplified and inserted into the pK18mobsacB vector using restriction digestion. The constructs were then cloned in *E. coli* PIR1 chemically competent cells, followed by plasmid confirmation via PCR and sequencing. The plasmids were then electroporated into *Pantoea* sp. YR343. Screening of constructs was carried out by antibiotic selection. To eliminate the vector backbone, the mutants were grown in media containing sucrose (0.5 w/v), since sucrose hydrolysis by the sacB gene is lethal for several gram-negative bacteria. Colonies of cells that survive sucrose selection were then used for colony PCR analysis.

### **Generation of insertion mutant in *Pantoea* sp. YR343**

To generate a disruption of mutant of any gene of interest, the first step includes the amplification of a approximately 500 base pairs (active site) of gene of interest. The fragment was then inserted in pKnock-Tc vector using restriction cloning and cloned in *E. coli* PIR1 chemically competent cells [3]. After plasmid extraction and purification, the constructs were cloned in *Pantoea* sp. YR343 by electroporation and selected on plates containing 5µg ml<sup>-1</sup> tetracycline. Disruption of the gene was confirmed PCR followed by sequencing.

### **Generation of deletion/insertion/point mutants in *Pantoea* sp. YR343 using Lambda Red recombination**

An alternative technique to homologous recombination is Lambda Red recombination that allows direct genome editing without the use of restriction sites. This strategy involves the use of a two-plasmid system [4]. The PCR fragment for the gene of interest is fused to a donor plasmid pTopo/xylA with a I-Sce I restriction site or pUC18. The mutagenesis plasmid pACBSR has the Lambda Red genes under the inducible control of arabinose

promoter. The donor plasmid with the gene of interest is then electroporated into *Pantoea* sp. YR343 containing the pACBSR mutagenesis plasmid. Co-transformants are then inoculated in LB medium with arabinose, generating desired gene mutations in the genome. The mutant clones are then identified via colony PCR and sequencing.

### **Gene deletion/insertion in *Pantoea* sp. YR343 using CRISPR-Cas system**

CRISPR-Cas is an efficient genome scale editing tool that can be used for generating both deletion and insertional mutant in bacteria. This technology has not yet been established in *Pantoea* sp. YR343. CRISPR technology heavily depends on the sgRNA specificity. The first step for gene deletion includes the binding of Cas9/sgRNA complex binding to the DNA sequences that match to the first 20 nucleotides of the sgRNA followed by the protospacer adjacent motif (PAM). Establishment of the technology requires precise identification of both sgRNA and promoter sequences for target gene expression. Optimal target design is necessary for identification of the position of target sites that affects the efficiency of silencing. Several studies on specific sgRNA is needed in *Pantoea* to prevent off-target effects of CRISPR-Cas9 system.

This methodology uses two vector system-pCas and pTarget [5]. pCas constitutively expresses cas9 and inducible expression of lambda RED and sgRNA. pCas contains the cas9 gene with a native promoter, an arabinose-inducible sgRNA guiding Cas9 to the pMB1 replicon of pTarget, the  $\lambda$ -Red recombination system to improve the editing efficiency, and the temperature-sensitive replication repA101 (Ts) for self-curing. pTarget on the other hand, constitutively expresses sgRNA without donor editing template DNA. pTarget was constructed to express the targeting sgRNA, with donor DNA as editing templates. Cas9, Cas9 endonuclease; pJ23119, synthetic promoter; N20, 20-bp region complementary to the targeting region; araC, arabinose-inducible transcription factor; pKD46K, a form of pKD46 in which the bla gene is replaced with the aadA gene that confers kanamycin resistance; pTrc99A-spec, a form of pTrc99A, in which bla was replaced by aadA, which confers streptomycin resistance.

The first step is the identification of NGG sites in the gene of interest for sgRNA (<http://www.multicrispr.net>). After identification of desired sgRNA, NEBase changer on PTarget sequence was used to substitute the 20 base pairs before the sgRNA with your desired sgRNA. Q5 site directed mutagenesis and restriction digestion was used to obtain desired sgRNA-pTarget plasmid and transformed into *E. coli* Top10 competent cells. The desired pTarget was then electroporated into *Pantoea* sp. YR343. Arabinose (10 mM final concentration) was added to the culture for  $\lambda$ -Red induction. Cells were recovered at 28°C for 1 h before being spread onto LB agar containing kanamycin (50 mg/liter) and

streptomycin (50 mg/liter). Transformants were identified by colony PCR and DNA sequencing.

For the curing of pTarget series, the edited colony harboring both pCas and pTarget series was inoculated into 2 ml of LB medium containing kanamycin (50 mg/liter) and IPTG (isopropyl- $\beta$ -D-thiogalactopyranoside; 0.5 mM). The culture was incubated for 16 h and spread onto LB plates containing kanamycin. The colonies were confirmed as cured by determining their sensitivity to streptomycin (50 mg/liter). The colonies cured of pTarget series were used in a second round of genome editing. pCas was cured by growing the colonies overnight at 37°C nonselectively. Mutants were further confirmed by PCR and sequencing.

### **Localization studies in *Pantoea* sp. YR343 and $\Delta crtB$ mutant cells using over expression plasmid**

To understand the expression patterns of genes of interest, we constructed a reporter plasmid using pPROBE vector [6]. The promoter region for the gene is usually defined as 350-500 base pairs upstream from the transcription start site and amplified using specific primers. The amplified fragment was fused to the pPROBE-NT vector and transformed into *Pantoea* sp. YR343 and  $\Delta crtB$ . Transformed cells were plated on R2A plates GFP expression and localization was measured using Zeiss LSM710 confocal laser scanning microscopy.

### **Localization studies in *Pantoea* sp. YR343 and $\Delta crtB$ mutant cells using transposon localization**

Localization studies using over-expression plasmids, though commonly used do not exactly provide useful information as the copy number of the protein of interest cannot be controlled. Another method that facilitates integration of single-copy genes into bacterial chromosomes is the use of mini-Tn7 vectors [7]. Gene of interest along with native promoter and a GFP fusion product was generated and confirmed with PCR. Using TOPO cloning pENTR vector, the GOI-GFP fusion product transformed into One Shot competent *E. coli* cells and streaked on LB plates with Kanamycin. Next GOI-GFP/pENTR plasmids were extracted and the fusion product was confirmed via PCR. Next, using gateway LR Clonase II enzyme mix, a LR recombination reaction was set up and transformed in *E. coli* TOP10 competent cells. This step ensures the transfer of the GOI from the entry vector to the destination vector. PCR was carried on destination vector constructs to check successful GOI transfer. The last step includes electro-competent transformation of the destination vector into *Pantoea* sp. YR343 and  $\Delta crtB$



mutant competent cells. using Zeiss LSM710 confocal laser scanning microscopy can be used to study the localization patterns in *Pantoea* sp. YR343 and  $\Delta crtB$  mutant cells.

**Table A.1: List of primers used in this study**

<b>Primer name</b>	<b>Sequence (5'-3')*</b>	<b>Purpose</b>
CrtZ up For (XbaI)	TGCT <u>CTAGAT</u> ACGCAGAATCG ATCCCA	For clean
CrtZ up Rev (KpnI)	CGGGGTAC <u>CTGTT</u> CG TCCATTTGTGGA	deletion
CrtZ down For (KpnI)	CGGGGTAC <u>CTCGCTAA</u> ACCTGCCCTT	using
CrtZ down Rev (XbaI)	TGCT <u>CTAGA</u> ACCGCATAACCGCGATGC	pk18mob
CrtZ up forward-SceI and XbaI	<u>TAGGGATAACAGGGTAATTGCTCTAGAT</u> ACGCAGAATCGATCCCA	For
CrtZ up reverse-KpnI	CGGGGTAC <u>CTGTT</u> CGTCCATTTGTGGA	lambda
CrtZ dw forward-KpnI	CGGGGTAC <u>CTCGCTAA</u> ACCTGCCCTT	red
CrtZ dw reverse- SceI and XbaI	<u>TAGGGATAACAGGGTAATTGCTCTAGA</u> ACCGCATAACCGCGATGC	cloning
crtY/XbaI	TGCT <u>CTAGAC</u> CCTACCAGCTCAGCCAGC	
crtY/KpnI	CGGGGTACCGGTA <u>AAACCC</u> ACGCAGGT	For
TonB/XbaI	TGCT <u>CTAGACTT</u> CTTACGCCGGCTATC	insertional
TonB/KpnI	CGGGGTACCGCATCCTGAAAATCCTGC	mutants
DGC3134/XbaI	TGCT <u>CTAGAT</u> GACATCGAGTGGGTGAT	using
DGC3134/KpnI	CGGGGTAC <u>CTCACCTT</u> TGAGATGGCCA	pKnock
pTargetF- crtY Up For/EcoRI	CGGAAT <u>TCGTT</u> GCATAATCGAGCTG	For
pTargetF- crtY Up Rev/BamHI	CGGGAT <u>CCAAC</u> GCACCTTATGTGATTG	CRISPR-
pTargetF- crtY Dw For/BamHI	CGGGAT <u>CCGTC</u> GCCTCCGCCAGCACA	Cas
pTargetF- crtY Dw rev/HindIII	CCCAAGCTTATTAAACAGCGCGCTGGAAGC	mutants

\*Restriction enzymes are underlined in the primer sequence.

## References

1. Schäfer, A., et al., Small mobilizable multi-purpose cloning vectors derived from the *Escherichia coli* plasmids pK18 and pK19: selection of defined deletions in the chromosome of *Corynebacterium glutamicum*. *Gene*, 1994. 145(1): p. 69-73.
2. Tan, Y., et al., Construction of a novel *sacB*-based system for marker-free gene deletion in *Corynebacterium glutamicum*. *Plasmid*, 2012. 67(1): p. 44-52.
3. Alexeyev, M.F., The pKNOCK series of broad-host-range mobilizable suicide vectors for gene knockout and targeted DNA insertion into the chromosome of gram-negative bacteria. *Biotechniques*, 1999. 26(5): p. 824-6, 828.
4. Mosberg, J.A., et al., Improving Lambda Red Genome Engineering in *Escherichia coli* via Rational Removal of Endogenous Nucleases. *PLOS ONE*, 2012. 7(9): p. e44638.
5. Li, Y., et al., Metabolic engineering of *Escherichia coli* using CRISPR–Cas9 mediated genome editing. *Metabolic engineering*, 2015. 31: p. 13-21.
6. Miller, W.G., J.H. Leveau, and S.E. Lindow, Improved *gfp* and *inaZ* broad-host-range promoter-probe vectors. *Mol Plant Microbe Interact*, 2000. 13(11): p. 1243-50.
7. Choi, K.-H. and H.P. Schweizer, mini-Tn7 insertion in bacteria with single *attTn7* sites: example *Pseudomonas aeruginosa*. *Nature Protocols*, 2006. 1: p. 153.

## Appendix-B

Appendix-B contains the list of transcripts/genes identified by transcriptomics. With a log<sub>2</sub> fold change  $\geq 2$  and a p-value  $\leq 0.05$ , upregulated and downregulated transcripts of  $\Delta crtB$  mutant cells were identified.

**Table B.1: List of transcripts upregulated in  $\Delta crtB$  mutant cells**

Using log<sub>2</sub>\_FC cutoff of  $\geq 2$  and p-value  $\leq 0.05$ , 5 transcripts were identified to be upregulated in  $\Delta crtB$  mutant cells.

Transcripts upregulated in $\Delta crtB$ mutant cells			
Locus tag	Gene Product Name	log <sub>2</sub> _FC	p_value
PMI39_00250	ribokinase	2.66904555	9.79E-74
PMI39_01552	anti-sigma B factor antagonist	3.20467	0.005816
PMI39_04409	glycerol-3-phosphate dehydrogenase	10.4384142	3.42E-285
PMI39_04621	metal resistance protein	2.11354001	1.75E-22
PMI39_04900	elongation factor G	2.50191556	3.99E-146

**Table B.1: List of transcripts downregulated in  $\Delta crtB$  mutant cells**

Using  $\log_2\_FC$  cutoff of  $\geq 2$  and  $p$ -value  $\leq 0.05$ , 5 transcripts were identified to be downregulated in  $\Delta crtB$  mutant cells.

Transcripts upregulated in $\Delta crtB$ mutant cells			
Locus tag	Gene Product Name	$\log_2\_FC$	p_value
PMI39_00128	holo-[acyl-carrier-protein] synthase	-2.798236	0.009270478
PMI39_00205	Site-specific DNA recombinase	-4.382789	5.17E-116
PMI39_00206	putatice virulence related protein PagC	-4.44461	1.47E-106
PMI39_00207	putatice virulence related protein PagC	-4.216057	1.23E-102
PMI39_00209	hypothetical protein	-4.33775	8.25E-120
PMI39_00210	hypothetical protein	-4.465043	1.45E-92
PMI39_00211	Uncharacterized homolog of phage Mu protein gp47	-4.257536	4.77E-145
PMI39_00212	hypothetical protein	-4.601179	4.59E-96
PMI39_00213	hypothetical protein	-4.344751	2.15E-111
PMI39_00214	hypothetical protein	-4.288323	5.76E-146
PMI39_00215	hypothetical protein	-4.280771	2.46E-83
PMI39_00216	Protease subunit of ATP-dependent Clp proteases	-4.080806	2.17E-176
PMI39_00217	Protein of unknown function (DUF2767)	-4.818347	9.23E-218
PMI39_00218	hypothetical protein	-4.377319	6.68E-123
PMI39_00219	SIR2-like domain-containing protein	-3.85704	6.41E-201
PMI39_00220	hypothetical protein	-3.920508	2.73E-103
PMI39_00221	Protein-disulfide isomerase	-4.425231	2.69E-111
PMI39_00222	hypothetical protein	-4.720376	1.91E-158
PMI39_00223	hypothetical protein	-4.4777	1.88E-137
PMI39_00224	hypothetical protein	-4.638454	4.33E-130
PMI39_00225	hypothetical protein	-4.598449	2.96E-104
PMI39_00226	hypothetical protein	-4.673895	2.51E-128
PMI39_00227	hypothetical protein	-4.555286	1.48E-105
PMI39_00228	hypothetical protein	-5.099756	2.05E-79
PMI39_00229	hypothetical protein	-4.853886	2.45E-28
PMI39_00230	hypothetical protein	-4.54698	1.82E-58
PMI39_00231	protein of unknown function (DUF4055)	-4.403778	1.64E-85
PMI39_00232	hypothetical protein	-4.207735	3.04E-184
PMI39_00233	phage terminase small subunit	-3.99862	6.20E-145
PMI39_00234	hypothetical protein	-4.101221	2.43E-165
PMI39_00235	Colicin immunity protein / pyocin immunity protein	-3.385193	5.38E-99
PMI39_00237	lysozyme	-4.478866	6.13E-84
PMI39_00238	Bacteriophage P21 holin S	-3.741967	1.64E-58

Table B.1 continued

<b>Locus tag</b>	<b>Gene Product Name</b>	<b>log2_FC</b>	<b>p_value</b>
PMI39_00239	Antitermination protein	-4.216044	3.31E-108
PMI39_00240	Response regulator	-3.901708	3.75E-82
PMI39_00241	hypothetical protein	-3.85888	9.65E-89
PMI39_00242	MFS transporter, DHA2 family, multidrug resistance protein	-3.952174	1.45E-163
PMI39_00243	DNA polymerase V	-4.1174	1.74E-145
PMI39_00244	DNA polymerase V	-3.873906	1.33E-102
PMI39_00245	hypothetical protein	-3.713643	3.79E-99
PMI39_00246	hypothetical protein	-3.963675	1.64E-150
PMI39_00247	hypothetical protein	-3.835641	3.52E-148
PMI39_00293	hypothetical protein	-3.748404	1.55E-125
PMI39_00294	hypothetical protein	-4.038532	7.07E-87
PMI39_00295	hypothetical protein	-4.022854	3.69E-83
PMI39_00296	transcriptional regulator, TetR family	-4.062069	3.40E-110
PMI39_00297	N-ethylmaleimide reductase	-3.782178	2.90E-77
PMI39_00298	hypothetical protein	-3.742426	5.44E-85
PMI39_00299	Short-chain dehydrogenase	-3.772589	4.85E-143
PMI39_00302	ATPase components of ABC transporters with duplicated ATPase domains	-3.620675	1.81E-147
PMI39_00303	Transmembrane transcriptional regulator (anti-sigma factor RsiW)	-3.470316	2.22E-87
PMI39_00304	RNA polymerase sigma-70 factor, ECF subfamily	-3.602549	1.78E-114
PMI39_00305	TPR repeat-containing protein	-3.757199	7.23E-130
PMI39_00306	membrane fusion protein, macrolide-specific efflux system	-3.504737	2.77E-109
PMI39_00307	macrolide transport system ATP-binding/permease protein	-3.567919	1.40E-128
PMI39_00308	transcriptional regulator, RpiR family	-3.584949	4.69E-77
PMI39_00309	PTS system, maltose and glucose-specific IIC component	-3.501648	1.54E-113
PMI39_00310	N-acylglucosamine-6-phosphate 2-epimerase	-3.669272	1.95E-131
PMI39_00311	choline/glycine/proline betaine transport protein	-3.737722	5.92E-192
PMI39_00312	transcriptional regulator, TetR family	-3.334475	4.64E-105
PMI39_00317	NAD-dependent aldehyde dehydrogenases	-3.098981	1.07E-86
PMI39_00318	choline dehydrogenase	-3.521412	5.62E-187
PMI39_00319	Cyanate permease	-4.192715	8.20E-72
PMI39_00320	transcriptional regulator, IclR family	-3.861767	6.06E-119
PMI39_00321	Mannose-6-phosphate isomerase, cupin superfamily	-3.961022	1.29E-79
PMI39_00322	Protein of unknown function (DUF1471)	-5.005554	1.18E-268
PMI39_00323	Protein of unknown function (DUF1471)	-5.514058	0
PMI39_00324	4-hydroxy-tetrahydrodipicolinate synthase	-3.818062	1.27E-82
PMI39_00325	hypothetical protein	-4.178008	1.49E-214
PMI39_00326	outer-membrane receptor for ferric coprogen and ferric-rhodotorulic acid	-4.376577	1.04E-222

Table B.1 continued

<b>Locus tag</b>	<b>Gene Product Name</b>	<b>log2_FC</b>	<b>p_value</b>
PMI39_00327	probable lipoprotein NlpC	-4.23914	1.49E-242
PMI39_00328	Isopenicillin N synthase	-4.71465	6.76E-75
PMI39_00329	NitT/TauT family transport system substrate-binding protein	-4.677395	1.65E-64
PMI39_00330	Cytosine/adenosine deaminase	-3.521239	3.35E-57
PMI39_00331	drug resistance transporter, EmrB/QacA subfamily	-4.086986	8.06E-181
PMI39_00332	transcriptional regulator, TetR family	-3.564052	2.84E-89
PMI39_00333	Peroxiredoxin	-4.220121	6.78E-92
PMI39_00334	thiol:disulfide interchange protein DsbD	-3.83058	2.33E-161
PMI39_00335	RNA polymerase sigma-70 factor, ECF subfamily	-3.96119	1.15E-57
PMI39_00336	Protein of unknown function (DUF1109)	-4.037772	3.70E-121
PMI39_00337	3-dehydro-L-gulonate 2-dehydrogenase	-4.03534	3.69E-215
PMI39_00338	oligogalacturonide transporter	-4.289066	6.25E-233
PMI39_00339	Protein of unknown function (DUF1471)	-3.399263	3.82E-49
PMI39_00340	Multidrug resistance efflux pump	-4.374927	5.58E-159
PMI39_00341	Protein of unknown function (DUF3302)	-4.52532	1.87E-180
PMI39_00342	Nucleoside-diphosphate-sugar epimerase	-3.755068	1.02E-81
PMI39_00343	DNA-binding transcriptional regulator, LysR family	-3.964928	1.23E-172
PMI39_00372	Uncharacterized membrane protein YhdT	-8.159252	3.22E-06
PMI39_00374	Chloride channel protein EriC	-4.034067	3.04E-124
PMI39_00375	Ferritin-like metal-binding protein YciE	-4.176782	2.25E-114
PMI39_00376	hypothetical protein	-4.163163	4.61E-76
PMI39_00377	hypothetical protein	-4.621629	3.07E-78
PMI39_00379	Cellobiose phosphorylase	-4.033398	5.70E-161
PMI39_00380	Cytosine/adenosine deaminase	-3.97627	8.31E-113
PMI39_00384	AraC-type DNA-binding protein	-3.667001	2.74E-69
PMI39_00385	DNA-binding transcriptional regulator, LysR family	-4.106883	1.58E-124
PMI39_00386	Glyoxylase, beta-lactamase superfamily II	-4.071537	1.30E-266
PMI39_00387	Permease of the drug/metabolite transporter (DMT) superfamily	-4.539063	3.81E-198
PMI39_00388	2-polyprenyl-6-methoxyphenol hydroxylase	-4.284708	1.27E-149
PMI39_00389	AraC-type DNA-binding protein	-4.074309	4.94E-80
PMI39_00390	Short-chain dehydrogenase	-4.259309	2.44E-39
PMI39_00391	hypothetical protein	-4.391799	2.35E-116
PMI39_00392	hypothetical protein	-4.095063	9.70E-164
PMI39_00393	Nicotinamidase-related amidase	-4.358591	1.06E-171
PMI39_00394	hypothetical protein	-4.398133	5.28E-97
PMI39_00395	DNA-binding transcriptional regulator, LacI/PurR family	-4.118139	2.14E-177
PMI39_00396	resistance to homoserine/threonine (RhtB) family protein	-4.413681	1.87E-123
PMI39_00397	Uncharacterized conserved protein YbaA, DUF1428 family	-4.347959	3.09E-130
PMI39_00398	hypothetical protein	-4.141326	1.15E-101

Table B.1 continued

Locus tag	Gene Product Name	log2_FC	p_value
PMI39_00399	6-phospho-beta-glucosidase	-3.768844	3.04E-94
PMI39_00400	PTS system, beta-glucosides-specific IIC component	-4.473577	2.84E-78
PMI39_00401	transcriptional regulator, RpiR family	-4.158164	6.35E-174
PMI39_00402	glutathione peroxidase	-3.902069	7.89E-67
PMI39_00403	transcriptional regulator, Lacl family	-4.149601	6.52E-107
PMI39_00404	NAD(P)-dependent dehydrogenase, short-chain alcohol dehydrogenase family	-4.301434	1.19E-208
PMI39_00405	Ectoine hydroxylase-related dioxygenase, phytanoyl-CoA dioxygenase (PhyH) family	-4.340428	4.44E-269
PMI39_00406	Predicted arabinose efflux permease, MFS family	-4.358983	5.01E-175
PMI39_00407	hypothetical protein	-4.355022	3.38E-132
PMI39_00408	transcriptional regulator, LysR family	-4.430966	3.79E-271
PMI39_00409	Glycosyltransferase involved in cell wall bisynthesis	-4.350227	4.29E-150
PMI39_00411	Pimeloyl-ACP methyl ester carboxylesterase	-4.250622	1.09E-123
PMI39_00412	Predicted arabinose efflux permease, MFS family	-4.691445	1.05E-166
PMI39_00413	transcriptional regulator, AraC family	-4.555403	1.29E-115
PMI39_00414	Protein of unknown function (DUF1471)	-5.673713	1.40E-233
PMI39_00415	Protein of unknown function (DUF1203)	-4.425425	2.87E-118
PMI39_00416	Acetyltransferases	-4.176464	7.60E-192
PMI39_00417	Ribosomal protein S18 acetylase RimI	-4.098378	8.43E-143
PMI39_00418	Threonine/homoserine/homoserine lactone efflux protein	-4.128176	1.26E-144
PMI39_00422	hypothetical protein	-4.42343	1.51E-174
PMI39_00423	Nucleoside-diphosphate-sugar epimerase	-4.260684	8.57E-151
PMI39_00424	DNA-binding transcriptional regulator, LysR family	-4.002754	2.13E-257
PMI39_00425	hypothetical protein	-3.564994	4.18E-94
PMI39_00426	Pimeloyl-ACP methyl ester carboxylesterase	-3.738777	1.27E-105
PMI39_00427	DNA-binding response regulator, OmpR family, contains REC and winged-helix (wHTH) domain	-3.566039	9.10E-86
PMI39_00428	Signal transduction histidine kinase	-3.63855	7.54E-130
PMI39_00429	Pimeloyl-ACP methyl ester carboxylesterase	-3.709593	1.33E-67
PMI39_00430	Cytochrome c biogenesis protein CcdA	-3.746406	1.50E-220
PMI39_00431	aldehyde dehydrogenase (NAD+)	-3.880339	2.13E-144
PMI39_00432	DNA-binding transcriptional regulator, LysR family	-4.127299	1.59E-217
PMI39_00433	putative restriction endonuclease	-4.131317	1.13E-171
PMI39_00435	hypothetical protein	-4.21354	2.13E-106
PMI39_00437	hypothetical protein	-4.330222	1.34E-174
PMI39_00438	hypothetical protein	-4.20472	1.11E-77
PMI39_00454	Pimeloyl-ACP methyl ester carboxylesterase	-3.951701	3.92E-272
PMI39_00896	flagellar protein FlgJ	-6.089472	3.72E-161

Table B.1 continued

<b>Locus tag</b>	<b>Gene Product Name</b>	<b>log2_FC</b>	<b>p_value</b>
PMI39_00935	Protoporphyrinogen oxidase	-3.62606	2.51E-171
PMI39_00937	hypothetical protein	-3.785523	7.02E-86
PMI39_00938	2-methylcitrate dehydratase PrpD	-3.582952	1.92E-182
PMI39_00939	amidohydrolase	-3.442435	1.24E-126
PMI39_00940	Acetyltransferase (GNAT) domain-containing protein	-3.455454	1.09E-93
PMI39_01724	formate dehydrogenase subunit gamma	-2.311072	5.41E-72
PMI39_02311	5-hydroxyisourate hydrolase	-3.608569	1.34E-125
PMI39_02312	AraC family transcriptional regulator, transcriptional activator FtrA	-3.901868	1.33E-168
PMI39_02313	drug resistance transporter, EmrB/QacA subfamily	-3.783325	8.93E-217
PMI39_02314	Pyridoxamine-phosphate oxidase	-3.76601	9.36E-79
PMI39_02315	transcriptional regulator, TetR family	-4.906643	1.54E-09
PMI39_02316	NAD(P)H dehydrogenase (quinone)	-3.879814	6.64E-75
PMI39_02317	outer membrane autotransporter barrel domain-containing protein	-3.958402	0
PMI39_02318	Uncharacterized membrane protein YfcC, ion transporter superfamily	-4.423153	2.97E-306
PMI39_02319	glutamate carboxypeptidase	-4.332136	3.34E-285
PMI39_02320	DNA-binding transcriptional regulator, LysR family	-4.563052	3.42E-251
PMI39_02322	hypothetical protein	-4.175121	3.29E-163
PMI39_02323	Pre-toxin domain with VENN motif-containing protein	-4.542985	2.06E-161
PMI39_02324	hypothetical protein	-4.832863	2.69E-170
PMI39_02325	hypothetical protein	-4.288155	1.98E-187
PMI39_02326	hypothetical protein	-4.470001	1.63E-132
PMI39_02327	Immunity protein 8	-4.481273	2.49E-288
PMI39_02328	Plasmid stabilization system protein ParE	-4.563714	2.19E-164
PMI39_02329	antitoxin ParD1/3/4	-4.507184	1.83E-256
PMI39_02330	hypothetical protein	-4.977299	1.23E-102
PMI39_02332	hypothetical protein	-4.19208	3.47E-148
PMI39_02503	LysR family transcriptional regulator, regulator of gene expression of beta-lactamase	-3.825383	2.90E-111
PMI39_02504	beta-lactamase class C	-3.772125	1.83E-43
PMI39_02506	Predicted arabinose efflux permease, MFS family	-3.859712	1.76E-183
PMI39_02507	transcriptional regulator, TetR family	-4.097635	1.32E-83
PMI39_02508	two component transcriptional regulator, LuxR family	-3.970934	1.77E-292
PMI39_02509	HPt (histidine-containing phosphotransfer) domain-containing protein	-4.18935	1.48E-127
PMI39_02510	major type 1 subunit fimbrin (pilin)	-4.239955	2.06E-40
PMI39_02511	chaperone protein EcpD	-4.631201	1.08E-81
PMI39_02512	outer membrane usher protein	-4.548347	1.24E-63
PMI39_02513	Pilin (type 1 fimbria component protein)	-4.491306	2.16E-135



Table B.1 continued

<b>Locus tag</b>	<b>Gene Product Name</b>	<b>log2_FC</b>	<b>p_value</b>
PMI39_02514	two-component system, NarL family, response regulator EvgA	-4.203675	1.26E-227
PMI39_02515	two-component system, NarL family, sensor histidine kinase EvgS	-4.364231	1.31E-183
PMI39_02516	two component transcriptional regulator, LuxR family	-3.84771	2.34E-120
PMI39_02517	two-component system, NarL family, sensor histidine kinase EvgS	-4.015152	1.17E-238
PMI39_02518	two component transcriptional regulator, LuxR family	-4.089643	3.95E-110
PMI39_02519	transcriptional regulator, RpiR family	-4.063905	7.61E-78
PMI39_02520	PTS system, cellobiose-specific IIB component	-3.726106	1.13E-57
PMI39_02521	PTS system, cellobiose-specific IIA component	-3.884395	5.39E-26
PMI39_02522	6-phospho-beta-glucosidase	-3.978147	7.47E-92
PMI39_02523	PTS system, cellobiose-specific IIC component	-4.367688	9.81E-196
PMI39_02524	Biofilm development protein YmgB/AriR	-4.097885	1.45E-62
PMI39_02526	L-arabinose isomerase	-4.026816	2.14E-146
PMI39_02527	Cytosine/adenosine deaminases	-4.130414	2.81E-186
PMI39_02528	Predicted oxidoreductase	-4.087784	1.68E-222
PMI39_02529	hypothetical protein	-3.474463	2.92E-56
PMI39_02530	molybdenum cofactor cytidyltransferase	-4.00853	2.23E-172
PMI39_02531	xanthine dehydrogenase accessory factor	-3.828596	1.98E-158
PMI39_02532	xanthine dehydrogenase YagR molybdenum-binding subunit	-3.844601	0
PMI39_02533	xanthine dehydrogenase YagS FAD-binding subunit	-3.794436	6.54E-118
PMI39_02534	xanthine dehydrogenase YagT iron-sulfur-binding subunit	-4.317017	9.95E-196
PMI39_02535	serine/threonine-protein kinase HipA	-4.417617	3.48E-251
PMI39_02536	Helix-turn-helix	-4.324455	1.06E-190
PMI39_02537	DNA-binding transcriptional regulator, LysR family	-4.483514	4.87E-197
PMI39_02538	Protein of unknown function (DUF2798)	-3.489834	7.54E-43
PMI39_02540	ADP-ribose pyrophosphatase	-4.023634	1.26E-89
PMI39_02541	Transposase	-4.044908	7.53E-139
PMI39_02542	Catechol 2,3-dioxygenase	-3.681631	3.63E-124
PMI39_02543	Protein N-acetyltransferase, RimJ/RimL family	-5.654301	7.31E-07
PMI39_02544	DNA-binding transcriptional regulator, GntR family	-3.296332	2.64E-61
PMI39_02545	Cytosine/adenosine deaminase	-4.127303	8.78E-131
PMI39_02546	Cytosine/adenosine deaminase	-4.219282	1.96E-196
PMI39_02547	cytosine deaminase	-4.395187	2.12E-47
PMI39_02548	peptide/nickel transport system ATP-binding protein	-4.156784	3.17E-103
PMI39_02549	peptide/nickel transport system ATP-binding protein	-4.323801	8.89E-09
PMI39_02550	peptide/nickel transport system permease protein	-3.611322	3.58E-53
PMI39_02551	peptide/nickel transport system permease protein	-5.192735	1.15E-57
PMI39_02552	peptide/nickel transport system substrate-binding protein	-4.887684	9.76E-75
PMI39_02553	hypothetical protein	-5.142805	1.18E-98
PMI39_02554	hypothetical protein	-5.081735	4.23E-18

Table B.1 continued

<b>Locus tag</b>	<b>Gene Product Name</b>	<b>log2_FC</b>	<b>p_value</b>
PMI39_02555	regulatory protein, luxR family	-4.458574	3.90E-54
PMI39_02556	two-component system, NarL family, sensor histidine kinase EvgS	-4.474027	1.04E-142
PMI39_02557	two component transcriptional regulator, LuxR family	-4.63091	2.77E-158
PMI39_02560	xylose isomerase	-4.542976	2.53E-93
PMI39_02561	lactoylglutathione lyase	-4.364759	3.69E-90
PMI39_02562	Sugar phosphate permease	-4.705583	1.51E-159
PMI39_02563	transcriptional regulator, DeoR family	-4.494722	2.11E-111
PMI39_02564	transcriptional regulator, LacI family	-4.386029	1.07E-216
PMI39_02565	monosaccharide ABC transporter substrate-binding protein, CUT2 family	-4.066917	6.44E-118
PMI39_02566	creatinine amidohydrolase	-4.397118	3.68E-64
PMI39_02567	DNA-binding transcriptional regulator, LysR family	-4.37304	5.71E-139
PMI39_02568	basic membrane protein A	-4.491495	2.14E-113
PMI39_02569	nucleoside ABC transporter ATP-binding protein	-3.624479	4.19E-95
PMI39_02570	simple sugar transport system permease protein	-3.550631	2.81E-75
PMI39_02571	simple sugar transport system permease protein	-3.942565	1.31E-77
PMI39_02572	Cupin domain-containing protein	-4.73815	2.58E-64
PMI39_02573	Nicotinamidase-related amidase	-3.77516	1.12E-61
PMI39_02574	5-methylthioadenosine/S-adenosylhomocysteine deaminase	-4.314484	2.87E-93
PMI39_02576	serine/threonine-protein kinase HipA	-4.272788	3.35E-188
PMI39_02577	2,4-dienoyl-CoA reductase	-3.773643	5.40E-121
PMI39_02578	Choline dehydrogenase	-4.00219	1.89E-243
PMI39_02579	Membrane bound FAD containing D-sorbitol dehydrogenase	-4.111215	2.04E-148
PMI39_02580	Cytochrome c, mono- and diheme variants	-4.217008	7.18E-112
PMI39_02581	hypothetical protein	-4.124113	6.03E-121
PMI39_02582	6-phosphogluconolactonase	-4.10822	1.92E-107
PMI39_02583	Ribulose-5-phosphate 4-epimerase/Fuculose-1-phosphate aldolase	-4.599227	4.12E-58
PMI39_02584	D-galactonate transporter	-4.626821	7.10E-86
PMI39_02585	transcriptional regulator, LacI family	-3.926047	2.68E-112
PMI39_02586	molybdate transport system substrate-binding protein	-3.679141	4.51E-70
PMI39_02587	L-lactate dehydrogenase (cytochrome)	-4.394261	9.26E-116
PMI39_02588	hypothetical protein	-4.511598	4.37E-52
PMI39_02589	Uncharacterized conserved protein YgbK, DUF1537 family	-4.479486	2.65E-74
PMI39_02590	tryptophan-specific transport protein	-4.64857	1.09E-93
PMI39_02591	myo-inositol 2-dehydrogenase / D-chiro-inositol 1-dehydrogenase	-4.274503	1.94E-97
PMI39_02592	2-keto-myo-inositol isomerase	-4.060995	1.50E-137
PMI39_02593	MFS transporter, SP family, major inositol transporter	-3.784518	1.30E-149
PMI39_02594	hypothetical protein	-3.791728	1.56E-69

Table B.1 continued

<b>Locus tag</b>	<b>Gene Product Name</b>	<b>log2_FC</b>	<b>p_value</b>
PMI39_02595	methyl-accepting chemotaxis protein-2, aspartate sensor receptor	-4.2412	8.10E-95
PMI39_02596	methionyl aminopeptidase	-3.91715	6.09E-145
PMI39_02597	ParD-like antitoxin of type II toxin-antitoxin system	-3.564727	8.95E-52
PMI39_02599	hypothetical protein	-3.779062	9.80E-65
PMI39_02600	MFS transporter, sugar porter (SP) family	-4.346216	5.54E-83
PMI39_02601	Uncharacterized membrane protein YoaK, UPF0700 family	-4.400765	2.62E-110
PMI39_02602	PTS system, beta-glucosides-specific IIC component	-3.55847	4.96E-109
PMI39_02603	6-phospho-beta-glucosidase	-2.354012	1.57E-47
PMI39_02604	transcriptional antiterminator, BglG family	-4.205992	2.77E-154
PMI39_02605	flagellar hook-associated protein 2	-4.314456	2.74E-233
PMI39_02606	HNH endonuclease	-4.126638	6.13E-168
PMI39_02607	Glucosyl transferase GtrII	-4.378743	2.17E-196
PMI39_02609	5-methyltetrahydropteroyltriglutamate--homocysteine methyltransferase	-3.971038	5.33E-187
PMI39_02610	protein of unknown function (DUF1852)	-3.656761	9.26E-171
PMI39_02612	hypothetical protein	-3.846546	3.76E-110
PMI39_02613	tRNA pseudouridine32 synthase / 23S rRNA pseudouridine746 synthase	-4.161592	2.14E-155
PMI39_02614	Cold shock protein, CspA family	-4.103545	1.38E-176
PMI39_02616	Protein of unknown function (DUF1493)	-3.447292	8.21E-37
PMI39_02617	hypothetical protein	-4.117243	1.10E-75
PMI39_02618	methyl-accepting chemotaxis protein	-4.160321	2.62E-273
PMI39_02620	glycogen operon protein	-3.768781	2.40E-223
PMI39_02621	(1->4)-alpha-D-glucan 1-alpha-D-glucosylmutase	-3.928274	3.96E-197
PMI39_02622	malto-oligosyltrehalose trehalohydrolase	-4.205862	8.77E-224
PMI39_02623	MFS transporter, MHS family, proline/betaine transporter	-4.408989	3.60E-147
PMI39_02624	hypothetical protein	-3.951048	2.91E-52
PMI39_02833	DNA-binding transcriptional regulator, LysR family	-4.127501	4.41E-101
PMI39_02834	aminobenzoyl-glutamate utilization protein B	-3.865156	3.52E-138
PMI39_02835	peptide/nickel transport system substrate-binding protein	-4.25528	2.41E-174
PMI39_02836	peptide/nickel transport system permease protein	-4.04083	1.23E-100
PMI39_02837	peptide/nickel transport system permease protein	-3.942933	6.74E-57
PMI39_02838	peptide/nickel transport system ATP-binding protein	-4.060985	2.06E-36
PMI39_02839	peptide/nickel transport system ATP-binding protein	-3.884901	1.63E-56
PMI39_02840	2-methylcitrate dehydratase PrpD	-4.192058	2.53E-136
PMI39_02841	NADP-dependent 3-hydroxy acid dehydrogenase YdfG	-3.933489	6.49E-132
PMI39_02842	hypothetical protein	-3.871195	2.17E-84
PMI39_02843	RNA polymerase sigma factor, sigma-70 family	-3.896	2.02E-158
PMI39_02844	L-ascorbate metabolism protein UlaG, beta-lactamase superfamily	-4.16442	1.23E-147

Table B.1 continued

Locus tag	Gene Product Name	log2_FC	p_value
PMI39_02845	Uncharacterized conserved protein YtfP, gamma-glutamylcyclotransferase (GGCT)/AIG2-like family	-4.341642	1.07E-110
PMI39_02846	Uncharacterized conserved protein, DUF1778 family	-4.199961	5.92E-143
PMI39_02847	Acetyltransferase (GNAT) domain-containing protein	-4.389089	2.62E-138
PMI39_02848	hypothetical protein	-4.357277	4.17E-204
PMI39_02849	D-methionine transport system substrate-binding protein	-4.040125	1.15E-287
PMI39_02850	KUP system potassium uptake protein	-4.153928	4.09E-196
PMI39_02851	Protein of unknown function (DUF1471)	-4.462203	2.10E-177
PMI39_02852	DNA-binding transcriptional regulator, LysR family	-4.281474	2.39E-169
PMI39_02853	haloacetate dehalogenase	-4.237584	5.61E-100
PMI39_02854	3-isopropylmalate/(R)-2-methylmalate dehydratase small subunit	-4.314831	3.83E-91
PMI39_02855	3-isopropylmalate/(R)-2-methylmalate dehydratase large subunit	-4.386672	2.12E-76
PMI39_02856	malate dehydrogenase (quinone)	-3.938279	5.40E-237
PMI39_02857	L-lactate dehydrogenase (cytochrome)	-3.655438	1.10E-13
PMI39_02858	putative flavoprotein involved in K <sup>+</sup> transport	-4.666621	1.75E-246
PMI39_02859	putative spermidine/putrescine transport system permease protein	-4.756132	5.65E-162
PMI39_02860	putative spermidine/putrescine transport system permease protein	-4.137429	1.34E-44
PMI39_02861	putative spermidine/putrescine transport system substrate-binding protein	-4.588801	7.36E-97
PMI39_02862	DNA-binding transcriptional regulator, LysR family	-4.601019	1.26E-71
PMI39_02863	glyoxylate/hydroxypyruvate reductase A	-4.327247	3.38E-132
PMI39_02864	3-dehydroquinate dehydratase	-3.777109	1.91E-56
PMI39_02865	glutathione S-transferase	-4.036539	5.53E-67
PMI39_02866	putative NAD(P)H quinone oxidoreductase, PIG3 family	-4.029122	5.77E-86
PMI39_02867	putative spermidine/putrescine transport system ATP-binding protein	-3.998453	1.12E-113
PMI39_02868	acetylornithine deacetylase	-3.935361	2.21E-77
PMI39_02869	Uncharacterized conserved protein, Ntn-hydrolase superfamily	-4.314782	2.34E-51
PMI39_02870	Enamine deaminase RidA, house cleaning of reactive enamine intermediates, YjgF/YER057c/UK114 family	-4.15731	5.15E-78
PMI39_02871	acyl-CoA thioester hydrolase	-3.979896	1.44E-57
PMI39_02872	Dienelactone hydrolase	-3.917833	3.95E-87
PMI39_02873	Sulfate permease and related transporters (MFS superfamily)	-4.653801	1.95E-139
PMI39_02875	Cd <sup>2+</sup> /Zn <sup>2+</sup> -exporting ATPase	-4.533804	4.73E-116
PMI39_02876	Protein of unknown function (DUF1471)	-4.456744	2.67E-116
PMI39_02877	gluconate:H <sup>+</sup> symporter, GntP family	-4.240306	3.38E-181
PMI39_02878	Peptidoglycan/LPS O-acetylase OafA/YrhL, contains acyltransferase and SGNH-hydrolase domains	-4.343427	2.91E-163

Table B.1 continued

<b>Locus tag</b>	<b>Gene Product Name</b>	<b>log2_FC</b>	<b>p_value</b>
PMI39_02879	transcriptional regulator, LacI family	-4.165394	2.12E-90
PMI39_02880	PTS system, arbutin-, cellobiose-, and salicin-specific IIC component	-4.087432	3.99E-105
PMI39_02881	6-phospho-beta-glucosidase	-3.90152	5.60E-174
PMI39_02882	Uncharacterized membrane protein YccC	-4.252981	2.80E-97
PMI39_02883	protein of unknown function (DUF4154)	-4.007141	1.30E-135
PMI39_02884	diguanylate cyclase (GGDEF) domain-containing protein	-3.963473	7.19E-222
PMI39_02885	Outer membrane protein and related peptidoglycan-associated (lipo)proteins	-4.238638	4.24E-173
PMI39_02886	UV-damage endonuclease	-3.878389	5.06E-188
PMI39_02887	choline/glycine/proline betaine transport protein	-3.768844	2.48E-87
PMI39_02888	transcriptional regulator, TetR family	-3.470398	4.78E-86
PMI39_02889	betaine aldehyde dehydrogenase	-3.292245	1.79E-131
PMI39_02890	choline dehydrogenase	-3.272344	5.60E-160
PMI39_02891	antitoxin VapB	-3.706984	4.73E-93
PMI39_02892	Acetyl esterase/lipase	-3.376526	1.02E-98
PMI39_02893	Nicotinamidase-related amidase	-3.654156	3.88E-82
PMI39_02894	cytosine permease	-3.947764	1.05E-07
PMI39_02895	aspartyl-tRNA(Asn)/glutamyl-tRNA(Gln) amidotransferase subunit A	-3.408261	1.51E-135
PMI39_02896	DNA-binding transcriptional regulator, LysR family	-3.287451	9.40E-61
PMI39_02897	Nucleoside-diphosphate-sugar epimerase	-3.822387	2.78E-107
PMI39_02898	small multidrug resistance pump	-4.392567	7.09E-111
PMI39_02899	Uncharacterized membrane protein YkgB	-4.18933	1.28E-121
PMI39_02900	Protein of unknown function (DUF1471)	-3.842353	3.44E-69
PMI39_02901	transcriptional regulator, TetR family	-4.210559	6.72E-241
PMI39_02902	iron complex transport system substrate-binding protein	-4.04613	3.95E-231
PMI39_02903	molybdate transport system substrate-binding protein	-3.808704	1.79E-159
PMI39_02904	Uncharacterized membrane protein HdeD, DUF308 family	-3.764457	4.85E-165
PMI39_02905	hypothetical protein	-4.438954	5.01E-118
PMI39_03108	L-lactate dehydrogenase (cytochrome)	-3.786932	2.00E-71
PMI39_03109	undecaprenyl phosphate-alpha-L-ara4N flippase subunit ArnF	-3.630142	4.35E-100
PMI39_03110	undecaprenyl phosphate-alpha-L-ara4N flippase subunit ArnE	-3.935862	7.02E-84
PMI39_03111	4-amino-4-deoxy-L-arabinose transferase	-3.47939	2.15E-176
PMI39_03112	undecaprenyl phosphate-alpha-L-ara4FN deformylase	-3.477436	2.29E-175
PMI39_03113	UDP-4-amino-4-deoxy-L-arabinose formyltransferase / UDP-glucuronic acid dehydrogenase (UDP-4-keto-hexauronic acid decarboxylating)	-3.556941	9.00E-152

Table B.1 continued

Locus tag	Gene Product Name	log2_FC	p_value
PMI39_03114	undecaprenyl-phosphate 4-deoxy-4-formamido-L-arabinose transferase	-3.437698	5.21E-183
PMI39_03115	UDP-4-amino-4-deoxy-L-arabinose-oxoglutarate aminotransferase	-3.426194	2.69E-131
PMI39_03116	hypothetical protein	-4.515944	1.19E-96
PMI39_03117	leader peptidase (prepilin peptidase) / N-methyltransferase	-4.413205	1.23E-306
PMI39_03118	diaminobutyrate aminotransferase apoenzyme	-4.068895	2.60E-287
PMI39_03119	L-2,4-diaminobutyrate decarboxylase	-3.950543	2.14E-261
PMI39_03120	fibronectin-binding autotransporter adhesin	-4.131957	2.08E-137
PMI39_03121	Small-conductance mechanosensitive channel	-4.39246	7.36E-211
PMI39_03122	Phosphoserine phosphatase	-4.144906	2.02E-288
PMI39_03123	Oxygen tolerance	-4.111139	1.09E-108
PMI39_03124	Ca-activated chloride channel family protein	-3.823446	1.49E-157
PMI39_03125	Ca-activated chloride channel family protein	-3.920405	6.67E-77
PMI39_03126	protein of unknown function (DUF4381)	-3.450258	1.10E-45
PMI39_03127	Uncharacterized conserved protein (some members contain a von Willebrand factor type A (vWA) domain)	-2.394857	0.001108283
PMI39_03128	MoxR-like ATPase	-3.26715	0.004580315
PMI39_03129	uncharacterized protein	-4.083276	1.74E-206
PMI39_03132	long-chain fatty acid transport protein	-4.187548	5.85E-181
PMI39_03133	hypothetical protein	-4.041534	1.94E-126
PMI39_03134	diguanylate cyclase (GGDEF) domain-containing protein	-4.092872	2.21E-196
PMI39_03135	Purine-cytosine permease	-4.716136	3.08E-183
PMI39_03136	Predicted amidohydrolase	-4.373742	9.87E-179
PMI39_03137	amino acid/amide ABC transporter substrate-binding protein, HAAT family	-3.842091	1.04E-155
PMI39_03138	Two-component response regulator, AmiR/NasT family, consists of REC and RNA-binding antiterminator (ANTAR) domains	-3.655088	6.62E-68
PMI39_03139	DNA-binding transcriptional regulator, LysR family	-3.984852	1.49E-76
PMI39_03140	Predicted oxidoreductase	-3.738118	1.02E-124
PMI39_03141	GntR family transcriptional regulator / MocR family aminotransferase	-4.021411	1.34E-94
PMI39_03142	4-aminobutyrate aminotransferase	-3.138018	1.88E-101
PMI39_03143	GABA permease	-3.737252	6.04E-132
PMI39_03144	hypothetical protein	-3.432319	5.20E-56
PMI39_03145	Uncharacterized lipoprotein YddW, UPF0748 family	-3.852785	1.03E-194
PMI39_03387	molybdate/tungstate transport system substrate-binding protein	-4.119089	1.80E-79
PMI39_03388	hypothetical protein	-4.317568	2.66E-110
PMI39_03389	hypothetical protein	-3.917198	1.06E-83
PMI39_03390	uncharacterized zinc-type alcohol dehydrogenase-like protein	-4.072406	4.23E-133
PMI39_03391	uncharacterized zinc-type alcohol dehydrogenase-like protein	-3.816596	1.54E-102

Table B.1 continued

Locus tag	Gene Product Name	log2_FC	p_value
PMI39_03392	Uncharacterized iron-regulated membrane protein	-3.885416	5.39E-113
PMI39_03393	Protein of unknown function (DUF2946)	-3.554653	4.90E-71
PMI39_03394	L-glutaminase	-4.179564	3.23E-205
PMI39_03395	cupin 2 domain-containing protein	-4.253383	7.46E-90
PMI39_03396	Uncharacterized protein, UPF0303 family	-4.271541	5.22E-125
PMI39_03397	Cytochrome c, mono- and diheme variants	-3.819224	4.70E-116
PMI39_03398	gluconate 2-dehydrogenase alpha chain	-4.386262	3.89E-198
PMI39_03399	gluconate 2-dehydrogenase gamma chain	-3.81056	3.80E-57
PMI39_03400	Sugar phosphate isomerase/epimerase	-3.921146	3.16E-127
PMI39_03402	Predicted dehydrogenase	-3.658191	7.79E-133
PMI39_03403	Sugar phosphate isomerase/epimerase	-3.864349	4.96E-84
PMI39_03404	DNA-binding transcriptional regulator, ArsR family	-3.883843	9.18E-146
PMI39_03405	MFS transporter, CP family, cyanate transporter	-3.513165	2.82E-89
PMI39_03406	RHH-type transcriptional regulator, rel operon repressor / antitoxin RelB	-4.13278	2.60E-102
PMI39_03407	beta-carotene 3-hydroxylase	-3.969177	1.33E-219
PMI39_03408	phytoene synthase	-3.81807	8.54E-101
PMI39_03409	phytoene desaturase	-3.679885	2.52E-287
PMI39_03410	lycopene beta-cyclase	-2.358535	4.23E-09
PMI39_03411	UDP-glucuronosyl and UDP-glucosyl transferase	-3.530769	4.79E-114
PMI39_03412	geranylgeranyl diphosphate synthase, type II	-3.94146	2.75E-122
PMI39_03413	hydroxypyruvate reductase	-3.988826	2.33E-109
PMI39_03414	Glycine/D-amino acid oxidase (deaminating)	-3.89107	1.43E-221
PMI39_03415	DNA-binding transcriptional regulator, MocR family, contains an aminotransferase domain	-4.504798	2.61E-227
PMI39_03416	EamA-like transporter family protein	-4.511233	1.00E-157
PMI39_03417	trehalose 6-phosphate synthase	-4.524627	2.97E-127
PMI39_03418	Predicted dehydrogenase	-4.115624	3.92E-164
PMI39_03419	Ribosomal protein S18 acetylase RimI	-4.267839	1.62E-285
PMI39_03420	Phage antirepressor protein YoqD, KilAC domain	-4.207824	0
PMI39_03421	Mannosyltransferase OCH1 and related enzymes	-4.402621	4.73E-169
PMI39_03422	Helix-turn-helix domain-containing protein	-3.967826	2.76E-255
PMI39_03423	Arabinose efflux permease	-4.142532	1.33E-173
PMI39_03424	Beta-barrel assembly machine subunit BamA	-4.430123	2.83E-120
PMI39_03425	multiple sugar transport system ATP-binding protein	-4.052948	5.23E-82
PMI39_03426	Sugar or nucleoside kinase, ribokinase family	-4.856409	1.86E-10
PMI39_03427	multiple sugar transport system permease protein	-3.850898	6.96E-69
PMI39_03428	multiple sugar transport system permease protein	-4.540708	3.43E-112
PMI39_03429	multiple sugar transport system substrate-binding protein	-4.217955	8.73E-109

Table B.1 continued

Locus tag	Gene Product Name	log2_FC	p_value
PMI39_03430	hypothetical protein	-4.054245	1.14E-101
PMI39_03431	hypothetical protein	-3.982597	3.66E-85
PMI39_03432	hypothetical protein	-4.23945	1.31E-142
PMI39_03433	Sugar kinase of the NBD/HSP70 family, may contain an N-terminal HTH domain	-3.899353	2.86E-221
PMI39_03434	L-asparagine transporter	-4.406581	3.53E-141
PMI39_03435	glutamate dehydrogenase (NAD(P)+)	-4.841749	1.18E-198
PMI39_03436	hypothetical protein	-4.086055	7.98E-80
PMI39_03437	hypothetical protein	-3.881512	1.43E-102
PMI39_03438	DNA-binding transcriptional regulator, LysR family	-4.046808	3.28E-103
PMI39_03440	Phenylpyruvate tautomerase PptA, 4-oxalocrotonate tautomerase family	-3.895305	1.70E-40
PMI39_03441	glutathione transport system ATP-binding protein	-3.666877	8.04E-165
PMI39_03442	Microcystin degradation protein Mlrc, contains DUF1485 domain	-3.880305	3.19E-152
PMI39_03443	Sugar kinase of the NBD/HSP70 family, may contain an N-terminal HTH domain	-4.029575	1.75E-161
PMI39_03444	glutathione transport system substrate-binding protein	-3.93433	6.71E-89
PMI39_03445	glutathione transport system permease protein	-3.744537	2.17E-121
PMI39_03446	glutathione transport system permease protein	-4.046998	1.93E-66
PMI39_03447	N-acetylglucosamine kinase	-4.263532	3.82E-09
PMI39_03628	hypothetical protein	-8.065918	4.02E-262
PMI39_03841	FAD/FMN-containing dehydrogenase	-4.368813	3.02E-218
PMI39_03842	amylovoran biosynthesis protein AmsF	-4.553305	1.72E-250
PMI39_03843	outer membrane lipase/esterase	-4.301921	2.65E-212
PMI39_03844	methyl-accepting chemotaxis sensory transducer with Pas/Pac sensor	-4.096119	3.16E-143
PMI39_03845	Glycine/D-amino acid oxidase (deaminating)	-4.305288	0
PMI39_03846	transcriptional regulator, XRE family with cupin sensor	-4.292899	1.15E-129
PMI39_03847	polar amino acid transport system substrate-binding protein	-4.209338	2.93E-64
PMI39_03848	polar amino acid transport system permease protein	-4.117346	9.96E-125
PMI39_03849	polar amino acid transport system ATP-binding protein	-4.137762	1.59E-152
PMI39_03850	hypothetical protein	-4.048844	2.78E-97
PMI39_03851	manganese/iron transport system substrate-binding protein	-4.806525	6.49E-276
PMI39_03852	manganese/iron transport system ATP-binding protein	-4.721495	1.31E-207
PMI39_03853	manganese/iron transport system permease protein	-4.542307	3.30E-228
PMI39_03854	manganese/iron transport system permease protein	-4.547951	1.27E-170
PMI39_03855	Enamine deaminase RidA, house cleaning of reactive enamine intermediates, YjgF/YER057c/UK114 family	-4.225228	1.15E-121
PMI39_03856	flavin reductase	-4.175568	2.33E-82



Table B.1 continued

Locus tag	Gene Product Name	log2_FC	p_value
PMI39_03857	Predicted oxidoreductase	-4.119708	1.22E-100
PMI39_03858	aminoacrylate peracid reductase	-4.183826	7.76E-83
PMI39_03859	simple sugar transport system permease protein	-4.371559	7.75E-79
PMI39_03860	simple sugar transport system permease protein	-4.388384	4.39E-104
PMI39_03861	simple sugar transport system ATP-binding protein	-4.024232	9.64E-101
PMI39_03862	basic membrane protein A	-4.436655	1.28E-116
PMI39_03863	pyrimidine oxygenase	-3.867092	3.19E-94
PMI39_03864	aminoacrylate hydrolase	-3.809969	1.71E-65
PMI39_03865	DNA-binding transcriptional regulator, LysR family	-4.247004	5.69E-151
PMI39_03866	outer membrane autotransporter barrel domain-containing protein	-4.281824	4.48E-169
PMI39_03867	DNA-binding transcriptional regulator, Lrp family	-4.106043	3.88E-180
PMI39_03868	Protein of unknown function (DUF2000)	-4.238443	1.37E-171
PMI39_03869	AraC-type DNA-binding protein	-3.547881	7.07E-178
PMI39_03870	NADP-dependent 3-hydroxy acid dehydrogenase YdfG	-4.153713	4.25E-75
PMI39_03871	transcriptional regulator, XRE family with cupin sensor	-3.867424	4.32E-86
PMI39_03872	B3/B4 domain-containing protein (DNA/RNA-binding domain of Phe-tRNA-synthetase)	-4.130808	3.79E-71
PMI39_03873	Predicted N-acetyltransferase YhbS	-4.168469	2.20E-85
PMI39_03874	8-oxo-dGTP diphosphatase	-4.146509	1.47E-133
PMI39_03875	protein of unknown function (DUF1543)	-4.101062	2.44E-144
PMI39_03876	MFS transporter, CP family, cyanate transporter	-4.207416	1.77E-110
PMI39_03877	DNA-binding transcriptional regulator, MarR family	-3.988205	1.20E-130
PMI39_03878	cytochrome b561	-4.14085	1.31E-192
PMI39_03879	Transcriptional regulator containing an amidase domain and an AraC-type DNA-binding HTH domain	-3.88038	4.00E-115
PMI39_03880	Predicted O-methyltransferase	-3.780448	3.31E-106
PMI39_03881	Predicted DNA-binding protein, MmcQ/YjbR family	-3.767032	1.07E-74
PMI39_03882	hypothetical protein	-4.091127	4.04E-172
PMI39_03883	transcriptional regulator, TetR family	-4.451555	2.70E-122
PMI39_03884	Predicted arabinose efflux permease, MFS family	-4.782544	1.65E-69
PMI39_03885	Predicted HD superfamily hydrolase	-4.49008	1.01E-45
PMI39_03886	Transcriptional regulator GlxA family, contains an amidase domain and an AraC-type DNA-binding HTH domain	-3.685455	3.48E-136
PMI39_03887	non-heme chloroperoxidase	-3.882837	1.67E-119
PMI39_03888	Transcriptional regulator GlxA family, contains an amidase domain and an AraC-type DNA-binding HTH domain	-3.582048	2.82E-151
PMI39_03889	Predicted arabinose efflux permease, MFS family	-3.636081	6.58E-202
PMI39_03890	methyl-accepting chemotaxis sensory transducer with Cache sensor	-3.640931	2.46E-246

Table B.1 continued

<b>Locus tag</b>	<b>Gene Product Name</b>	<b>log2_FC</b>	<b>p_value</b>
PMI39_03891	Fic family protein	-3.741595	6.08E-274
PMI39_03892	hypothetical protein	-3.679887	1.98E-73
PMI39_03893	SIR2-like domain-containing protein	-4.269512	4.33E-159
PMI39_03894	XTP/dITP diphosphohydrolase	-4.184382	8.65E-78
PMI39_03895	EAL domain, c-di-GMP-specific phosphodiesterase class I (or its enzymatically inactive variant)	-4.259413	4.63E-189
PMI39_03897	hypothetical protein	-4.004743	5.16E-111
PMI39_03898	polar amino acid transport system substrate-binding protein	-3.942371	3.29E-89
PMI39_03899	polar amino acid transport system ATP-binding protein	-3.688261	4.10E-113
PMI39_03900	polar amino acid transport system permease protein	-3.813245	1.35E-76
PMI39_03901	N-acetylglutamate synthase and related acetyltransferases	-3.785762	1.24E-66
PMI39_03902	polar amino acid transport system substrate-binding protein	-4.080552	2.90E-118
PMI39_03903	FMN-dependent oxidoreductase, nitrilotriacetate monooxygenase family	-3.679235	2.03E-123
PMI39_03904	amidohydrolase	-3.970055	7.49E-116
PMI39_03905	luciferase family oxidoreductase, group 1	-3.789618	2.39E-100
PMI39_03906	tripartite ATP-independent transporter solute receptor, DctP family	-4.085289	4.40E-227
PMI39_03907	TRAP-type C4-dicarboxylate transport system, small permease component	-3.929616	2.66E-119
PMI39_03908	TRAP transporter, DctM subunit	-4.379356	4.45E-140
PMI39_03909	peptide/nickel transport system substrate-binding protein	-3.480945	1.11E-54
PMI39_03910	peptide/nickel transport system permease protein	-3.026893	5.56E-33
PMI39_03911	peptide/nickel transport system permease protein	-3.183953	1.50E-88
PMI39_03912	peptide/nickel transport system ATP-binding protein	-3.380879	7.56E-125
PMI39_03913	putative FMN-dependent luciferase-like monooxygenase, KPN_01858 family	-3.190191	1.60E-96
PMI39_03914	alkylhydroperoxidase domain protein, Avi_7169 family	-3.025784	2.26E-110
PMI39_03915	amidohydrolase	-3.607044	1.83E-87
PMI39_03916	Glyoxalase-like domain-containing protein	-3.423026	1.20E-130
PMI39_03917	Protein N-acetyltransferase, RimJ/RimL family	-3.318488	6.23E-120
PMI39_03918	hypothetical protein	-3.613826	4.53E-206
PMI39_03919	4-hydroxy-tetrahydrodipicolinate synthase	-3.480037	2.80E-217
PMI39_03920	transcriptional regulator, GntR family	-3.621747	1.25E-108
PMI39_03921	leucine efflux protein	-3.94514	6.17E-115
PMI39_03922	quaternary ammonium compound-resistance protein SugE	-3.821436	5.68E-90
PMI39_03923	Predicted transcriptional regulators	-3.53777	2.12E-167
PMI39_03924	B3/B4 domain-containing protein (DNA/RNA-binding domain of Phe-tRNA-synthetase)	-3.431631	2.45E-104
PMI39_03925	L-lysine exporter family protein LysE/ArgO	-3.585573	3.55E-217

Table B.1 continued

<b>Locus tag</b>	<b>Gene Product Name</b>	<b>log2_FC</b>	<b>p_value</b>
PMI39_03926	outer membrane autotransporter barrel domain-containing protein	-3.495599	4.78E-262
PMI39_03927	hypothetical protein	-4.362462	8.57E-129
PMI39_03928	hypothetical protein	-4.249075	6.59E-102
PMI39_03929	Outer membrane protein and related peptidoglycan-associated (lipo)proteins	-4.638159	6.32E-85
PMI39_03930	AraC-type DNA-binding protein	-4.549498	2.91E-164
PMI39_03931	2,4-dienoyl-CoA reductase	-4.387369	1.87E-191
PMI39_03932	Predicted oxidoreductase	-4.273177	7.87E-251
PMI39_03933	hypothetical protein	-4.170395	8.38E-56
PMI39_04053	2-keto-4-pentenoate hydratase/2-oxohepta-3-ene-1,7-dioic acid hydratase (catechol pathway)	-3.992186	5.90E-107
PMI39_04054	2-keto-3-deoxy-L-fuconate dehydrogenase	-3.914772	3.21E-119
PMI39_04055	DNA-binding transcriptional regulator, FadR family	-4.089338	4.78E-128
PMI39_04056	ABC transporter transmembrane region	-4.044201	3.65E-91
PMI39_04057	transcriptional regulator, TetR family	-4.27273	5.37E-200
PMI39_04058	Membrane protein involved in the export of O-antigen and teichoic acid	-4.643874	1.95E-108
PMI39_04059	TupA-like ATPgrasp	-4.304669	1.83E-114
PMI39_04060	Small-conductance mechanosensitive channel	-4.188	3.23E-119
PMI39_04061	O-acetylserine/cysteine efflux transporter	-4.416921	8.60E-79
PMI39_04062	aspartyl-tRNA(Asn)/glutamyl-tRNA(Gln) amidotransferase subunit A	-3.842805	5.03E-143
PMI39_04063	hypothetical protein	-4.313859	2.09E-34
PMI39_04064	NitT/TauT family transport system substrate-binding protein	-4.020822	1.97E-111
PMI39_04065	NitT/TauT family transport system permease protein	-4.518876	6.46E-77
PMI39_04066	NitT/TauT family transport system ATP-binding protein	-4.65424	6.64E-74
PMI39_04067	Predicted amidohydrolase	-3.732716	2.57E-72
PMI39_04068	transcriptional regulator, XRE family with cupin sensor	-4.255248	5.75E-102
PMI39_04069	Organic hydroperoxide reductase OsmC/OhrA	-3.840677	6.38E-158
PMI39_04070	diguanylate cyclase (GGDEF) domain-containing protein	-4.158017	1.77E-200
PMI39_04071	Methyl-accepting chemotaxis protein	-3.944733	0
PMI39_04072	DNA-binding transcriptional regulator, LysR family	-4.483603	0
PMI39_04073	Predicted ester cyclase	-4.305793	6.03E-99
PMI39_04074	uncharacterized zinc-type alcohol dehydrogenase-like protein	-4.324353	2.55E-101
PMI39_04075	transcriptional regulator, HxlR family	-3.862192	1.53E-58
PMI39_04076	Helix-turn-helix domain-containing protein	-4.143629	4.88E-115
PMI39_04078	Nucleoside-diphosphate-sugar epimerase	-4.323971	3.44E-136
PMI39_04079	hypothetical protein	-4.468902	6.32E-234
PMI39_04080	hypothetical protein	-4.702321	7.86E-116

Table B.1 continued

<b>Locus tag</b>	<b>Gene Product Name</b>	<b>log2_FC</b>	<b>p_value</b>
PMI39_04081	Biotin carboxylase	-4.4255	5.67E-140
PMI39_04082	Permease of the drug/metabolite transporter (DMT) superfamily	-4.138994	4.57E-71
PMI39_04083	hypothetical protein	-4.542037	6.02E-172
PMI39_04084	transcriptional regulator, TetR family	-4.245582	3.14E-68
PMI39_04085	Predicted O-methyltransferase	-4.273949	7.27E-102
PMI39_04086	GTPase, G3E family	-4.68344	4.81E-87
PMI39_04087	iron complex transport system substrate-binding protein	-3.734481	8.69E-71
PMI39_04088	transcriptional regulator, lclR family	-4.121135	1.74E-155
PMI39_04089	Enamine deaminase RidA, house cleaning of reactive enamine intermediates, YjgF/YER057c/UK114 family	-4.295618	4.05E-88
PMI39_04090	polar amino acid transport system substrate-binding protein	-4.199638	2.69E-110
PMI39_04091	polar amino acid transport system permease protein	-4.315292	2.52E-119
PMI39_04092	polar amino acid transport system permease protein	-4.692621	3.39E-109
PMI39_04093	polar amino acid transport system ATP-binding protein	-4.470433	2.95E-81
PMI39_04094	D-serine deaminase, pyridoxal phosphate-dependent	-3.890052	2.94E-87
PMI39_04095	aspartate racemase	-4.444003	2.28E-136
PMI39_04096	Uncharacterized membrane protein YccC	-4.399164	9.68E-155
PMI39_04097	sulfonate transport system substrate-binding protein	-4.384859	1.71E-189
PMI39_04099	Acyl-CoA dehydrogenase	-4.162931	1.69E-124
PMI39_04100	Predicted arabinose efflux permease, MFS family	-4.243639	7.12E-126
PMI39_04101	ABC-type metal ion transport system, substrate-binding protein/surface antigen	-3.785379	1.39E-120
PMI39_04102	ABC-type methionine transport system, permease component	-3.756147	2.92E-110
PMI39_04103	D-methionine transport system ATP-binding protein	-3.934873	7.08E-65
PMI39_04104	FMN-dependent oxidoreductase, nitrilotriacetate monooxygenase family	-3.471582	2.46E-72
PMI39_04105	Uncharacterized NAD(P)/FAD-binding protein YdhS	-3.598759	5.43E-211
PMI39_04106	alkanesulfonate monooxygenase	-3.761671	8.30E-136
PMI39_04107	ABC transporter, substrate-binding protein, aliphatic sulfonates family	-4.29071	1.58E-91
PMI39_04108	chromosome partitioning protein, ParB family	-3.570124	2.08E-163
PMI39_04109	Cellulose biosynthesis protein BcsQ	-3.955752	5.70E-275
PMI39_04110	Initiator Replication protein	-3.982311	1.10E-127
PMI39_04111	succinate-semialdehyde dehydrogenase	-4.622004	3.27E-90
PMI39_04112	nucleoside transporter	-4.683156	3.49E-129
PMI39_04113	ADP-ribosylglycohydrolase	-3.960585	9.14E-154
PMI39_04114	Sugar or nucleoside kinase, ribokinase family	-3.89177	1.99E-135
PMI39_04115	DNA-binding transcriptional regulator, GntR family	-3.93443	3.94E-194
PMI39_04116	ADP-heptose:LPS heptosyltransferase	-3.530988	1.29E-49

Table B.1 continued

<b>Locus tag</b>	<b>Gene Product Name</b>	<b>log2_FC</b>	<b>p_value</b>
PMI39_04117	4-oxalocrotonate tautomerase	-4.139767	2.23E-80
PMI39_04118	peptide/nickel transport system substrate-binding protein	-3.991721	6.80E-77
PMI39_04119	peptide/nickel transport system permease protein	-3.950737	5.04E-68
PMI39_04120	peptide/nickel transport system permease protein	-4.358257	2.47E-85
PMI39_04121	peptide/nickel transport system ATP-binding protein	-3.838854	3.19E-164
PMI39_04122	phosphinothricin acetyltransferase	-3.834934	2.14E-80
PMI39_04123	transcriptional regulator, XRE family with cupin sensor	-4.358384	2.09E-143
PMI39_04124	4-azaleucine resistance probable transporter AzIC	-3.836826	1.11E-112
PMI39_04125	Branched-chain amino acid transport protein (AzID)	-3.775214	7.55E-85
PMI39_04126	Protein N-acetyltransferase, RimJ/RimL family	-3.488018	2.06E-97
PMI39_04127	N-acetylglutamate synthase and related acetyltransferases	-3.769334	7.37E-202
PMI39_04128	magnesium transporter	-3.90509	7.98E-161
PMI39_04129	cyclohexyl-isocyanide hydratase	-4.017067	2.48E-161
PMI39_04130	NADP-dependent 3-hydroxy acid dehydrogenase YdfG	-3.902584	3.60E-65
PMI39_04131	AraC-type DNA-binding protein	-3.653042	2.73E-123
PMI39_04133	NAD(P)-dependent dehydrogenase, short-chain alcohol dehydrogenase family	-4.019911	4.06E-68
PMI39_04134	LysR family transcriptional regulator, glycine cleavage system transcriptional activator	-3.479341	7.88E-124
PMI39_04135	amidohydrolase	-3.625233	4.86E-129
PMI39_04136	octopine/nopaline transport system substrate-binding protein	-3.928295	1.35E-121
PMI39_04137	octopine/nopaline transport system permease protein	-3.833842	2.91E-14
PMI39_04138	octopine/nopaline transport system permease protein	-3.542876	5.76E-103
PMI39_04139	octopine/nopaline transport system ATP-binding protein	-3.746512	4.27E-95
PMI39_04140	His Kinase A (phospho-acceptor) domain-containing protein	-3.817806	3.34E-145
PMI39_04141	two component transcriptional regulator, LuxR family	-3.608949	4.51E-121
PMI39_04142	Uncharacterized conserved protein GlcG, DUF336 family	-3.631351	1.01E-79
PMI39_04161	ArsR family transcriptional regulator	-4.442047	9.22E-198
PMI39_04162	arsenical pump membrane protein	-4.057941	4.14E-167
PMI39_04163	arsenate reductase	-4.066336	1.57E-83
PMI39_04164	arsenical resistance protein ArsH	-3.708813	1.41E-77
PMI39_04165	DNA-binding transcriptional regulator, ArsR family	-4.298366	3.79E-109
PMI39_04166	Phage integrase family protein	-4.404508	1.07E-137
PMI39_04167	Excisionase-like protein	-4.524499	3.17E-102
PMI39_04168	hypothetical protein	-4.848758	7.35E-113
PMI39_04169	hypothetical protein	-4.080309	1.23E-62
PMI39_04170	hypothetical protein	-4.474707	1.95E-111
PMI39_04172	hypothetical protein	-4.4863	5.40E-80
PMI39_04173	hypothetical protein	-4.203619	1.05E-106

Table B.1 continued

Locus tag	Gene Product Name	log2_FC	p_value
PMI39_04174	hypothetical protein	-4.414262	3.50E-172
PMI39_04175	DNA polymerase-3 subunit theta	-4.222363	2.65E-91
PMI39_04176	Putative SOS response-associated peptidase YedK	-4.354785	2.02E-106
PMI39_04177	YadA-like C-terminal region	-4.443776	4.96E-88
PMI39_04179	hypothetical protein	-4.781786	1.80E-133
PMI39_04180	RecT family protein	-4.517296	3.02E-169
PMI39_04181	exodeoxyribonuclease VIII	-4.620318	5.31E-147
PMI39_04182	hypothetical protein	-4.526007	1.44E-122
PMI39_04183	hypothetical protein	-4.2401	1.83E-101
PMI39_04185	Uncharacterized low-complexity proteins	-4.279934	1.59E-105
PMI39_04187	hypothetical protein	-4.354018	8.24E-90
PMI39_04189	hypothetical protein	-4.750205	5.69E-91
PMI39_04190	SOS-response transcriptional repressor LexA (RecA-mediated autopeptidase)	-3.97271	1.45E-115
PMI39_04192	hypothetical protein	-5.039282	1.49E-107
PMI39_04204	D-methionine transport system permease protein	-4.306888	6.58E-68
PMI39_04205	D-methionine transport system ATP-binding protein	-3.858064	4.83E-115
PMI39_04206	D-methionine transport system substrate-binding protein	-4.256603	1.61E-100
PMI39_04207	FMN-dependent oxidoreductase, nitrilotriacetate monooxygenase family	-4.048002	3.71E-177
PMI39_04208	sulfur acquisition oxidoreductase, SfnB family	-3.692692	1.54E-71
PMI39_04209	sulfur acquisition oxidoreductase, SfnB family	-3.748211	1.05E-104
PMI39_04210	hypothetical protein	-3.981953	2.39E-242
PMI39_04211	amidase	-3.737833	5.91E-137
PMI39_04212	Transcriptional regulator containing an amidase domain and an AraC-type DNA-binding HTH domain	-3.680252	4.97E-79
PMI39_04213	Two-component response regulator, AmiR/NasT family, consists of REC and RNA-binding antiterminator (ANTAR) domains	-3.682044	8.94E-60
PMI39_04214	urea transport system ATP-binding protein	-3.680826	5.22E-161
PMI39_04215	urea transport system ATP-binding protein	-3.954993	4.84E-140
PMI39_04216	branched-chain amino acid transport system permease protein	-4.084927	2.48E-10
PMI39_04217	branched-chain amino acid transport system permease protein	-3.672408	4.73E-106
PMI39_04218	branched-chain amino acid transport system substrate-binding protein	-4.032005	2.29E-115
PMI39_04219	6-phosphogluconolactonase, cycloisomerase 2 family	-4.306265	5.06E-141
PMI39_04220	L-lysine exporter family protein LysE/ArgO	-3.752147	1.19E-76
PMI39_04221	myo-inositol-1(or 4)-monophosphatase	-3.730299	3.09E-52
PMI39_04222	iron(III) transport system ATP-binding protein	-4.446058	1.40E-06
PMI39_04223	iron(III) transport system permease protein	-3.996068	9.24E-123

Table B.1 continued

Locus tag	Gene Product Name	log2_FC	p_value
PMI39_04224	iron (III) transport system substrate-binding protein	-4.081388	2.47E-70
PMI39_04225	transcriptional regulator, LacI family	-3.696768	1.11E-129
PMI39_04226	DNA-binding transcriptional regulator, LysR family	-3.545919	1.33E-128
PMI39_04227	NAD(P)-dependent dehydrogenase, short-chain alcohol dehydrogenase family	-3.661646	1.82E-52
PMI39_04228	DNA-binding transcriptional regulator, LysR family	-3.834321	9.09E-40
PMI39_04229	Zn-dependent hydrolases, including glyoxylases	-4.261769	2.64E-80
PMI39_04230	mandelamide amidase	-3.678782	3.31E-147
PMI39_04231	hypothetical protein	-3.908799	1.99E-98
PMI39_04232	AraC-type DNA-binding protein	-3.581187	3.08E-82
PMI39_04233	anion transporter	-3.875866	7.72E-173
PMI39_04273	FMN-dependent oxidoreductase, nitrilotriacetate monooxygenase family	-3.392289	3.97E-106
PMI39_04274	aspartate aminotransferase	-3.814414	4.16E-226
PMI39_04275	adenosylhomocysteine nucleosidase	-4.058092	5.93E-305
PMI39_04276	DNA-binding protein H-NS	-3.970277	1.61E-127
PMI39_04277	outer-membrane receptor for ferric coprogen and ferric-rhodotorulic acid	-4.261975	3.39E-221
PMI39_04278	succinyl-diaminopimelate desuccinylase	-3.608314	0.035026785
PMI39_04279	Uncharacterized membrane protein	-4.110017	4.64E-132
PMI39_04280	phosphotriesterase-related protein	-4.19359	2.48E-96
PMI39_04281	monosaccharide ABC transporter membrane protein, CUT2 family	-4.040382	5.83E-167
PMI39_04282	monosaccharide ABC transporter ATP-binding protein, CUT2 family	-4.854697	3.12E-66
PMI39_04283	transcriptional regulator, LacI family	-3.765895	4.31E-187
PMI39_04284	ribose transport system substrate-binding protein	-4.36757	1.05E-119
PMI39_04285	ribokinase	-4.140743	3.37E-96
PMI39_04286	hypothetical protein	-4.097175	7.67E-87
PMI39_04287	thiaminase (transcriptional activator TenA)	-4.342453	8.96E-92
PMI39_04288	ABC transporter	-4.00247	1.86E-105
PMI39_04289	rhamnose transport system substrate-binding protein	-4.436382	2.44E-97
PMI39_04290	Al-2 transport system permease protein	-4.625393	2.62E-85
PMI39_04291	ribose transport system permease protein	-3.937798	5.64E-96
PMI39_04292	acetylmethionine deacetylase	-3.983993	8.16E-66
PMI39_04293	alkanesulfonate monooxygenase	-3.775942	1.17E-72
PMI39_04294	Acyl-CoA dehydrogenase	-4.13685	1.66E-84
PMI39_04295	NitT/TauT family transport system substrate-binding protein	-3.71799	3.45E-65
PMI39_04296	cysteine synthase A	-3.661079	4.02E-125
PMI39_04297	NitT/TauT family transport system permease protein	-3.748629	1.31E-85
PMI39_04299	NitT/TauT family transport system ATP-binding protein	-3.890688	5.25E-97

Table B.1 continued

Locus tag	Gene Product Name	log2_FC	p_value
PMI39_04302	lipid A ethanolaminephosphotransferase	-4.290606	2.54E-274
PMI39_04303	Uncharacterized membrane-anchored protein	-4.507221	2.19E-98
PMI39_04304	two-component system, OmpR family, response regulator	-4.027094	2.54E-56
PMI39_04305	two-component system, OmpR family, sensor kinase	-4.168552	8.05E-113
PMI39_04306	undecaprenyl-diphosphatase	-4.253916	1.51E-124
PMI39_04307	phosphatidylglycerophosphatase B	-4.630789	1.40E-117
PMI39_04309	iron complex transport system substrate-binding protein	-4.413797	7.95E-50
PMI39_04310	iron complex outermembrane receptor protein	-4.240499	3.00E-119
PMI39_04311	transcriptional regulator, RpiR family	-4.291815	2.82E-99
PMI39_04312	putative ABC transport system ATP-binding protein	-3.65684	1.06E-76
PMI39_04313	putative ABC transport system permease protein	-3.657022	4.85E-72
PMI39_04314	transcriptional regulator, LysR family	-4.047628	3.17E-158
PMI39_04315	hypothetical protein	-4.195306	6.38E-130
PMI39_04316	2,4-dienoyl-CoA reductase	-3.659356	1.17E-227
PMI39_04350	MFS transporter, ENTS family, enterobactin (siderophore) exporter	-4.405109	4.07E-159
PMI39_04351	iron complex transport system substrate-binding protein	-3.797315	1.64E-77
PMI39_04362	Enamine deaminase RidA, house cleaning of reactive enamine intermediates, YjgF/YER057c/UK114 family	-3.60466	1.63E-58
PMI39_04363	cytosine deaminase	-4.406223	2.79E-33
PMI39_04364	vanillate O-demethylase ferredoxin subunit	-3.960255	6.06E-153
PMI39_04365	DNA-binding transcriptional regulator, LysR family	-3.875951	6.81E-147
PMI39_04644	LysR family transcriptional regulator, glycine cleavage system transcriptional activator	-3.834282	4.65E-62
PMI39_04645	2OG-Fe(II) oxygenase superfamily protein	-3.80261	1.55E-109
PMI39_04646	Protein of unknown function (DUF2817)	-3.855085	1.54E-109
PMI39_04647	lysine/arginine/ornithine transport system substrate-binding protein	-4.372496	4.31E-167
PMI39_04648	Pimeloyl-ACP methyl ester carboxylesterase	-4.877218	1.14E-55
PMI39_04649	two component heavy metal response transcriptional regulator, winged helix family	-3.840069	3.05E-151
PMI39_04650	two-component system, OmpR family, heavy metal sensor histidine kinase CusS	-4.256511	1.39E-192
PMI39_04651	nitroreductase / dihydropteridine reductase	-3.968208	1.25E-155
PMI39_04652	zinc-binding alcohol dehydrogenase family protein	-3.632172	1.91E-111
PMI39_04653	DNA-binding transcriptional regulator, LysR family	-3.338261	1.48E-67
PMI39_04654	transcriptional regulator, TetR family	-3.787312	7.94E-116
PMI39_04655	aspartate aminotransferase	-3.727061	1.98E-126
PMI39_04656	NADP-dependent 3-hydroxy acid dehydrogenase YdfG	-3.841054	2.92E-73
PMI39_04658	N-methylhydantoinase A	-3.441174	1.48E-111



Table B.1 continued

<b>Locus tag</b>	<b>Gene Product Name</b>	<b>log2_FC</b>	<b>p_value</b>
PMI39_04659	MFS transporter, MHS family, proline/betaine transporter	-3.832215	1.90E-102
PMI39_04660	Regulator of RNase E activity RraA	-3.858822	1.21E-50
PMI39_04661	GntR family transcriptional regulator, xuxAB operon transcriptional repressor	-3.797028	2.78E-84
PMI39_04662	PTS system, cellobiose-specific IIB component	-4.115381	8.35E-48
PMI39_04663	6-phospho-beta-glucosidase	-4.737428	1.05E-83
PMI39_04664	PTS system, cellobiose-specific IIC component	-4.707848	3.44E-165
PMI39_04665	PTS system, cellobiose-specific IIA component	-4.033436	6.99E-55
PMI39_04666	Uncharacterized conserved protein, DUF1778 family	-4.553939	0
PMI39_04667	Acetyltransferase (GNAT) domain-containing protein	-4.742295	0
PMI39_04668	Threonine/homoserine/homoserine lactone efflux protein	-4.599564	0
PMI39_04688	2-dehydropantoate 2-reductase	-4.162174	8.40E-185
PMI39_04689	transcriptional regulator, DeoR family	-4.292522	1.01E-93
PMI39_04690	hypothetical protein	-4.250666	2.79E-56
PMI39_04691	NAD(P)-dependent dehydrogenase, short-chain alcohol dehydrogenase family	-4.206272	1.68E-84
PMI39_04692	DNA-binding transcriptional regulator, LysR family	-4.292098	6.65E-189
PMI39_04693	NAD(P)-dependent dehydrogenase, short-chain alcohol dehydrogenase family	-4.070633	1.15E-96
PMI39_04694	hypothetical protein	-3.897826	2.83E-61
PMI39_04695	iron complex transport system substrate-binding protein	-4.200988	4.18E-58
PMI39_04696	iron complex outermembrane receptor protein	-4.394581	7.15E-82
PMI39_04697	transcriptional regulator, RpiR family	-4.14306	7.52E-74
PMI39_04698	Threonine/homoserine efflux transporter RhtA	-4.272625	2.91E-108
PMI39_04699	Pimeloyl-ACP methyl ester carboxylesterase	-4.730906	1.27E-61
PMI39_04700	outer membrane autotransporter barrel domain-containing protein	-4.533139	8.00E-291
PMI39_04701	outer membrane receptor for ferrienterochelin and colicins	-4.32697	1.41E-228
PMI39_04702	polar amino acid transport system substrate-binding protein	-4.042142	8.59E-54
PMI39_04703	polar amino acid transport system permease protein	-4.064309	1.45E-76
PMI39_04704	polar amino acid transport system ATP-binding protein	-4.074336	6.98E-115
PMI39_04705	biotin/methionine sulfoxide reductase	-3.186627	3.66E-185
PMI39_04706	antitoxin ChpS	-3.767306	5.86E-75
PMI39_04904	L-alanine-DL-glutamate epimerase and related enzymes of enolase superfamily	-3.857193	2.24E-75
PMI39_04905	L-fuconolactonase	-3.759893	2.17E-89
PMI39_04906	L-fucose dehydrogenase	-3.673689	1.07E-70
PMI39_04907	L-rhamnose mutarotase	-4.271434	2.27E-82
PMI39_04908	MFS transporter, FHS family, L-fucose permease	-4.372326	2.95E-171
PMI39_04909	Putative motility protein	-4.229838	1.94E-90

Table B.1 continued

Locus tag	Gene Product Name	log2_FC	p_value
PMI39_04910	2-desacetyl-2-hydroxyethyl bacteriochlorophyllide A dehydrogenase	-4.414943	7.56E-257
PMI39_04911	DNA-binding transcriptional regulator, LysR family	-4.359616	7.30E-132
PMI39_04912	Thymidylate kinase	-4.682217	3.47E-177
PMI39_04913	cold shock protein (beta-ribbon, CspA family)	-3.786584	2.96E-81
PMI39_04914	Peptidoglycan/LPS O-acetylase OafA/YrhL, contains acyltransferase and SGNH-hydrolase domains	-4.851216	8.09E-123
PMI39_04915	palmitoyl transferase	-4.131974	7.87E-91
PMI39_04916	Lysophospholipase, alpha-beta hydrolase superfamily	-3.907366	4.94E-171
PMI39_04917	Surface polysaccharide O-acyltransferase, integral membrane enzyme	-4.170569	1.83E-182
PMI39_04918	Multidrug efflux pump subunit AcrB	-4.208872	1.75E-215
PMI39_04919	RND family efflux transporter, MFP subunit	-3.874445	2.55E-51
PMI39_04921	potassium and/or sodium efflux P-type ATPase	-4.238932	4.04E-136
PMI39_04922	AI-2 transport protein TqsA	-4.337715	2.10E-159
PMI39_04923	Multidrug efflux pump subunit AcrB	-3.76538	3.32E-125
PMI39_04924	RND family efflux transporter, MFP subunit	-4.352664	3.69E-104
PMI39_04926	ATPase, P-type (transporting), HAD superfamily, subfamily IC	-3.877956	4.46E-120
PMI39_04927	protein of unknown function (DUF903)	-3.72936	1.19E-51
PMI39_04928	protein of unknown function (DUF903)	-3.721387	9.82E-50
PMI39_04929	GntR family transcriptional regulator	-3.962393	6.14E-70
PMI39_04930	succinyl-diaminopimelate desuccinylase	-4.017724	4.54E-117
PMI39_04931	peptide/nickel transport system substrate-binding protein	-3.837052	1.02E-178
PMI39_04932	peptide/nickel transport system permease protein	-3.807919	3.74E-41
PMI39_04934	peptide/nickel transport system ATP-binding protein	-3.803233	3.05E-154
PMI39_04935	acetylornithine deacetylase	-5.538087	1.59E-06
PMI39_04936	Xaa-Pro dipeptidase	-3.957725	4.61E-151
PMI39_04937	D-alanyl-D-alanine dipeptidase	-3.892351	1.13E-145
PMI39_04938	transcriptional regulator, TraR/DksA family	-3.83024	1.49E-54
PMI39_04940	Coenzyme F390 synthetase	-3.628753	5.94E-145
PMI39_04941	Acyl-CoA reductase (LuxC)	-3.962486	5.05E-203
PMI39_04942	3-oxoacyl-[acyl-carrier protein] reductase	-3.58063	2.98E-144
PMI39_04944	type VI secretion system secreted protein Hcp	-3.887603	6.46E-151
PMI39_04945	O-acetyl-ADP-ribose deacetylase (regulator of RNase III), contains Macro domain	-4.079793	1.52E-204
PMI39_04946	maltooligosaccharide ABC transporter membrane protein	-3.925197	1.85E-164
PMI39_04947	maltose/maltodextrin transport system permease protein	-3.900935	1.21E-144
PMI39_04948	maltose/maltodextrin transport system substrate-binding protein	-4.161742	5.55E-148
PMI39_04949	multiple sugar transport system ATP-binding protein	-3.732575	1.02E-71

Table B.1 continued

<b>Locus tag</b>	<b>Gene Product Name</b>	<b>log2_FC</b>	<b>p_value</b>
PMI39_04950	maltoporin	-4.096643	3.34E-101
PMI39_04951	maltose operon protein	-3.764856	5.74E-106
PMI39_04952	4-alpha-glucanotransferase	-4.172782	6.35E-141
PMI39_04953	starch phosphorylase	-4.137186	8.41E-136
PMI39_04954	LuxR family transcriptional regulator, maltose regulon positive regulatory protein	-4.265099	0
PMI39_04966	MFS transporter, DHA1 family, arabinose polymer transporter	-3.973773	1.70E-68
PMI39_04967	DNA-binding transcriptional regulator, LysR family	-3.515575	1.66E-46
PMI39_04968	hypothetical protein	-3.975284	7.43E-159
PMI39_04969	Sugar phosphate permease	-3.918522	3.06E-218
PMI39_04970	6,7-dimethyl-8-ribityllumazine synthase	-4.440229	3.68E-138
PMI39_04972	glycine oxidase	-3.767547	4.93E-51
PMI39_04973	sulfur carrier protein	-3.96307	2.91E-24
PMI39_04974	thiazole synthase	-3.493134	1.34E-66
PMI39_04975	Molybdopterin or thiamine biosynthesis adenylyltransferase	-3.701978	8.41E-91
PMI39_04976	putative hydroxymethylpyrimidine transport system ATP-binding protein	-3.493996	2.70E-121
PMI39_04977	putative hydroxymethylpyrimidine transport system permease protein	-3.799816	2.48E-96
PMI39_04978	putative hydroxymethylpyrimidine transport system substrate-binding protein	-3.935247	2.44E-150
PMI39_04989	NitT/TauT family transport system substrate-binding protein	-3.842591	1.15E-86
PMI39_04990	NitT/TauT family transport system ATP-binding protein	-4.694812	3.66E-50
PMI39_04991	NitT/TauT family transport system permease protein	-3.751047	1.11E-72
PMI39_04994	filamentous hemagglutinin	-4.155844	1.11E-260
PMI39_04995	Hemolysin activation/secretion protein	-4.274873	2.30E-170
PMI39_04996	KDO II ethanolaminephosphotransferase	-4.583976	2.71E-251
PMI39_04997	Predicted transcriptional regulators	-4.397141	2.68E-100
PMI39_04999	Protein N-acetyltransferase, RimJ/RimL family	-4.183066	7.00E-95
PMI39_05000	non-ribosomal peptide synthase domain TIGR01720/amino acid adenylation domain-containing protein	-4.176868	4.37E-209
PMI39_05001	MbtH protein	-3.872643	8.54E-54
PMI39_05002	enterochelin esterase	-4.374362	6.44E-176
PMI39_05003	iron complex outer membrane receptor protein	-4.843568	0
PMI39_05004	hypothetical protein	-4.162545	7.93E-256

## VITA

Sushmitha Vijaya Kumar was born on January 14th, 1989, in Hyderabad, Telangana, India. She obtained her Bachelor of Science degree in Biotechnology and Microbiology from Osmania University, Hyderabad, India in 2009. She got her Master of Science in Biotechnology from Vellore Institute of Technology, Vellore, India in 2011. After her post graduate studies, she was accepted as a Biotech Consortium India Limited (BCIL) fellow, where she worked on “*In vivo* testing of biologicals” at Biological E Pvt Ltd, Hyderabad. Following that she worked as a research associate at Dr. Iravathams clinical laboratory. In 2013, she joined the University of Southern Mississippi, as a graduate student under the guidance of Dr. Hao Xu. Her research was focused on understanding the role of VAMP7 proteins in mast cell degranulation. During the time, she published a research paper where she contributed as the second author. In 2015, she joined the Genome Science and Technology graduate program at the University of Tennessee and joined Dr. Jennifer Morrell-Falvey’s lab at ORNL. Her project is understanding the role of carotenoids in bacterial membrane organization. Currently, she is working on two first author publications.